INOSITOL PHOSPHATES REGULATE PHOSPHATE STORAGE IN ACIDOCALCISOMES OF *TRYPANOSOMA BRUCEI*

by

CIRO DAVI CORDEIRO

(Under the Direction of ROBERTO DOCAMPO)

ABSTRACT

Trypanosoma brucei is a protist parasite that infects human and animals, currently found in sub-Saharan Africa. *T. brucei* human infection is called African trypanosomiasis or sleeping sickness and it leads to death if untreated. The cattle disease (Nagana) has harsh socioeconomic impacts in developing nations affected. Inorganic phosphate (Pi) is vital for all organisms, as cells need it for the synthesis of essential compounds such as nucleotides and phospholipids. Deprivation or excess of Pi can be harmful, therefore normal metabolism requires a balance in cytosolic phosphate. One form of regulating Pi levels is to store it as polyphosphate (polyP), a polymer of phosphates that can be degraded to release Pi to the cytosol. The main organelles for polyP storage in *T. brucei* are the acidocalcisomes, acidic compartments that store phosphate, polyphosphate, calcium and other metal ions. The physiological regulation of acidocalcisomes is not well understood. This work demonstrated that signaling molecules named inositol phosphates are key regulators of acidocalcisome phosphate storage. We first studied the inositol pyrophosphate synthetic pathway of *T. brucei* and characterized the activity of inositol phosphate kinases TbIPMK, TbIP5K and TbIP6K. Our experiments revealed that *T. brucei* produces inositol hexakisphosphate (IP_6) and 5-diphospho-inositol pentakisphosphate (5-IP_7). We discovered that depletion of TbIPMK causes a reduction in polyphosphate synthesis in

acidocalcisomes. Interestingly, we also observed that the sodium/phosphate symporter TbPho91, located in acidocalcisomes, is stimulated by 5-IP_7. Additionally, TbPho91 knockout cells are more sensitive to DNA damage, revealing that an imbalance in cytosolic Pi may reduce nucleotide synthesis and consequently delay DNA repair. This mechanism for regulation of polyP synthesis in acidocalcisomes and phosphate release by the transporter Pho91 is also found in *Saccharomyces cerevisiae*, revealing a conserved mechanism of phosphate homeostasis regulation. We also investigated enzymes involved in control of polyP outside acidocalcisomes. Our research led to the identification and characterization of the polyphosphatase activity of two nudix hydrolases TbNH2 and TbNH4. TbNH2 was detected in glycosomes and TbNH4 in cytosol of the parasites. Current results suggest that nudix hydrolases may help control polyP levels in glycosomes and cytosol.

INDEX WORDS: Acidocalcisomes, Inositol phosphate, Inositol pyrophosphate, *Trypanosoma brucei*, *Saccaromices cerevisiae*, Phosphate transporter, SPX domain, Nudix hydrolases, Polyphosphate

INOSITOL PHOSPHATES REGULATE PHOSPHATE STORAGE IN ACIDOCALCISOMES OF *TRYPANOSOMA BRUCEI*

by

CIRO DAVI CORDEIRO

B.S., Universidade de Brasília, Brazil, 2009

M.S., Universidade de Brasília, Brazil, 2011

A Dissertation Submitted to the Graduate Faculty of The University of Georgia in Partial Fulfillment of the Requirements for the Degree

DOCTOR OF PHILOSOPHY.

ATHENS, GEORGIA

2018

INOSITOL PHOSPHATES REGULATE PHOSPHATE STORAGE IN ACIDOCALCISOMES OF *TRYPANOSOMA BRUCEI*

by

CIRO DAVI CORDEIRO

Major Professor: Roberto Docampo

Committee: Robert S. Sabatini
Ronald Drew Etheridge
Vasant Muralidharan

Electronic Version Approved:

Suzanne Barbour
Dean of the Graduate School
The University of Georgia
August 2018

DEDICATION

To my parents Eudes Davi Cordeiro and Olímpia Valda de Souza Cordeiro who made notable efforts to give my siblings and I the basic education and English skills we needed to succeed in our careers. Though they missed me, they still always encouraged me and unconditionally supported my decisions.

ACKNOWLEDGEMENTS

This work was only made possible by a collaboration of many young and experienced scientists. First, I would like to thank my advisor, Roberto Docampo, for dedicating so much of his time to my training during the last six years. Roberto is a knowledgeable scientist and devoted mentor. He continued to keep my best interest in mind, encouraging me to pursue many scholarship and collaboration opportunities and providing strong support during challenging times. I am thankful for his mentorship and look forward to keeping in contact with him for years to come.

I likewise would like to thank Adolfo Saiardi, my mentor during the summers of 2013 and 2014 at the University College London. Adolfo was a key collaborator for our study of inositol phosphates and I had a productive time working with him at his lab.

I thank all members of Docampo lab and Moreno lab who shared the last six years of lab work and made my experience at University of Georgia enjoyable and unforgettable. The lab colleagues, A. J. Stasic, Abigail Calixto, Beejan Asady, Brian Windle, Brian Mantilla, Catherine Li, Christina Moore, Evgeniy Potapenko, Guozhong Huang, Eric Dykes, Karla Marie Márquez-Nogueras, Manuel Fierro, Melina Galizzi, Melissa Storey, Michael Ahmed, Myriam Andrea Hortua-Triana, Nuria Nugrao, Nathan Chasen, Noelia Lander, Raquel Negreiros, Sayantanee Niyogi, Silvia Moreno, Srinivasan Ramakrishnan, Stephen Vella, Teresa Bustos and Zhu-hong Li, taught me important lessons all along the way and helped me solve my daily science challenges. I wouldn't have made it without them. Additionally, Beejan, Melissa and Melina

were lab managers during my time at UGA and I want to thank them for doing amazing work in helping maintain a productive work environment for all of us.

Some colleagues deserve a special acknowledgement for being directly involved in our work. Noelia first trained me when I arrived and helped with cloning experiments at the very beginning. Brian Windle and Michael Ahmed were undergraduate trainees who dedicated avidly to learning and helping with experiments with the Nudix hydrolases characterization. Evgeniy Potapenko invited me to participate in the work on Pho91 transporter, which led to a successful collaboration. Evgeniy is a skilled electrophysiologist who performed patch-clamp experiments on yeast vacuoles. Melissa Storey participated in the study of the Pho91 transporter by helping with experimental design, generating knockout cell lines and immunofluorescence of acidocalcisomes. She was also helpful for my learning of new idiomatic English expressions and the Southern accent. Additionally, Dr. James Umen and Yu Liu from Donald Danforth Plant Science Center in Saint Louis (MO) performed the mass spectrometry experiment with our samples that allowed us to detect IP_7 from *T. brucei* for the first time.

I gratefully thank my family for all the support and endless love. My father and mother always believed in my potential and encouraged me to pursue higher education. My brother, Bernardo, and sisters, Carolina and Talita, always provided valuable advices and ideas and it has been a pleasure to share our experiences. My fiancé, Emily, and my friend, Diego, were my family in Athens, providing English writing assistance, cooking tips, and extra support and motivation when I needed it.

TABLE OF CONTENTS

Page

LIST OF TABLES

Page

LIST OF FIGURES

Page

CHAPTER 1

INTRODUCTION AND LITERATURE REVIEW

Trypanosoma brucei

Trypanosomes are unicellular protozoan parasites that belong to the class Kinetoplastida. Trypanosomes have evolved the ability to infect a wide variety of hosts, which makes them an interesting model to understand parasitism at a cell and molecular level. The study of the basic biology of Trypanosomes has vital medical relevance and therefore can lead to discoveries that may directly impact many aspects of the disease, such as finding new drug targets, diagnostic tools, preventing transmission and vaccine development. Additionally, advancements on the understanding of Trypanosomes unique cells may shine light on the cell biology of other protozoa that are distant from more mainstream cell models. Another benefit of parasite cell biology is that it may help uncover new findings on the human host's physiology and cell biology. In this work we studied two topics that are important for polyP and phosphate homeostasis of *T. brucei*: The inositol phosphate pathway and Nudix hydrolases.

Trypanosoma brucei can infect several mammalian hosts: humans, domestic animals and wild animals, all of which can act as reservoirs of the disease. Inside the mammalian host, the parasites live mainly in the bloodstream and it is referred to as bloodstream trypomastigote form (BSF). When the mammalian host gets bitten by flies from the Glossina genus (tsetse fly), the parasite is ingested with blood and differentiates into the procyclic form (PCF) that replicates inside the midgut of the insect host. The parasite then differentiates to mesocyclic

trypomastigotes and later epimastigotes that will migrate to salivary glands, where they finally differentiate to metacyclic trypomastigotes. The next time the fly has a blood meal, the parasite will be injected with saliva and infect a new mammalian host again (Franco, Simarro et al. 2014).

Currently, *T. brucei* is only naturally transmitted in sub-Saharan Africa. The human disease is called African trypanosomiasis or sleeping sickness and it is caused by two sub-species called *T. brucei gambiense* and *T. brucei rhodesiense*. There was a rise in total cases during the decade of 1990 with a peak of almost 40,000 cases annually. Since then the number of cases have been reducing gradually and WHO estimated in 2012 less than 10,000 new cases per year. However, 57 million people still live in areas of risk of transmission of *T. b. gambiense* and 12.3 million live in endemic areas for *T. b. rhodesiense*. The people more exposed to the tsetse fly are in rural areas, with less access to treatment and information. Sleeping sickness leads to death if untreated (Franco, Simarro et al. 2014).

Animal African trypanosomiasis is called Nagana, which means powerless or useless in Zulu and it is caused by *T. congolense, T. vivax, T. brucei* spp. Nagana makes domestic animals progressively weaker and ultimately unfit for work, which impacts significantly the livestock production of endemic areas. Although it is not fatal, Nagana induces substantial weight loss creating an economic barrier for development and food production (Steverding 2008). Additionally, wild animal infection may be a reservoir of trypanosomes that infect humans (Njiokou, Laveissiere et al. 2006). *T. brucei brucei* only infects animals and is commonly used as a lab model for Trypanosomes, so we chose this organism for our study.

Phosphate and polyphosphates

One of the indispensable elements to life as we know it is phosphorous, which is mostly found combined with oxygen on the form of phosphate. Phosphate is required to build vital macromolecules like DNA, RNA and phospholipids. It can form a polymer of inorganic orthophosphate bound by phospho-anhydride bonds named polyphosphate (PolyP). PolyP has been found in bacteria, protists, animals and fungi (Rao, Gomez-Garcia et al. 2009). The majority of polyP is synthesized from ATP. Bacteria can synthesize ATP from polyP (Rao, Gomez-Garcia et al. 2009), but such a reaction has not been found in eukaryotes. Cellular energy state is suggested to be the result of an equilibrium between inorganic phosphate, ATP and polyP. In yeast, for example, polyP constitutes about 50% of total phosphate content of the cell, and at least 90% of this polyP is stored in the vacuoles (Freimoser, Hurlimann et al. 2006). Cells use a lot of energy to produce this much polyphosphate, so it is reasonable to conclude that polyP must be extremely important for those cells. The universal use of energy from phospho-anhydride bonds (e.g. nucleoside triphosphates) by living organisms highlights how important phosphate and polyP have been for the evolution of life on Earth (Piast and Wieczorek 2017). Cells need to manage phosphate concentration since it also can be a limiting nutrient. Adequate phosphate balance is crucial for preserving basic cellular functions as energy metabolism, nucleotides synthesis and cell signaling. For this purpose, polyP is an important reserve of phosphate commonly used by bacteria, protozoa and fungi. Understanding the processes that regulate polyP/phosphate homeostasis may help reveal interesting aspects of cell biology.

A screen for genes that affect polyP metabolism in yeast found genes involved in very diverse cellular processes and localized to different cellular compartments, a suggestion that polyP may be involved in pathways other than phosphate storage (Freimoser, Hurlimann et al.

2006). Some of the known polyP functions are: structural function as part of the cell wall in some fungi and algae (Werner, Amrhein et al. 2007, Werner, Amrhein et al. 2007); signaling properties, polyP secreted by human platelets can induce blood clotting (Smith, Mutch et al. 2006); polyP has been found to act as a chaperone in bacteria, preventing protein denaturation induced by various stresses (Gray, Wholey et al. 2014); polyP increase biofilm formation in bacteria (Cremers, Knoefler et al. 2016); polyP can be covalently attached to PASK domain of proteins, generating a new post-translational modification called polyphosphorylation, which has been observed to regulate protein activity (Azevedo, Livermore et al. 2015). Several proteins involved in ribosome biogenesis have been identified as polyphosphorylated in yeast. Interestingly, expression of bacterial polyphosphate kinase (EcPPK1) in human cells resulted in polyphosphorylation of ribosome related genes. This finding highlights a potential conserved mechanism of regulation by protein polyphosphorylation. Hundreds of proteins containing PASK domain from various organisms are yet to be characterized (Bentley-DeSousa, Holinier et al. 2018). *S. cerevisiae* vacuolar transporter chaperone 4 (VTC4) knockout (KO), which produces no polyP, stores less magnesium in vacuoles resulting in lower tolerance to survive when transferred to low magnesium conditions (Klompmaker, Kohl et al. 2017). Polyphosphate of long and short chain has been observed binding bacteria ribosomes *in vitro* and the function of this interaction is unknown. Evidence by *in vitro* translation tests suggest polyP addition improves translation fidelity (McInerney, Mizutani et al. 2006). *T. cruzi* increases polyP production during hyperosmotic stress and degrades polyP upon hyposmotic shock. The changes were observed using two different purification methods that allow quantification of short-chain and long-chain polyP (Ruiz, Rodrigues et al. 2001). Additionally, overexpression of TcVSP (acidocalcisomal Vacuolar Soluble Pyrophosphatase) leads to reduction in polyP, reduced

response to hyperosmotic stress and impaired ability to infect the host (Galizzi, Bustamante et al. 2013). Likewise, *T. brucei* cells deprived of VTC4, the acidocalcisome polyP synthase, have less short chain polyP, reduced capability to regulate cell volume during hyper and hypoosmotic shock and its virulence is seriously compromised (Lander, Ulrich et al. 2013).

In this study we aim at exploring pathways that are important for phosphate homeostasis in *Trypanosoma brucei*. First, we decided to characterize the inositol phosphate pathway and how it helps control phosphate homeostasis in eukaryotic cells via synthesis of polyphosphate and release of phosphate from stores. Then we shifted to studying Nudix phosphatases that may participate in various signaling events and help balance polyphosphate levels.

Acidocalcisomes and the yeast vacuole

Acidocalcisomes were first described in *Trypanosoma brucei* (Vercesi, Moreno et al. 1994) and *T. cruzi* (Docampo, Scott et al. 1995). They are acidic compartments that accumulate phosphate, polyphosphate, basic amino acids, calcium, zinc, magnesium and other cations (Docampo and Moreno 2011). Further analysis revealed that acidocalcisomes from Trypanosomes are very similar in composition to volutin granules, also known as polyphosphate bodies. Volutin granules have been observed in bacteria, archaea, protist and algae. Like acidocalcisomes from Trypanosomes, they have a membrane, H^+-PPase and store calcium, polyphosphate and metal ions. The distribution of acidocalcisome-like organelles across various domains of life suggests that they appeared early on evolution of cells and they are one of the most conserved organelles with membrane (Seufferheld, Kim et al. 2011).

The number of acidocalcisomes and quantity of elements per cell varies among species. Additionally, analysis of cell volume shows that acidocalcisomes occupy around 1-4% of cell

volume in different trypanosomatids, and cells with less acidocalcisomes tend to have larger ones (Miranda, Docampo et al. 2004). Acidocalcisomes from *T. brucei* have a V-H^+-ATPase and a V-H^+-PPase that generate the proton gradient; calcium gradient is maintained by a Ca^{2+}-ATPase and a calcium exchanger Ca^{2+}/H^+. Other cation exchangers are common, such as Na^+/H^+, Vacuolar Iron Transporter (VIT), zinc transporter (ZnT) (Docampo and Huang 2016). Ca^{2+} can be released by inositol 1,4,5-trisphosphate receptor (IP3R), a feature so far only found in acidocalcisomes from *T. brucei* (Huang, Bartlett et al. 2013) and *T. cruzi* (Lander, Chiurillo et al. 2016). Phosphate is transported inside by the Vacuolar Transporter Chaperone (VTC) Complex, a membrane protein that uses cytosolic ATP to produce polyP that is released inside the lumen. VTC complex has two identified subunits: Vtc1 and Vtc4. Depletion of VTC4 subunit results in reduced short chain polyP synthesis, reduced acidocalcisome numbers, lower growth rate, less resistance to osmotic stress and severe loss of infectivity (Lander, Ulrich et al. 2013, Ulrich, Lander et al. 2014). Depletion of VTC1 also lead to less polyP, less acidocalcisomes and impaired growth (Fang, Rohloff et al. 2007). In the lumen, the Vacuolar Soluble Pyrophosphatase (VSP) can degrade pyrophosphate and polyP into orthophosphate (Galizzi, Bustamante et al. 2013), which probably is released to the cytosol by the uncharacterized phosphate transporter Pho91 (TbPho91) (Huang, Ulrich et al. 2014).

The *Saccharomyces cerevisiae* vacuole is known as a model of the mammalian lysosome, but it also shares traits with acidocalcisomes (e.g. acidic pH, high polyphosphate content, basic amino acids and cations storage) and many orthologs of pumps and transporters (e.g. V-H^+-ATPase, Ca^{2+}-ATPase, Ca^{2+}-exchanger, ZnT) (Docampo and Huang 2016). Unlike acidocalcisomes, vacuoles are large organelles that occupy larger cell volume. Still, the composition is similar, with basic amino acids, polyP, calcium, zinc, iron, and other metal ions.

Vacuoles evolved many functions: protein degradation, detoxification of cytosol, calcium signaling, metabolite storage and resistance to various stresses like osmotic shock and nutrient deprivation (Li and Kane 2009). The yeast vacuole shares phosphate homeostasis homolog proteins with *T. brucei* acidocalcisomes. The VTC complex and the phosphate transporter Pho91 are found in both organelles (Docampo and Huang 2016). Both proteins from the VTC complex and the Pho91 contain an N-terminal SPX domain. This suggests that the phosphate mechanisms regulated by these organelles may have been conserved.

The yeast Pho91 is a transporter that apparently releases phosphate from the vacuole stores to the cytosol. The *T. brucei* TbPho91 ortholog contains 9 transmembrane domains. It was found in a proteome study of the acidocalcisome and its localization was validated by endogenous C-terminal tagging (Huang, Ulrich et al. 2014). In *T. cruzi*, TcPho91 was found in the contractile vacuole and not in acidocalcisomes (Jimenez and Docampo 2015). The acidocalcisome in this organism was observed fusing with the contractile vacuole, which shows a mechanism to release phosphate content from acidocalcisomes (Niyogi, Jimenez et al. 2015).

Inositol phosphates and inositol pyrophosphates

Inositol is a stable sugar-like six carbon molecule synthesized from glucose in archea and eukayotes. Myo-inositol is the most common stereoisomer used by cells to build signaling molecules by adding phosphate or lipids, which generate soluble inositol phosphates (IP) and phophatidylinositols (PI), respectively. Phosphoinositides can be phosphorylated generating phosphatidylinositol phosphates (PIPs). IPs are originated from hydrolysis of phosphatidylinositol 4,5-bisphosphate ($PI(4,5)P_2$), a common phosphoinositide in the plasma membrane, by the phospholipase C, which generates inositol 1,4,5-triphosphate (IP_3) and

diacylglycerol. IP_3 is phosphorylated to produce higher phosphorylated inositol phosphates. IPs and PIP pathways and signaling are widely distributed among eukaryotes (Saiardi 2017). Inositol pyrophosphates (InsPP) are generated when a pyrophospho-anhydride bond is created by phosphorylation. For example, when inositol 1,3,4,5,6-pentakisphosphate (IP_5) and Inositol hexakisphosphate (IP_6) are phosphorylated by IP6K, they generate 5-diphospho-inositol 1,4,5,6-tetrakisphosphate (5PP-IP_4) and 5-diphospho-inositol 1,2,4,5,6-pentakisphosphate (5PP-IP_5 or IP_7) respectively (Wilson, Livermore et al. 2013).

The known inositol phosphate kinases comprise the most studied pathway for inositol phosphate synthesis. However, there are few reports of an alternative pathway for IP_3 synthesis that is independent from phospholipase C, in *Dictyostelium discoideum* (Van Dijken, de Haas et al. 1995, Van Dijken, Bergsma et al. 1997). Furthermore, there is also in vitro evidence of a IP_6 generation from inositol by stepwise phosphorylation (Stephens and Irvine 1990). Still, the enzymes involved in this pathway are not known and there are no other further studies of PLC-independent synthesis of IPs and its relevance to eukaryotic cells.

Inositol pyrophosphate synthesis pathway

The pathway for conversion of I(1,4,5)P_3 to IP_7 is conserved among eukaryotes. The I(1,4,5)P_3 released by PLC is phosphorylated by Inositol Polyphosphate Multikinase (IPMK) to form I(1,3,4,5)P_4, which is phosphorylated again by the same enzyme into I(1,3,4,5,6)P_5. It was found that in mammalian cells this enzyme can also further phosphorylate I(1,3,4,5,6)P_5 to produce 5PP-I(1,3,4,5,6)P_4 (Saiardi, Nagata et al. 2001). Human IPMK can also phosphorylate PI(4,5)P_2 to make PI(3,4,5)P_3 (PI3K activity) (Resnick, Snowman et al. 2005). Inositol Pentakisphosphate Kinase (IP5K) is the only known kinase that phosphorylates position 2-

hydroxy of I(1,3,4,5,6)P_5 to produce IP_6. The next on the pathway is the Inositol Hexakisphosphate Kinase (IP6K) that produces inositol pyrophophosphates by phosphorylating phosphate 5 of I(1,3,4,5,6)P_5 or IP_6, generating 5PP-I(1,3,4,5,6)P_4 and 5PP-I(1,2,3,4,6)P_5 (5-IP_7) respectively. Another kinase named PPIP5K (mammalian) or Vip (yeast) can phosphorylate phosphate 1 of IP_6 or IP_7, generating 1PP-I(2,3,4,5,6)P_5 (1-IP_7) and 1,5$(PP)_2$-I(2,3,4,6)P_4 (1,5-IP_8), respectively (Thota and Bhandari 2015) (Figure 2.1).

There are reports of IP6K enzymatic reverse transfer of phosphate from 5-IP_7 and IP_6 to ADP forming ATP (Voglmaier, Bembenek et al. 1996, Wundenberg, Grabinski et al. 2014). It is not clear what is the role of this phosphate transfer to the energy metabolism in the cells, the amount of ATP generated is insignificant compared to the amount generated by glycolysis and oxidative phosphorylation. This was detected only *in vitro*, and it is likely that it consists of a signaling event that is regulated by ATP/ADP ratio (Wundenberg, Grabinski et al. 2014).

In yeast, two types of phosphatases that hydrolyze pyrophospho-anhydride bonds of InsPP have been discovered: Ddp1 (Nudix hydrolase) and Siw14 (Tyrosine phosphatase-like). Ddp1 has been characterized as 1-IP_7 to IP_6 and 1,5-IP_8 to 5-IP_7 degrading enzyme (Lonetti, Szijgyarto et al. 2011). Siw14 was characterized in yeast as the enzyme that remove β-phosphate from 5-IP_7 and 1,5-IP_8 making IP_6 and 1-IP_7 respectively (Steidle, Chong et al. 2016).

We searched the genome *T. brucei* and we found one ortholog of IPMK, IP5k and IP6K. There are no orthologs of other known inositol phosphate kinases. *T. brucei* also has five Nudix hydrolases and a couple of Tyrosine phosphatase-like that could be involved in InsPP signaling.

Inositol Pyrophosphates Signaling

Although the concentration of InsPP is lower than that of IPs, its effects are significant for various pathways and essential for many cell types. InsPP have been described as signaling molecules. InsPP have been found as energy sensors in some cells. IPMK, IP5K, PPIP5K have a low Km range for ATP comparing to IP6K which has a Km between 1 and 1.4 mM. Therefore, IP6K is extremely sensitive to fluctuations in ATP concentration (Thota and Bhandari 2015). Treatment of cell lysates and intact mammalian cells with fluoride, which inhibits InsPP phosphatases, leads to fast accumulation of InsPP. The current understanding of InsPP signaling is that following synthesis by kinases there is a rapid reduction in InsPP by specific phosphatases, restoring their basal levels. This phenomenon was described as a rapid turnover of InsPP (Glennon and Shears 1993, Menniti, Miller et al. 1993), which suggests there is tight control of InsPP concentration.

There are two mechanisms of InsPP signaling: binding to targets and phosphate transfer. Binding regulation can be through competition for a specific protein domain or allosteric interaction. The former has been observed in competitive binding of IP_7 to Pleckstrin Homology (PH) domain of Akt, which normally binds PIP_3, regulating its activity (Pavlovic, Thakor et al. 2016). Allosteric interaction was detected by observation of crystal structure of the SPX domain of VTC4 with IP_6 bound to its positive-charged surface. Functional experiments revealed that 5-IP7 is an effector that binds the allosteric site on the SPX domain and stimulate VTC complex activity with 1000 fold higher affinity than IP_6 (Wild, Gerasimaite et al. 2016). The second mode of action, phosphate transfer to proteins, has been reported for inositol pyrophosphate 5-IP_7, which can transfer a phosphate from its high energy phosphoanhydride bond to a phosphorylated serine generating protein pyrophosphorylation (Bhandari, Saiardi et al. 2007, Saiardi 2016). For

example, the β sub-unit of adaptor protein complex AP-3 was found to be pyrophosphorylated by IP_7, resulting in change in the protein interaction with its binding partner Kif3A (Azevedo, Burton et al. 2009). Also, *in vitro* experiments showed yeast RNA Polymerase I is pyrophosphorylated by IP_7. In the absence of Kcs1-generated 5-IP_7, the RNA Pol I activity is reduced resulting in less ribosomal RNA synthesis and global protein translation (Thota, Unnikannan et al. 2015). In addition, several other pyrophosphorylated yeast proteins have been identified (Szijgyarto, Garedew et al. 2011, Wu, Chong et al. 2016).

Protein domains that interact with inositol phosphates

IP3R

The inositol phosphates second messenger role gained attention when IP_3-induced calcium release from intracellular stores was first reported in 1983 (Streb, Irvine et al. 1983). A few years later, the channel that is responsible for calcium release was identified and named IP_3-Receptor (IP3R) (Ross, Meldolesi et al. 1989). Interestingly, *T. brucei* and *T. cruzi* have a functional IP3R that is located on the acidocalcisome membrane and not on the ER as do mammals and other model organisms (Huang, Bartlett et al. 2013) (Lander, Chiurillo et al. 2016).

PH domains

Pleckstrin Homology Domains (PH domains) are commonly found in eukaryotic proteins and perform various functions, including mediating protein-protein interaction (Scheffzek and Welti 2012). PH domains can bind to inositol phosphates and phosphoinositides to regulate protein activity and signal transduction. For example, IP_7 is an inhibitor of the kinase known as Akt, which is important for numerous cellular processes. IP_7 binds the PH domain of Akt with

high affinity (IC_{50} is 20 nM) preventing its phosphorylation and activation, even in the presence of 1 µM PIP_3 (IC_{50} is 35 nM), an Akt activator (Chakraborty, Koldobskiy et al. 2010). Furthermore, it was observed that when IP_7 binds to the PH domain it induces Akt translocation from the membrane to the cytoplasm (Pavlovic, Thakor et al. 2016). *T. brucei* has 29 proteins annotated as containing PH-domains (Tritryp.org), but the interaction with inositol phosphates or phosphoinositides has not yet been studied.

The SPX Domain

The SPX domain was initially identified in yeast. It was named after three proteins: Syg1, Pho81 and the human Xpr1. It is found at the N-terminus of proteins with a sequence of about 300 amino acids long, containing three conserved sub-domains of about 30 amino acids separated by variable regions. SPX has been considered a phosphate sensor domain because it is found in genes associated with Pi homeostasis (Secco, Wang et al. 2012). In yeast, 1PP-IP_5 (generated by Vip1) binds the N-terminal segment of Pho81, which contains an SPX domain. 5PP-IP_5 generated by Kcs1 (IP6K) did not bind Pho81, showing its specificity for one IP_7 isomer (Lee, Huang et al. 2008). Likewise, the yeast VTC complex has specificity for different IP_7 or IP_8 isomers. 1PP-IP_5 and 5PP-IP_5 generated by Vip1 and Kcs1 have a similar capacity to induce polyP synthesis by this complex, whereas IP_6 has negligible effect under physiological conditions (Gerasimaite, Pavlovic et al. 2017). The crystal structure of the SPX domain from yeast VTC4 revealed a strong interaction with IP_6, which was used for generating crystals since it is more stable and abundant than IP_7 or IP_8. Point mutations on conserved residues important for binding with phosphate groups from IPs resulted in suppression of IP_7 ability to stimulate polyP synthesis (Wild, Gerasimaite et al. 2016). Additionally, ΔKcs1 leads to reduction in polyP synthesis whereas Vip1Δ has no significant changes in polyP content (Lonetti, Szijgyarto et al.

2011, Gerasimaite, Pavlovic et al. 2017), which indicates that Kcs1 activity is more relevant for polyP synthesis. *Ipk1Δ* generates an increase in polyphosphate, confirming IP_6 does not stimulate polyP synthesis in vacuole. *Ipk1Δ* shows elevated synthesis of PP-IP_4 (also capable of stimulating VTC activity) that would explain the higher polyP content of those cells (Lonetti, Szijgyarto et al. 2011).

In *T. brucei* there are only three proteins containing SPX domain. Two are the acidocalcisomal proteins TbVtc4 and TbPho91 (Huang, Ulrich et al. 2014). The other is a ribose-phosphate pyrophosphokinase, a protein that has not yet been studied in trypanosomes.

Relevance of the inositol pyrophosphate synthesis pathway

The genes that produce IPs are widely distributed in eukaryotes, suggestive of the ancient origin of inositol signaling. A large number of cellular functions have been associated with inositol pyrophosphates. Cell growth, stress response, DNA repair, vesicular trafficking, cell cycle regulation, phosphate homeostasis, energy metabolism, ribosome biogenesis, chromatin remodeling and autophagy (Thota and Bhandari 2015).

IP6K deletion in the pathogenic yeast *Cryptococcus neoformans* results in cell wall defects, lower ability to grow in non-fermentable carbon sources, impaired mitochondria activity, and lower pathogenicity (Lev, Li et al. 2015). However, IP5K depletion (mutants without IP_6 synthesis) does not affect growth or stress survival to the same level as IP6K depletion. Infection in mice demonstrated that IP6K, and not IP5K, is required for virulence of *C. neoformans* (Li, Lev et al. 2016).

The most abundant inositol phosphate IP_6 can range at concentrations of 10-60 µM in mammalian cells, while IP_7 range from 500 nM to 1.3 µM (Wilson, Livermore et al. 2013). The

yeast and mammalian IP6K have low affinity for ATP (Km ~ 1mM), close to the physiological ATP concentration, resulting in direct fluctuation of IP6K activity according to ATP levels (Thota and Bhandari 2015). Yeast knockout of Kcs1 (IP6K), but not Vip1, display elevated ATP, increased glycolysis and reduced mitochondrial activity. Synthesis of 5-IP7 is required for yeast growth in non-fermentable carbon sources. One of the mechanisms for this regulation is by pyrophosphorylation of the transcription factor GCR1, which participates in transcription control of glycolytic genes. Interestingly, $IP6K^{-/-}$ mouse fibroblasts show the same phenotype of high ATP and reduced mitochondrial activity (Szijgyarto, Garedew et al. 2011). These observations suggest that 5-IP_7 synthesis by IP6K help govern cellular ATP levels.

Knockout of yeast Kcs1 (IP6K) leads to numerous other phenotypes: lower growth; stress sensitivity; impaired DNA recombination; decreased endocytic membrane trafficking; reduced polyphosphate quantity; small fragmented vacuoles; increase in glycolysis and reduced ATP synthesis by electron transport chain (Thota and Bhandari 2015). Inositol phosphate has been associated with telomere stability in yeast, but the mechanism has not yet been proposed (Thota and Bhandari 2015). Additionally, Inositol Phosphates and Inositol Pyrophosphates affect prion spread in yeast (Wickner, Kelly et al. 2017). Remarkably, it is puzzling how the same signaling molecules produced by IP6K (5-IP_7 and 1,5-IP_8) directly regulate all these cellular functions. Some of the reported observations may be downstream effects of alterations on other cellular process. For example, polyphosphate synthesis is ablated in Kcs1 knockout. Interestingly, recent screen for polyphosphorylated proteins found several yeast proteins that are important for ribosome function and biogenesis. Lack of polyphosphate lead to ribosomal assembly defects (Bentley-DeSousa, Holinier et al. 2018), which lead us to believe that ribosomal phenotypes

observed in Kcs1 may stem from lack of polyphosphate and not only for direct regulation of ribosomal assembly by 5-IP_7.

One approach used to investigate processes affected by IPs or InsPPs was to detect binding partners by mass spectrometry. Pyrophosphorylation only happens in presence of Mg^{2+}, so the pulldown of proteins interacting with 5-IP_7 was performed with and without Mg^{2+} to differentiate targets that are pyrophosphorylated from targets regulated by binding. The researchers tested yeast lysates and found many proteins that belong to processes associated with ribosome biogenesis. Differently, the binding partners of 5-IP_7, without Mg^{2+}, were more diverse including phosphoproteins involved in signaling pathways, purine nucleotide synthesis, regulation of translation, polyphosphate synthesis, carbohydrate metabolism, tRNA aminoacylation and regulation of cellular pH (Wu, Chong et al. 2016).

Conditional Knockout of TbIPMK in *T. brucei* arrests replication 24h after gene repression and leads to all culture collapse in 4 days, therefore IP synthesis is essential. TbIPMK depletion did not affect the number of telomeric foci (Cestari and Stuart 2015). Unlike mammalian IPMK, TbIPMK does not have PI3K activity on PI(4,5)P_2 or other PIPs substrates (Cestari, Haas et al. 2016). PI3K activity of IPMK is crucial for some of the phenotypes related to nuclear signaling, gene expression and mRNA export observed in mammalian cells (Wickramasinghe, Savill et al. 2013). This suggests that TbIPMK role in *T. brucei* is different than what has been proposed in mammalian cells, and synthesis of I(1,3,4,5)P_4 and I(1,3,4,5,6)P_5, subsequently converted to other IPs and InsPP, may be most important catalytic activity of this enzyme.

Nudix Hydrolases

Nudix Hydrolases belong to a large family of diverse proteins found in archaea, bacteria, eukaryotes and viruses that can degrade a wide range of organic pyrophosphates, such as nucleoside di- and triphosphates, nucleotide sugars, NAD(P)H and guanosine-3',5'-tetraphosphate (ppGpp) (McLennan 2006). It was discovered that the human Nudix DIPP can cleave inositol pyrophosphates (Safrany, Caffrey et al. 1998), which are important regulators of energy metabolism (Szijgyarto, Garedew et al. 2011). Interestingly, *in vitro* assays identified the same human DIPP and its yeast ortholog as a highly active polyphosphatases (Lonetti, Szijgyarto et al. 2011). Many of the Nudix identified substrates are involved in energy metabolism and regulation of phosphate rich compounds, therefore it is believed that Nudix are important for cellular energy dynamics.

There is little information on enzymes that can degrade polyP (polyphosphatases) from trypanosomes. In *Trypanosoma brucei*, two exopolyphosphatases have been characterized: TbPPX1 (Luginbuehl, Kunz et al. 2011) and TbVSP1 (Lemercier, Espiau et al. 2004). There is no endopolyphosphatase identified, although one homolog of yeast PPN1 is in the genome of *T. brucei*. In contrast, *S. cerevisiae* has four known polyphosphatases: ScPPX (YHR201C), ScPPN1 (YDR452W), ScPPN2 (YNL217W) and Ddp1 (YOR163W). All yeast polyphosphatases, except ScPPX, are endopolyphosphatases. PolyP levels are not only regulated by synthesis but also by degradation. In bacteria, a balance between production and hydrolysis by PPX are crucial for maintaining polyP levels (Gray, Wholey et al. 2014), and, in yeast, vacuolar endopolyphosphatases activity is required for normal polyP degradation and turnover (Gerasimaite and Mayer 2017). We aim to find new polyphosphatases that may regulate polyP in *T. brucei*. *Trypanosoma brucei* has five Nudix proteins identified, and their possible function as

regulators of polyP and InsPP have not been explored. The characterization of Nudix hydrolases activity found in different compartments provides new insight on this family of enzymes.

CHAPTER 2

THE INOSITOL PYROPHOSPHATE SYNTHESIS PATHWAY IN *TRYPANOSOMA BRUCEI* IS LINKED TO POLYPHOSPHATE SYNTHESIS IN ACIDOCALCISOMES

Cordeiro, C. D., A. Saiardi and R. Docampo (2017). "The inositol pyrophosphate synthesis pathway in Trypanosoma brucei is linked to polyphosphate synthesis in acidocalcisomes." Mol Microbiol **106**(2): 319-333.
Reprinted with permission of the publisher.

Introduction

Myo-inositol is an essential precursor for the synthesis of soluble inositol phosphates (IPs) and lipid-bound inositols called phosphoinositides (PIPs) (Irvine and Schell 2001). After inositol incorporation into the lipid phosphatidylinositol (PI), the inositol ring is phosphorylated to PIPs such as phosphatidylinositol 4,5-bisphosphate (PIP_2) through the action of a phosphatidylinositol phosphate (PIP) kinase. PIP_2 is cleaved by a phosphoinositide phospholipase C (PI-PLC) (Cocco, Follo et al. 2015) to inositol 1,4,5-trisphosphate (IP_3) (Figure 2.1) and 1,2-diacylglycerol (DAG), which are important second messengers. While DAG stimulates a protein kinase C (Nishizuka 1986), IP_3 stimulates an IP_3 receptor to release Ca^{2+} from intracellular stores (Berridge 2009) and can be further metabolized to other soluble IPs by several kinases and phosphatases.

The inositol phosphate multikinase (IPMK) has dual 3-kinase/6-kinase activity and catalyzes the conversion of IP_3 into inositol tetrakisphosphate (IP_4) and inositol pentakisphosphate (IP_5). IP_5 is converted into inositol hexakisphosphate (IP_6), the fully phosphorylated *myo*-inositol also known as phytic acid, by the 2-kinase activity of inositol pentakisphosphate kinase (IP5K, or IPPK). Further phosphorylation of IP_6 by the inositol hexakisphosphate kinase (IP_6 kinase or IP6K) results in the production of diphosphoinositol polyphosphates (PP-IPs), also known as inositol pyrophosphates. These are IPs characterized by containing one or more high-energy pyrophosphate moiety. PP-IPs were discovered in the early 1990's, in *Dictyostelium discoideum* (Europe-Finner, Gammon et al. 1991, Mayr GW 1992, Stephens, Radenberg et al. 1993), *Entamoeba histolytica* (Martin, Bakker-Grunwald et al. 1993), and in mammalian cells (Menniti, Miller et al. 1993). The best-characterized member of this class is 5-diphosphoinositol pentakisphosphate (5-PP-P_5 or IP_7), which has five of the *myo*-

inositol hydroxyls monophosphorylated, while the sixth, at the 5-position, contains a pyrophosphate group (Albert, Safrany et al. 1997). The IP6K can also metabolize IP_5 to disphosphoinositol tetrakisphosphate (PP-IP_4) (Saiardi, Caffrey et al. 2000, Losito, Szijgyarto et al. 2009). Another isomer of IP_7, containing a pyrophosphate at the 1-position, can also be formed by a more recently identified enzyme termed diphosphoinositol pentakisphosphate kinase (PP-IP5K), though this enzyme appears to be predominantly associated physiologically with the formation of diphosphoinositol hexakisphosphate (PP_2-IP_4 or IP_8) (Choi, Williams et al. 2007).

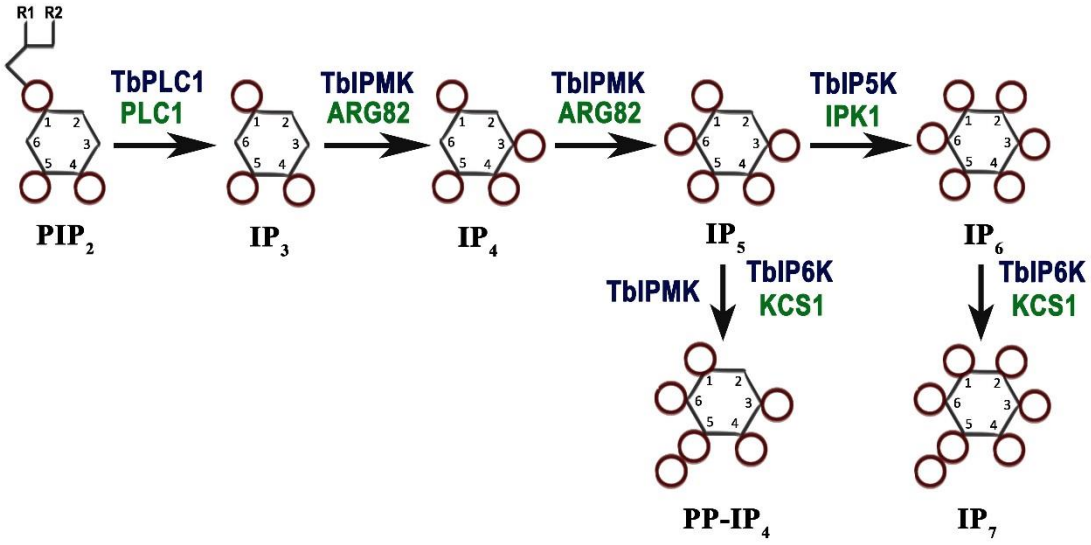

Figure 2.1. Inositol phosphate pathway in *Trypanosoma brucei*. The soluble IP pathway starts with hydrolysis of PIP_2 by TbPI-PLC1, releasing IP_3 that is phosphorylated by TbIPMK to generate IP_4 and IP_5. IP_5 is phosphorylated by TbIP5K to generate IP_6. IP_5 and IP_6 can be further phosphorylated by TbIPMK or TbIP6K to generate inositol pyrophosphates PP-IP_4 and IP_7. Names of the equivalent yeast enzymes are in green.

Among the many roles attributed to PP-IPs are the regulation of telomere length (Saiardi, Resnick et al. 2005, York, Armbruster et al. 2005), DNA repair by homologous recombination (Luo, Saiardi et al. 2002, Jadav, Chanduri et al. 2013), response to hyperosmotic stress (Pesesse, Choi et al. 2004, Choi, Williams et al. 2007), vesicle trafficking (Saiardi, Caffrey et al. 2000,

Saiardi, Sciambi et al. 2002), apoptosis (Morrison, Bauer et al. 2001, Nagata, Luo et al. 2005), autophagy (Nagata, Saiardi et al. 2010), binding of pleckstrin homology domains to phospholipids and proteins (Luo, Huang et al. 2003, Gokhale, Zaremba et al. 2013), transcription of glycolytic enzymes (Szijgyarto, Garedew et al. 2011), hemostasis (Ghosh, Shukla et al. 2013), phagocytic and bactericidal activities of neutrophils (Prasad, Jia et al. 2011), epigenetic modifications to chromatin (Burton, Azevedo et al. 2013) and exocytic insulin secretion (Illies, Gromada et al. 2007). PP-IPs may signal through allosteric interaction with proteins (i.e. binding to pleckstrin homology (PH) or other domains of proteins) or by phosphotransfer reactions (Saiardi 2012, Shears 2015, Wild, Gerasimaite et al. 2016). The phosphotransfer reaction is non-enzymatic and requires a phospho-serine residue within an acidic region and consists in adding a second phosphate to the phosphor-serine resulting in pyrophosphorylation (Saiardi 2012).

Trypanosoma brucei, which belongs to the group of parasites that causes African trypanosomiasis (sleeping sickness), possesses a PI-PLC that is stimulated by very low Ca^{2+} concentrations (King-Keller, Moore et al. 2015) and an IP_3 receptor that localizes to the acidocalcisomes instead of the endoplasmic reticulum (Huang, Bartlett et al. 2013). We now found that they also possess orthologs to IPMK, IP5K and IP6K, but do not have recognizable orthologs to PP-IP5K, inositol 1,4,5-trisphosphate 3-kinases (ITPKs) and inositol tetrakisphosphate 3-kinase 1 (ITPK1) (Table 2.1). The ortholog to IPMK (TbIPMK) was recently reported as essential for the bloodstream forms of the parasites (Cestari and Stuart 2015), suggesting that the soluble inositol phosphate pathway is essential for the parasite. The orthologs to IP5K and IP6K were not recognizable by sequence only and were wrongly annotated as a putative hypothetical protein and as inositol polyphosphate-like protein, respectively. In the

present study, we thoroughly characterized the soluble inositol phosphate pathway of *T. brucei*. We cloned, expressed and biochemically characterized the recombinant enzymes from *T. brucei*, complemented yeast mutants to demonstrate their function, analyzed their products, studied the inositol phosphate metabolism of *T. brucei* cells, and revealed the link of this pathway to the synthesis of polyphosphate in acidocalcisomes.

Experimental procedures

Chemicals and reagents

Mouse antibodies against HA were from Covance (Hollywood, FL). Inositol, myo-[1,2-^{3}H(N)] (60 Ci/mmol, ART 0261A) was from American Radiolabeled Chemicals, Inc. Goat anti-mouse antibodies were from LI-COR Biosciences (Lincoln, NE). Laemmli sample buffer was from Bio-Rad Laboratories (Hercules, CA). The bicinchoninic (BCA) protein assay kit was from Pierce (Thermo Fisher Scientific, USA). Titanium dioxide (TiO_2) beads (Titansphere ToO 5 µm) were from GL Sciences (USA). PrimeSTAR HS DNA polymerase was from Clontech Laboratories Inc. (Takara, Mountain View, CA). Vector pET32 Ek/LIC was from Novagen (Merck KGaA, Darmstadt, Germany). Acrylamide mix was from National Diagnostics (Chapel Hill, NC). CelLytic M cell lysis reagent, P8340 protease inhibitor, protease inhibitors, Benzonase Nuclease, antibody against c-Myc, inositol phosphates, and other analytical reagents were from Sigma-Aldrich (St. Louis, MO).

Table 2.1. Soluble inositol phosphate kinases identified in the human genome and orthologs from *S. cerevisiae* and *T. brucei*. Listed below the enzyme definition is the primary, but not exclusive, enzymatic reaction.

Inositol phosphate kinase	***H. sapiens*** Gene ID	***S. cerevisiae*** SGD	***T. brucei*** TriTrypDB
Inositol-trisphosphate 3-kinase $I(1,4,5)P_3$ => $I(1,3,4,5)P_4$	**ITPKA,B,C** 3706 3707 80271		
Inositol polyphosphate multikinase $I(1,4,5)P_3$ => IP_4 => $I(1,3,4,5,6)P_5$	**IPMK** 253430	**Arg82** YDR173C	**TbIPMK** Tb427tmp.211.3460
Inositol-tetrakisphosphate 1-kinase $I(1,3,4)P_3$ => IP_4 => $I(1,3,4,5,6)P_5$	**ITPK1** 3705		
Inositol pentakisphosphate 2-kinase $I(1,3,4,5,6)P_5$ => IP_6	**IPPK** 64768	**Ipk1** YDR315C	**TbIP5K** Tb427.04.1050
Inositol hexakisphosphate kinase IP_6 => 5PP-IP_5	**IP6K1,2,3** 9807 51447 117283	**Kcs1** YDR017C	**TbIP6K** Tb427.07.4400
Diphosphoinositol pentakisphosphate kinase 5PP-IP_5 => PP_2-IP_4	**PPIP5K1,2** 9677 23262	**Vip1** YLR410W	

Cell cultures

T. brucei Lister strain 427 BSF and PCF were used. The BSF were cultivated at 37ºC in HMI-9 medium (Hirumi and Hirumi 1989) supplemented with 10% heat inactivated fetal bovine serum (FBS, Sigma). The PCF were cultivated at 28ºC in SDM-79 medium (Cunningham 1977) supplemented with 10% heat-inactivated FBS and hemin (7.5 µg/ml). To determine the presence of IP_6 by PAGE analysis *T. brucei* BSF were also isolated from infected mice (Balb/c, female, 6-8 weeks old) and rats (Wistar, male retired breeders), as described previously (Cross 1975). *T. brucei IPMK* conditional knockout cell line was obtained and grown as described previously (Cestari and Stuart 2015).

Yeast strains

The yeast strains used in this study are isogenic to DDY1810 (MATa leu2-3,112 trp1-Δ901 ura3-52 prb1-1122 pep4-3 prc1-407), except for the *ipk1*□*kcs1*□ strain that is isogenic to BY4741 (MATa his3Δ1 leu2Δ0 met15Δ0 ura3Δ0) and was previously described (Saiardi, Sciambi et al. 2002). The DDY1810 protease deficient strain is often used to increase the expression of exogenous proteins upon overexpression due to a deletion on the Pep4 protease. The generation of DDY1810 *kcs1*□ strain was previously described (Onnebo and Saiardi 2009). The *arg82*□, *ipk1*□ yeast strains in the DDY1810 genetic background were generated following standard homologous recombination techniques (Gueldener, Heinisch et al. 2002) using oligonucleotides listed in Table 2.2. Initially diagnostic PCR was performed to confirm the correct integration of the deletion constructs. Subsequently, the soluble inositol polyphosphate profile of these new strains was used to phenotypically validate the correct homologous recombination event.

Epitope tagging, cloning expression and biochemical characterization of inositol phosphate kinases

We followed a one-step epitope-tagging method (Oberholzer, Morand et al. 2006) to produce the C-terminal HA- or cMyc-tagging cassettes for transfection of *T. brucei* PCF (Table 2.2). Briefly, the tagging cassettes containing selection markers were generated for cell transfection by PCR using pMOTag4H and pMOTag33M as templates with the corresponding PCR primers of the genes (Table 2.2). Transfection was performed using 2.5 x 10^7 PCF parasites from log phase. Cells were harvested at 1,000 x *g* for 10 min, washed with 10 ml of ice-cold sterile Cytomix buffer (2 mM EGTA, 3 mM $MgCl_2$, 120 mM KCl, 0.5% glucose, 0.15 mM $CaCl_2$, 0.1 mg/ml bovine serum albumin, 10 mM K_2HPO_4/KH_2PO_4, 1 mM hypoxanthine, 25 mM

Hepes, pH 7.6), centrifuged at 1,000 x *g* for 7 min, suspended in 0.5 ml Cytomix and transferred to an ice-cold 4 mm gap cuvette (Bio-Rad) containing 15 µg of PCR amplicon. Cuvettes were incubated 5 min on ice and immediately electroporated twice in Bio-Rad GenePulser Xcell^{TM} Electroporation System at 1.5 kV, 25 µF. Cuvettes were kept on ice for one minute between electroporation pulses. Cell mixture was transferred to SDM-79 medium with 15% FBS. After 6 h appropriate antibiotics were added. The sequences of the three kinases *TbIPMK, TbIP5K* and *TbIP6K* were amplified from genomic DNA by PCR (Table 2.2) using PrimeSTAR HS DNA polymerase and cloned into ligation independent expression vector pET32 Ek/LIC, as recommended by the manufacturer. Constructs were cloned into *Escherichia coli* BL21-CodonPlus(DE3) and protein expression was induced with 1 mM isopropyl β-D-1-thiogalactopyranoside **(**IPTG) in Luria Bertani broth for 3 h. Protein purification was performed using affinity chromatography HIS-Select® Cartridge, according to the manufacturer's instructions. We tested activity of the kinases on commercially available substrates. Enzyme assays were performed at 37°C using approximately 50 ng of recombinant protein, 20 mM Hepes buffer, pH 7.0, 0.2-0.5 mM substrate, 6 mM $MgCl_2$, 100 mM NaCl, 1 mM dithiotreitol (DTT), 0.5 mM ATP, 10 mM phosphocreatine, and 40 U creatine kinase. Enzymatic reactions were stopped with 3 µl of 100 mM EDTA and kept on ice or frozen until further use. Reaction products were resolved by PAGE using 35% acrylamide/bis-acrylamide 19:1 gels in Tris/Borate/EDTA (TBE) buffer as described by (Losito, Szijgyarto et al. 2009). Gels were stained with toluidine blue (Losito, Szijgyarto et al. 2009).

Table 2.2. *S. cerevisiae* strains, plasmids and primers used in this study.

Strain	Genotype	Source
DDY1810	*MATa leu2-3,112 trp1-Δ901 ura3-52 prb1-1122 pep4-3 prc1-407*	(Onnebo and Saiardi 2009)
*kcs1*Δ	DDY1810 kcs1:Leu2	(Onnebo and Saiardi 2009)
*ipk1*Δ	DDY1810 ipk1::Leu2	this study
*arg82*Δ	DDY1810 arg82::Leu2	this study
BY4741	MATa his3Δ1 leu2Δ0 met15Δ0 ura3Δ0	(Saiardi, Sciambi et al. 2002)
*Ipk1Δkcs1*Δ	BY4741 ipk1:kanMX4 kcs1:kanMX4	(Saiardi, Sciambi et al. 2002)

Plasmids	Source
pET-32 Ek/LIC	Novagen
pADH:GST	(Azevedo, Burton et al. 2009)
pMOTag4H	(Oberholzer, Morand et al. 2006)
pMOTag33M	(Oberholzer, Morand et al. 2006)

Primer	Sequence	Use
1	GACGACGACAAGATGTTAAATATTTGCCAAAAC	(fwd); cloning of *TbIPMK* in pET32
2	GAGGAGAAGCCCGGTTCATGAAAGAAGAAAAATAATT	(rev); cloning of *TbIPMK* in pET32
3	GACGACGACAAGATGTTGTCGGAAGAGGAGGCACG	(fwd); cloning of *TbIP5K* in pET32
4	GAGGAGAAGCCCGGTCTAACAATGGAACTCAGGTGCG	(rev); cloning of *TbIP5K* in pET32
5	GACGACGACAAGATGGGGGAAGAGGAGAATTTAC	(fwd); cloning of *TbIP6K* in pET32
6	GAGGAGAAGCCCGGTTATGTGAGCATGTCAAGTACA	(rev); cloning of *TbIP6K* in pET32

7	TCAGGTGACAGGCGGTTACACTTTCCT GAGGAGGTGGTTGGGTTTGTTCAAGGT TTGGAAAAAATTATTTTTCTTCTTTCAG GTACCGGGCCCCCCCTCGAG	(fwd); tagging *TbIPMK*; template pMOTag4H
8	AAAAGAGAGTGAGATCGAATAAATAT AAGACACCATGTCATACTACCAAATTT AAAACAACCGAAATACCGAAGATCGC CGGTTCTCATGGCGGCCGCTCTAGAAC TAGTGGAT	(rev); tagging *TbIPMK*; template pMOTag4H
9	CTGAGCCGCTATTTTGAGCTTGACCGT GAAGTCCTTGCAGCGTGGGAGGATTAT AAAGTTGTAAGCGCACCTGAGTTCCAT TGTGGTACCGGGCCCCCCCTCGAG	(fwd); tagging *TbIP5K*; template pMOTag4H or pMOTag33M
10	GATACACACAAACAAACAAACGAACG TTTACGCAACTTCGTCTCACATGGACTA AACCTAAAGAGGTGATCACACCCCCAC AAAAAGTGGCGGCCGCTCTAGAACTAG TGGAT	(rev); tagging *TbIP5K*; template pMOTag4H or pMOTag33M
11	AGCTGCTACGAGGTGGCGATGCAGACG CGGAACAGGATAAGGACGTGGGATAT ATTGAGGCCCTGAAAACTGTACTTGAC ATGCTCACAGGTACCGGGCCCCCCCTC GAG	(fwd); tagging *TbIP6K*; template pMOTag4H
12	TCCCGCACAAAACTCTGCTGCTTATGCT CCATTCATGCGTCCTGAAACGAACGTC CGCGATCATTTGGGAAGACACACTGTT GAAGGTATGGCGGCCGCTCTAGAACTA GTGGAT	(rev); tagging *TbIP6K*; template pMOTag4H
13	ACGCGTCGACAATGTTAAATATTTGCC AAAACTTGTCTTCCGTTG	(fwd); cloning of *TbIPMK* in pADH:GST
14	ATAAGAATGCGGCCGCTCATGAAAGAA GAAAAATAATTTTTTCCAAACCTTGAA C	(rev); cloning of *TbIPMK* in pADH:GST
15	ACGCGTCGACAATGCGCTTCCTCGGTG C	(fwd); cloning of *TbIP5K* in pADH:GST
16	ATAAGAATGCGGCCGCCTAACAATGGA ACTCAGGTGCGC	(rev); cloning of *TbIP5K* in pADH:GST
17	ACGCGTCGACAATGGGGGAAGAGGAG AATTTACGTAGAA	(fwd); cloning of *TbIP6K* in pADH:GST
18	ATAAGAATGCGGCCGCTTATGTGAGCA TGTCAAGTACAGTTTTCAGG	(rev); cloning of *TbIP6K* in pADH:GST
19	ACATGGATATGTGCATACGTGTGCCTA AGTAGAAATTTTTTTCACATGCAGCTG AAGCTTCGTACGC3	(fwd); generation of *arg82Δ*
20	TGTACCATATACCATAAACAAGGTAAA CTTCACCTCTCAATATATCTAGCATAGG CCACTAGTGGTACTG	(rev); generation of *arg82Δ*
21	TCGAAAATTGTCAGAGATAAGTTCCTT TTTTGAAAAGAAAGATCGATGCAGCTG AAGCTTCGTACGC3	(fwd); generation of ipk1*Δ*

22	TATGTGCATCTGCCAGTACCAAAGGTG GAAAGAAAAGTATACAGTTTAGCATAG GCCACTAGTGGTACTG	(rev); generation of *ipk1Δ*
23	TGACTTCTCTCGCTCAGGTG	(fwd); qRT-PCR *TbIPMK*
24	TCATGAAAGAAGAAAAATAATTTTTTC CAAACC	(rev); qRT-PCR *TbIPMK*
25	GTATAGCGTGTGGATTGGCGG	(fwd); qRT-PCR *Actin*
26	TGCTGTGTACGATGCTGGG	(rev); qRT-PCR *Actin*

RNA quantification

The *TbIPMK* conditional knockout cell line was grown with or without 1 µg/ml tetracycline and harvested at room temperature. RNA was extracted with TRI reagent (Sigma) and used as template for cDNA synthesis with SuperScript III RNA Polymerase (ThermoFisher) and oligo-dT as recommended by the manufacturer. We then performed qRT-PCR analysis using specific primers (Table 2.2) and SYBR Green Supermix (Bio-Rad). Relative *TbIPMK* gene expression relative to actin was calculated using CFX Manager™ Software (Bio-Rad).

Western blot analyses

Cells were harvested, washed twice in PBS, and lysed with CelLytic M cell lysis reagent containing protease inhibitor cocktail (Sigma P8340) diluted 1:250, 1 mM EDTA, 1 mM phenylmethanesulfonyl fluoride (PMSF), 20 µM *trans*-epoxysuccinyl-L-leucylamido(4-guanidino)butane (E64) and 50 U/ml Benzonase Nuclease (Millipore). The protein concentration was determined by using a BCA protein assay kit. The total cell lysates were mixed with 2X Laemmli sample buffer at 1:1 ratio (vol/vol) and directly loaded in 10% SDS-PAGE. The separated proteins were transferred onto nitrocellulose membranes using a Bio-Rad transblot apparatus. The membranes were blocked with 5% (wt/vol) nonfat milk in PBS containing 0.5% Tween-20 (PBS-T) at 4ºC overnight. The blots were incubated for 1 hour with mouse antibodies

against HA (1:1000) or mouse antibodies against c-Myc (1:1000). After five washings with PBS-T the blots were incubated with goat anti-mouse antibodies at a dilution of 1:15000 and developed using an Odyssey CLx Infrared Imaging System (LI-COR) according to the manufacturer instructions.

Yeast complementation

S. cerevisiae strains generated from DDY1810 were used: *arg82Δ, ipk1Δ*, *kcs1Δ, ipk1Δkcs1Δ*. *TbIPMK*, *TbIP5K* and *TbIP6K* were amplified from *T. brucei* Lister 427, cloned into plasmid pADH:GST (pYES-ADH1-GST) (Azevedo, Burton et al. 2009). Yeast cells were grown for 48 h in CSM plates. One colony was collected and suspended in 0.2 M lithium acetate with 25% polyethylene glycol solution and 0.1 M DTT. Cells were homogenized in 100 µl of solution with 100 ng of plasmid DNA and 5 µl of salmon sperm (Sigma D76560). Cells were incubated at 42ºC for 30 min and immediately plated in CSM -URA plates. Colonies were used for further experiments.

Titanium dioxide bead extraction

We adapted the method of Wilson et al. (Wilson, Bulley et al. 2015) for cell extraction of inositol polyphosphates. Cells (5×10^9) were harvested and washed twice in washing buffer A with glucose (BAG, 116 mM NaCl, 5.4 mM KCl, 0.8 mM $MgSO_4$, 50 mM Hepes, ph 7.3, and 5.5 mM glucose). The pellet was then mixed with 1 M perchloric acid, resuspended by sonication (40% amplitude) for 10 s and kept at room temperature for 15 min. The sample was centrifuged art 18,000 *x g* for 5 min and the supernatant was transferred to a new tube and boiled for 30 min to remove the large amount of polyphosphate present in *T. brucei*. Seven mg of TiO_2 beads were washed with water and 1 M perchloric acid, and added to the sample and left rotating for 30 min. Beads were centrifuged at 3,500 *x g* and inositol phosphates eluted with 1 M KOH,

10 mM EDTA. The sample was neutralized with perchloric acid and split into two. One half was digested with phytase (0.1 mg/ml) in the same medium at pH 5.0 and 37ºC for 1 h. Extracts were resolved by 35% PAGE analysis as described above.

HPLC analysis

Inositol phosphate analysis was performed according to (Azevedo and Saiardi 2006). Briefly, yeast liquid cultures were diluted to OD_{600} 0.005 in inositol free media supplemented with 5 µCi/ml [^{3}H] inositol and grown overnight at 30ºC with shaking. Cells were washed twice with water and immediately incubated with ice-cold 1 M perchloric acid and 3 mM EDTA. Glass beads were added and cells lysed by vortexing at 4ºC for 2 min, 3 times. Lysates were centrifuged and supernatants neutralized with 1 M K_2CO_3 and 3 mM EDTA. Samples were analyzed by strong anion exchange HPLC using SAX 4.6125 mm column (Whatman cat. no. 4621-0505). The column was eluted with two slightly different gradients generated by mixing buffer A (1 mM Na_2EDTA) and buffer B [buffer A plus 1.3 M $(NH_4)_2HPO_4$ (pH 3.8 with H_3PO_4)] as follows: 0–5 min, 0% B; 5–10 min, 0–30% B; 10–60 min, 30–100% B; 60–80 min, 100% B; or as follow: 0–5 min, 0% B; 5–10 min, 0–10% B; 10–85 min, 20–100% B; 85–100 min 100% B. Four mL of Ultima-Flo AP liquid scintillation cocktail (Perkin-Elmer cat. no. 6013599) was added to each fraction, mixed and radioactivity quantified in a scintillation counter.

T. brucei labeling for HPLC analysis

T. brucei PCF (~3x10^6 cells) were labeled with 5 µCi/ml of 1,2-[^{3}H]-inositol in SDM-79 medium (with 10% FBS) and grown for approximately 72 h. *T. brucei* BSF (~2x10^5 cells) were labeled with 5 µCi/ml of 1,2-[^{3}H]-inositol in HMI-9 medium (with 10% FBS) and grown for approximately 40 h. Cells were washed with PBS or BAG twice and frozen immediately. Soluble

inositol phosphates were extracted and analyzed as described before (Azevedo and Saiardi 2006), with minor modifications. Briefly, cells were suspended in ice-cold perchloric acid and broken by vortexing for 2 min. All steps were performed at 4^{o}C. Lysates were centrifuged for 5 min at 18,000 *x g* and supernatants transferred to new tubes, where the pH was neutralized with 1 M K_2CO_3 and 3 mM EDTA. Samples were stored at 4^{o}C and resolved by HPLC.

Polyphosphate extraction and measurement

Short chain polyphosphate was extracted from BSF *T. brucei* and quantified as described previously (Ulrich, Lander et al. 2014).

Immunofluorescence Assay

T. brucei BSF were washed with BAG and fixed with 2% paraformaldehyde in BAG for 1 h at room temperature. Then they were adhered to poly-L-lysine coated coverslips and permeabilized with 0.1% Triton X-100 in PBS for 5 min. Blocking was performed overnight at 4^{o}C in PBS containing 100 mM NH_4Cl, 3% BSA, 1% fish gelatin and 5% goat serum. Cells were then incubated with anti-TbVP1 polyclonal Guinea pig antibody (1:100) for 1 h and subsequently with Alexa 488-conjugated goat anti-Guinea pig antibody (1:1000) for 1h. Microscopy images were taken with a 100X oil immersion objective, a high-power solid-state 405 nm laser and EM-CCD camera (Andor iXon) under nonsaturating conditions in a Zeiss ELYRA S1 (SR-SIM) super resolution microscope. Images were acquired and processed with ZEN 2011 software with SIM analysis module.

Electron microscopy

Imaging of whole *T. brucei* BSF and determination of morphometric parameters were done as described previously (Ulrich, Lander et al. 2014).

Statistical analysis

All experiments were repeated at least three times (biological replicates) with several technical replicates as indicated in the figure legends, and where indicated results are expressed as means ± s.d. or s.e.m. of *n* experiments. Statistical analyses were performed using the Student's t-test. Results are considered significant when $P < 0.05$.

Results

Sequence analysis of T. brucei inositol phosphate kinases

Gene homology searches followed by validation of their activity (see below) have allowed to identify in the *T. brucei* genome (http://www.tritrypdb.org/tritrypdb/) the presumably gene orthologs to the inositol phosphate kinases encoding inositol polyphosphate multikinase (IPMK in mammals, and Arg82p or Ipk2p in yeast) (Tb427tmp.211.3460); the IP_5 kinase (IPPK or IP5K in mammals, and Ipk1p in yeast) (Tb427.04.1050); and the IP_6 kinase (IP6K in mammals, and Kcs1p in yeast) (Tb427.07.4400), (Figure 2.1), and named *TbIPMK*, *TbIP5K*, and *TbIP6K*, respectively (Table 2.1). No orthologs to diphosphoinositol pentakisphosphate kinase (PP-IP5K in mammals, or Vip1 in yeasts) were found, although orthologs to this gene are present in Apicomplexan (Laha, Johnen et al. 2015) and *Giardia* (EuPathDB). The orthologs to TbIPMK, TbIP5K, and TbIP6K identified in *T. cruzi* (TcCLB.510741.110, TcCLB.506405.90, TcCLB.504213.90) and *Leishmania major* (LmjF.35.3140, LmjF.34.3700, LmjF.14.0340) shared 45%, 36%, 35%, and 29%, 28%, 24% amino acid identity, respectively. Those of *T. brucei* share 15%, 16%, and 15% identity with the human enzymes, respectively. Structural analyses (ELM and TMHMM servers) predicted no transmembrane domains. A signal peptide was predicted for TbIP5K, but not for TbIPMK or TbIP6K. Mature proteins of 342, 461, and 756 amino acids with predicted molecular weights of 38.8, 51, and 82.6 kDa, for TbIPMK, TbIP5K,

and TbIP6K, respectively, were also predicted. Amino acids 138-147 of TbIPMK, and 588-596 of TbIP6K contained the conserved sequence PCVLDL(I)KL(M)G demonstrated previously as the putative inositol phosphate binding site that catalyzes the transfer of phosphate from ATP to inositol phosphates (Bertsch, Deschermeier et al. 2000). TbIP5K possesses the sequence PVLDIELL (amino acids 269-276) instead. Both TbIPMK and TbIP6K have a SASLL or TSSLL domain present in most members of this family of enzymes and required for enzymatic activity (Saiardi, Nagata et al. 2001, Nalaskowski, Deschermeier et al. 2002).

We utilized homologous recombination to add a hemagglutinin (HA) or c-Myc tag to the endogenous loci (Oberholzer, Morand et al. 2006) of TbIPMK, TbIP5K and TbIP6K. All three inositol phosphate kinases are expressed in procyclic forms (PCF) of *T. brucei* (Figure 2.2 A). Although the predicted MW of TbIP6K is 82.6 kDa the enzyme has multiple phosphorylations (Urbaniak, Martin et al. 2013) and these post-translational modifications (in addition to the HA tag) could result in a higher apparent MW. Interestingly, TbIP5K revealed no expression when using the HA-tag, but a protein with the expected size was detected when using a c-Myc tag (Figure 2.2 A). In addition, we tagged the three IP kinases in *T. brucei* bloodstream forms (BSF) but no clear bands were detected by western blot analyses although the tagged genes were expressed at the mRNA level (data not shown), suggesting that protein expression is lower in BSF than in PCF.

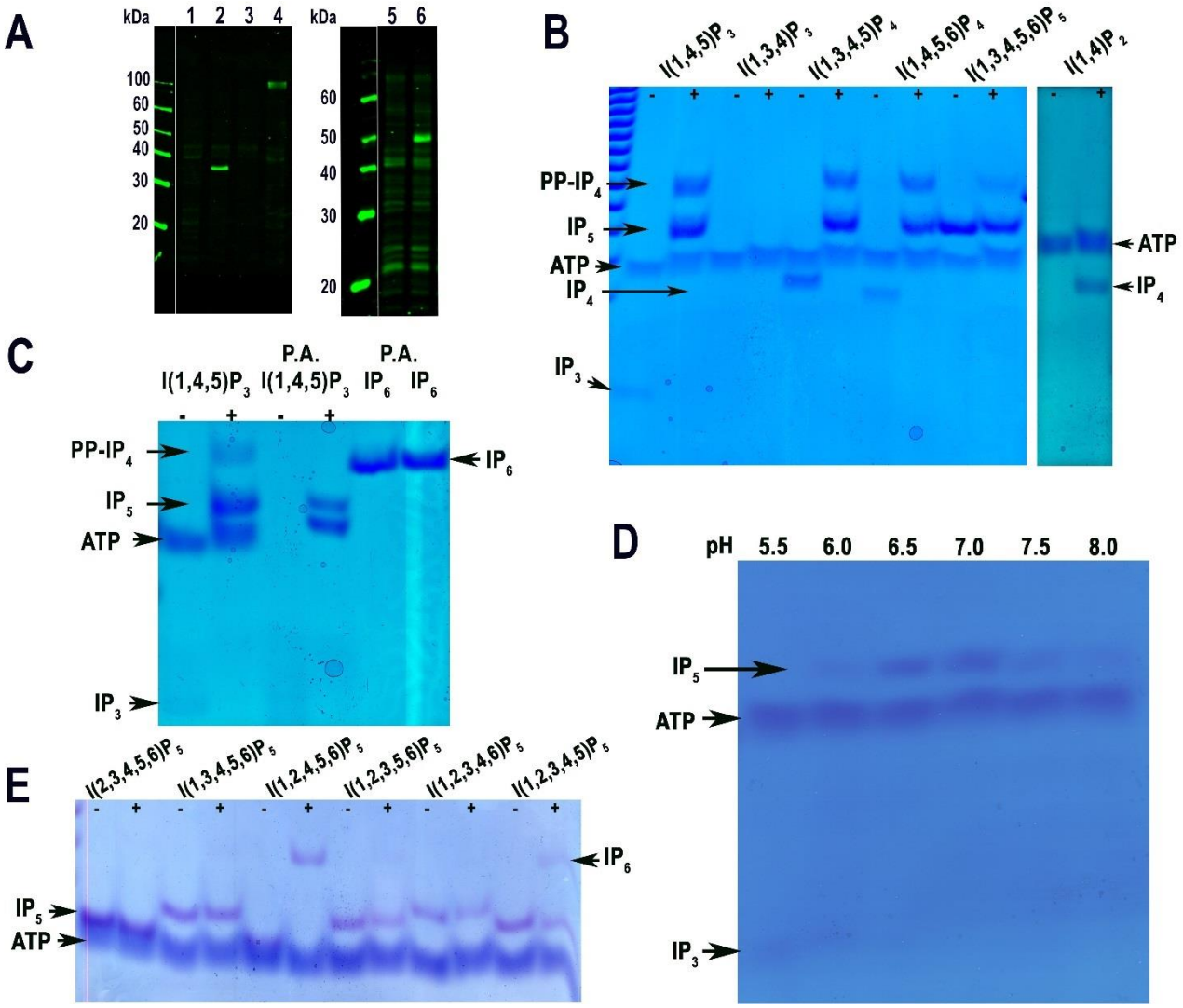

Figure 2.2. Western blot analyses and enzymatic activity of TbIPMK. A. Western blot analyses of *T. brucei* PCF expressing epitope-tagged TbIPMK, TbIP5K and TbIP6K. *Left panel* are HA tagged cell lines: 1, wild-type; 2, TbIPMK-HA; 3, wild-type; 4, TbIP6K-HA. *Right panel* is a c-Myc tagged line: 5, wild-type; 6, TbIP5K-cMyc. B. Kinase reactions performed with recombinant TbIPMK (2 µg) using the indicated substrates at 250 µM for 1 hour at 37ºC. TbIPMK can phosphorylate I(1,4,5)P_3 but not I(1,3,4)P_3 to produce I(1,3,4)P_5 and PP-IP_4, and can phosphorylate I(1,3,4,5)P_4, and I(1,4,5,6)P_4 to produce IP_5 and PP-IP_4. It can also phosphorylate I(1,3,4,5,6)P_5 to PP-IP_4. Other *arrows* show bands corresponding to ATP, IP_4, and IP_3. TbIPMK can phosphorylate I(1,4)P_2 to produce IP_4, and I(1,4,5)P_3 to produce IP_5 and PP-IP_4. C. Treatment of the sample with perchloric acid (PA) eliminates the band corresponding to PP-IP_4 but has no effect on IP_6. Other *arrows* indicate bands corresponding to ATP and IP_3. D. Optimum pH for TbIPMK activity is within the physiological range. E. TbIPMK can only phosphorylate positions 3 and 6 of different IP_5 derivatives to generate IP_6. Note the lower synthesis of PP-IP_4 using I(1,3,4,5,6)P_5 as substrate compared to results obtained in (B) and (C). We observed that shorter enzymatic reaction time resulted in less PP-IP_4 synthesis. All results are representative of three or more independent experiments.

Characterization of the inositol phosphate multikinase (TbIPMK)

To characterize the enzymatic activity of TbIPMK we expressed it as fusion protein with an *N*-terminal polyhistidine tag, purified and tested its activity *in vitro*. We found that it catalyzes the formation of IP_5 from IP_3 or IP_4, as detected by polyacrylamide gel electrophoresis (Figure 2.2 B). Inositol-1,4,5-trisphosphate ($I(1,4,5)P_3$) but not inositol-1,3,4-trisphosphate ($I(1,3,4)P_3$) could be used as substrate while both inositol-1,3,4,5-tetraphosphate ($I(1,3,4,5)P_4$) and inositol-1,4,5,6-tetraphosphate ($I(1,4,5,6)P_4$) could be used for the generation of inositol-1,3,4,5,6-pentakisphosphate ($I(1,3,4,5,6)P_5$) (Figure 2.2 B), indicating that TbIPMK has a dual 3-kinase/6-kinase activity. An additional product, which runs closely but not identically to IP_6, was also detected when IP_3, IP_4, or IP_5 was used as substrate (Figures 2.2 B and 2.2 C). The ability of IPMK to form PP-IP_4, an inositol pyrophosphate containing 6 phosphates and thus migrating closely to IP_6, has been demonstrated for the mammalian and yeast ortholog (Saiardi, Nagata et al. 2001, Zhang, Caffrey et al. 2001), and we therefore suspected that TbIPMK could have the same activity. A treatment with perchloric acid (PA), which degrades high-energy phosphoanhydride bonds (pyrophosphates) and is inactive against the phosphoester bond of IP_6 (Figure 2.2 C) (Pisani, Livermore et al. 2014), demonstrated that the highly phosphorylated product of TbIPMK is a pyrophosphate containing species, therefore PP-IP_4. The pH optimum of rTbIPMK was determined. TbIPMK has the maximum activity for IP_3 at the pH range of 6.5-7.0 (Figure 2.2 D). We also tested the ability of TbIPMK to phosphorylate different isomers of IP_5. Recombinant TbIPMK was able to phosphorylate $I(1,2,4,5,6)P_5$ and $I(1,2,3,4,5)P_5$ to IP_6 after short incubation times, but it was not able to use $I(2,3,4,5,6)P_5$, $I(1,3,4,5,6)P_5$, ($I(1,2,3,5,6)P_5$, or ($I(1,2,3,4,6)P_5$ as substrate (Figure 2.2 E). Although $I(1,2,4,5,6)P_5$ and $I(1,2,3,4,5)P_5$ would not be physiological substrates, the results again confirms a 3/6-kinase activity. Interestingly,

TbIPMK could also phosphorylate I(1,4)P_2 to IP_4 (Figure 2.2 B). The mammalian IPMK has been reported to have PI3-kinase activity that produces PIP_3 from PIP_2 (Resnick, Snowman et al. 2005). However, our in vitro activity tests using PIP_2 as substrate revealed no such activity (data not shown) in agreement with the results of a previous report (Cestari, Haas et al. 2016).

The ability of TbIPMK to act on IP_3 *in vivo* was tested by complementation of a *null* mutant for its ortholog *ARG82* (*arg82Δ* in *Saccharomyces cerevisiae*. Figure 2.3 A shows the HPLC analysis of soluble inositol phosphates isolated from yeast labeled with [^{3}H]inositol. Arg82p phosphorylates IP_3 to produce IP_4 and IP_5, and in its absence there is accumulation of IP_3, instead of the accumulation of IP_6 that occurs in wild type yeast (Figure 2.3 A). The metabolic pathway from IP_3 to IP_6 was restored by complementation with *TbIPMK* (Figure 2.3 A). These results indicate that TbIPMK function as part of the IP_6 biosynthetic pathway established in yeast (York, Odom et al. 1999). We also examined the ability of TbIPMK to rescue the growth defect of *arg82Δ* yeast. Complementation of *arg82Δ* with *TbIPMK* rescued their growth defect (Figure 2.3 B, and 2.3 C). Therefore, TbIPMK was able to complement yeast deficient in its ortholog Arg82p, providing molecular evidence of its function. The results also suggest that the pathway for IP_5 synthesis is similar to that present in yeast with conversion of I(1,4,5)P_3 into I(1,4,5,6)P_4 and I(1,3,4,5,6)P_5, TbIPMK acting as a 3/6-kinase. This is different from the pathway for synthesis of I(1,3,4,5,6)P_5 present in humans, where the major activity of IP_4 kinase is phosphorylation at the D-5 position (Chang, Miller et al. 2002).

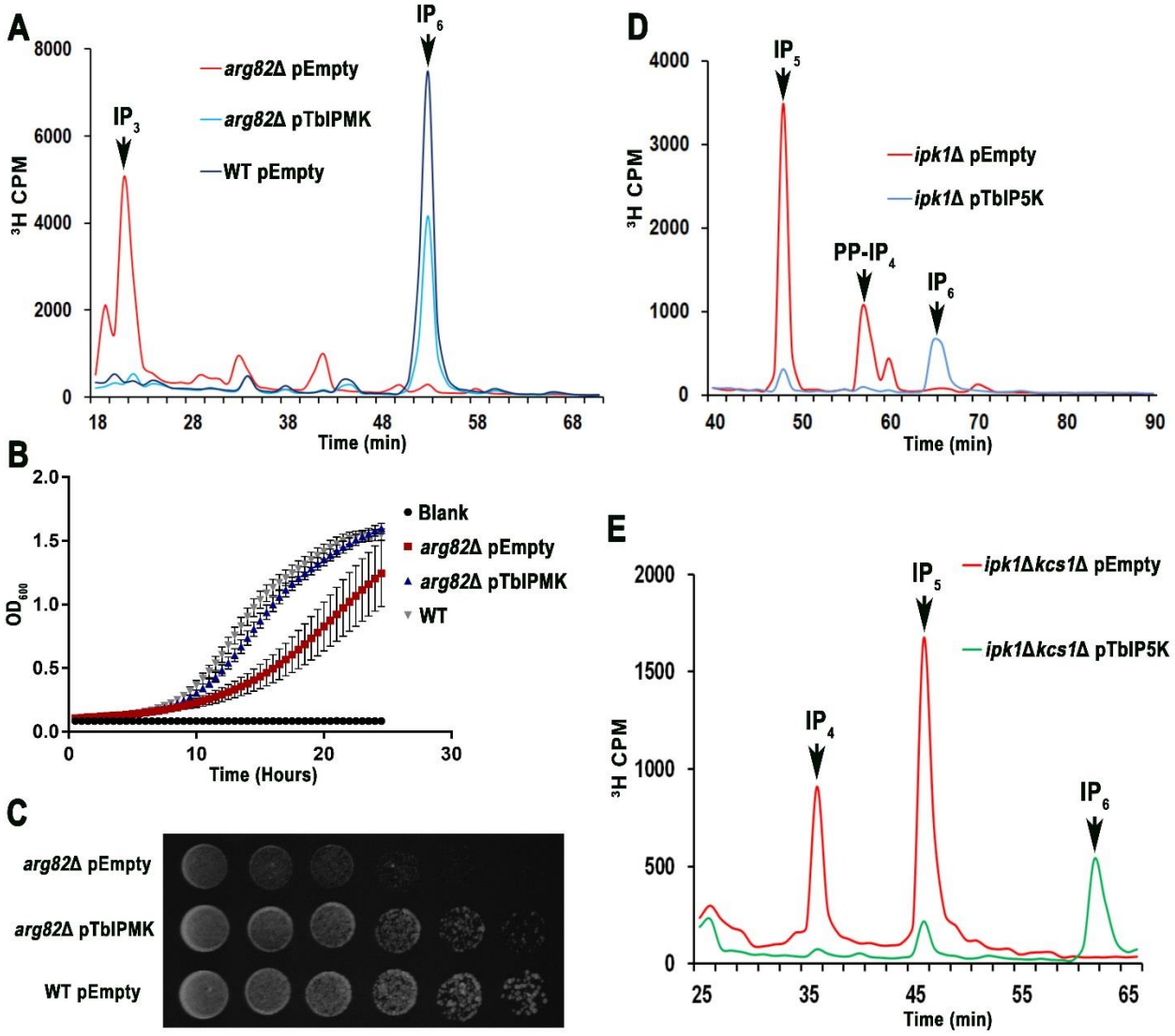

Figure 2.3. *TbIPMK*, and *TbIP5K* complementation of yeast mutants. A. HPLC analysis of soluble inositol phosphates of *S. cerevisiae arg82* mutants transformed with an empty vector (*red*) or a vector containing the entire open reading frame of *TbIPMK* (*blue*), and compared to those of wild-type (WT) yeast transformed with empty vector (*black*). B. Growth of the same cells in liquid medium as estimated by measuring optical density at 660 nm. *arg82*Δ mutants had reduced growth, which was restored by expression of *TbIPMK*. Mean ± S.D. for three independent experiments, each one with 6 duplicates. C. WT, and *arg82* transformed with empty vector or *arg82* transformed with *TbIPMK* (serially diluted 10-fold, 10^6-10 cells/spot from left to right) were spotted on YPD plates and incubated at 30ºC for 2 days. D. HPLC analysis of soluble inositol phosphates of *Scipk1* mutants transformed with an empty vector (*red*) or a vector containing the entire open reading frame of *TbIPMK* (*blue*) and compared with wild type transformed with an empty vector (*black*). E. HPLC analysis of *Scipk1Kcs1* complemented with empty vector (*red*) or *TbIP5K* (*green*) shows reconstitution of IP_6 synthesis. In *black*, wild type transformed with empty vector. All results are representative of three or more independent experiments.

Characterization of the inositol pentakisphosphate kinase (TbIP5K)

Although expression of polyhistidine-tagged TbIP5K was obtained in bacteria and the recombinant protein had the expected molecular mass, we were not able to detect its activity *in vitro*, even in the presence of different isomers of IP_5 (data not shown) suggesting that additional post-translational modifications are needed. In this regard, activity of human IP5K could only be obtained when expressed in insect cells (Verbsky, Wilson et al. 2002). However, *TbIP5K* was able to complement *null* mutant yeast deficient in its ortholog *IPK1* (*Ipk1Δ*) (Figure 2.3 D). Ipk1p phosphorylates IP_5 to produce IP_6, and in its absence there is accumulation of IP_5, instead of the accumulation of IP_6 that occurs in wild type yeast. The metabolic pathway from IP_5 to IP_6 was restored by complementation with *TbIP5K* (Figure 2.3 D). The presence of a shoulder close to the PP-IP_4 eluting peak in the mutant yeast suggests the existence of two isomeric PP-IP_4 species. We also complemented yeast mutants for both *ipk1Δ* (*IP5K*) and *kcs1Δ* (IP6K). These mutants accumulate IP_2, IP_3, IP_4, and IP_5 but no PP-IPs. While complementation with either *TbIPMK* or *TbIP6K* (not shown) alone did not change appreciably the inositol polyphosphate profile, synthesis of IP_6 was restored by complementation with *TbIP5K* alone (Figure 2.3 E), demonstrating that TbIP5K is the only inositol phosphate kinase identified in *T. brucei* genome that can produce IP_6.

Characterization of the inositol hexakisphosphate kinase (TbIP6K)

TbIP6K catalyzes the formation of IP_7 from IP_6. *TbIP6K* was also tagged with an HA tag using homologous recombination with the endogenous gene loci (Oberholzer, Morand et al. 2006). We detected expression of the enzyme in *T. brucei* procyclic forms (PCF) by western blot analysis (Figure 2.2 A). Recombinant TbIP6K was found to generate PP-IP_4 from IP_5 and IP_7

from IP_6 (Figure 2.4 A). Interestingly TbIP6K was not able to generate IP_8 using a 5PP-IP_7 as substrate, which suggests that, as IP6K from yeast and mammals, TbIP6K phosphorylates phosphate position D-5. Therefore, TbIP6K is able to generate two PP-IPs *in vitro*: PP-IP_4, and IP_7. The activity of TbIP6K was tested *in vivo* by complementation of a *null* mutant for its IP6K ortholog (*KCS1)* in *S. cerevisiae*. In the absence of *KCS1* there is no accumulation of IP_7, but the metabolic pathway from IP_6 to IP_7 is restored by complementation with *TbIP6K* (Figure 2.4 B). Complementation of *Kcs1Δ TbIP6K* also rescued the growth defect of these mutants (Figure 2.4 C and 2.4 D). The TbIP6K enzymatic activity has optimum pH 6.0-7.0 (Figure 2.4 E).

Characterization of inositol phosphates from *T. brucei* cells

Previous attempts to characterize soluble inositol phosphates from *T. brucei* (Moreno, Docampo et al. 1992) and *T. cruzi* (Docampo and Pignataro 1991) only detected IP, IP_2 and IP_3. We used increased labeling time to 40 hours (BSF) and 75 hours (PCF) with [^{3}H]inositol and used an improved protocol for purifying and analyzing inositol phosphates (see Materials and methods). Using these conditions, we were able to detect a small peak of IP_6 in PCF but not in BSF of the parasite (Figures 2.5 A, and 2.5 B). The inability to detect radiolabeled IP_6 in the BSF might simply reflect the lower number of cells that can be obtained in culture. To improve the detection of IP_6 we used a different approach that does not require metabolic labeling with [^{3}H]inositol. We extracted IPs from large amounts of cells (see Materials and methods) and assayed extracts by 35% polyacrylamide gel electrophoresis (PAGE). A band that runs like the IP_6 standard and that disappears after treatment of the extracts with phytase (Phy) was observed in both PCF and BSF (Figures 2.5 C, and 2.5 D). Other highly phosphorylated inositol

phosphates were not detected. These results confirm that both PCF and BSF TbIPMK and TbIP5K can sequentially synthesize IP_6 in *T. brucei.*

Biological relevance of the TbIPMK pathway

Yeast lacking Arg82p have no observable inorganic polyphosphate accumulation (Lonetti, Szijgyarto et al. 2011). As polyphosphate has important roles in trypanosomes, including growth, response to osmotic stress, and maintenance of persistent infections (Lander, Cordeiro et al. 2016), we investigated whether deletion of soluble inositol polyphosphates affected the levels of polyphosphate in *T. brucei*. We used the *TbIPMK* conditional knockout BSF cell line previously described (Cestari and Stuart 2015). Removal of tetracycline to induce the knockdown of *TbIPMK* dramatically reduced its expression more than 100-fold (Figure 2.6 A). Growth stalled after the first day without tetracycline (Figure 2.6 B). A resulting progressive reduction in polyphosphate levels was detected (Figure 2.6 C). Acidocalcisomes are the main cellular storage compartment for polyphosphate in trypanosomes (Lander, Cordeiro et al. 2016). However, examination of the cells by super-resolution microscopy with antibodies against the vacuolar proton pyrophosphatase (TbVP1) showed no apparent difference in labeling or distribution of acidocalcisomes between control and *TbIPMK* mutant cells (Figure 2.7). In previous work we demonstrated that a knockdown of the TbVtc4, which catalyzes the synthesis and translocation of polyphosphate into acidocalcisomes, results in less electron-dense organelles, as examined by electron microscopy (Ulrich et al., 2014). We hypothesized that if the polyphosphate reduction observed (Figure 2.6 C) was primarily within acidocalcisomes, we should observe similar changes in the *TbIPMK* mutant cells. Indeed, electron microscopy of the *TbIPMK* mutants showed a reduction in the number (Figure 2.6 D), size, and electron density

(compare figure. 2.6 E and 2.6 F) of electron-dense organelles identifiable as acidocalcisomes. This result indicates that acidocalcisome polyphosphate synthesis is disrupted by ablation of the inositol phosphate signaling pathway.

Discussion

Our work establishes the presence of an inositol pyrophosphate (PP-IPs) synthesis pathway in *T. brucei*. We demonstrated that genes encoding proteins with homology to kinases involved in the generation of IP_5 from IP_4 and IP_3 (TbIPMK), of IP_6 from IP_5 (TbIP5K), and of IP_7 from IP_6 (TbIP6K) are present in the *T. brucei* genome (*TbIPMK, TbIP5K*, and *TbIP6K*). To demonstrate that these genes encode for functional enzymes we complemented yeast strains deficient in their corresponding orthologs and compared their products with those produced in the wild type strain providing *in vivo* genetic evidence of their function. We did not compare them with the knockout strains overexpressing the endogenous genes because the heterologous gene expression is often hampered by a diverse genetic code usage and by the lack of yeast specific post-translational processing. Thus, the heterologous genes are regularly expressed from a stronger promoter. The overexpressing of the endogenous gene from a stronger promoter might generate, to the contrary, 'hyper' phenotype and not a normal WT phenotype and our aim was to demonstrate their function and not to compare their activities to those of the overexpressed endogenous genes. Suppression of this pathway in *T. brucei* BSF resulted in a significant decrease in polyphosphate levels and in morphological alterations of the acidocalcisomes. The results suggest that this pathway is important for polyphosphate synthesis in acidocalcisomes.

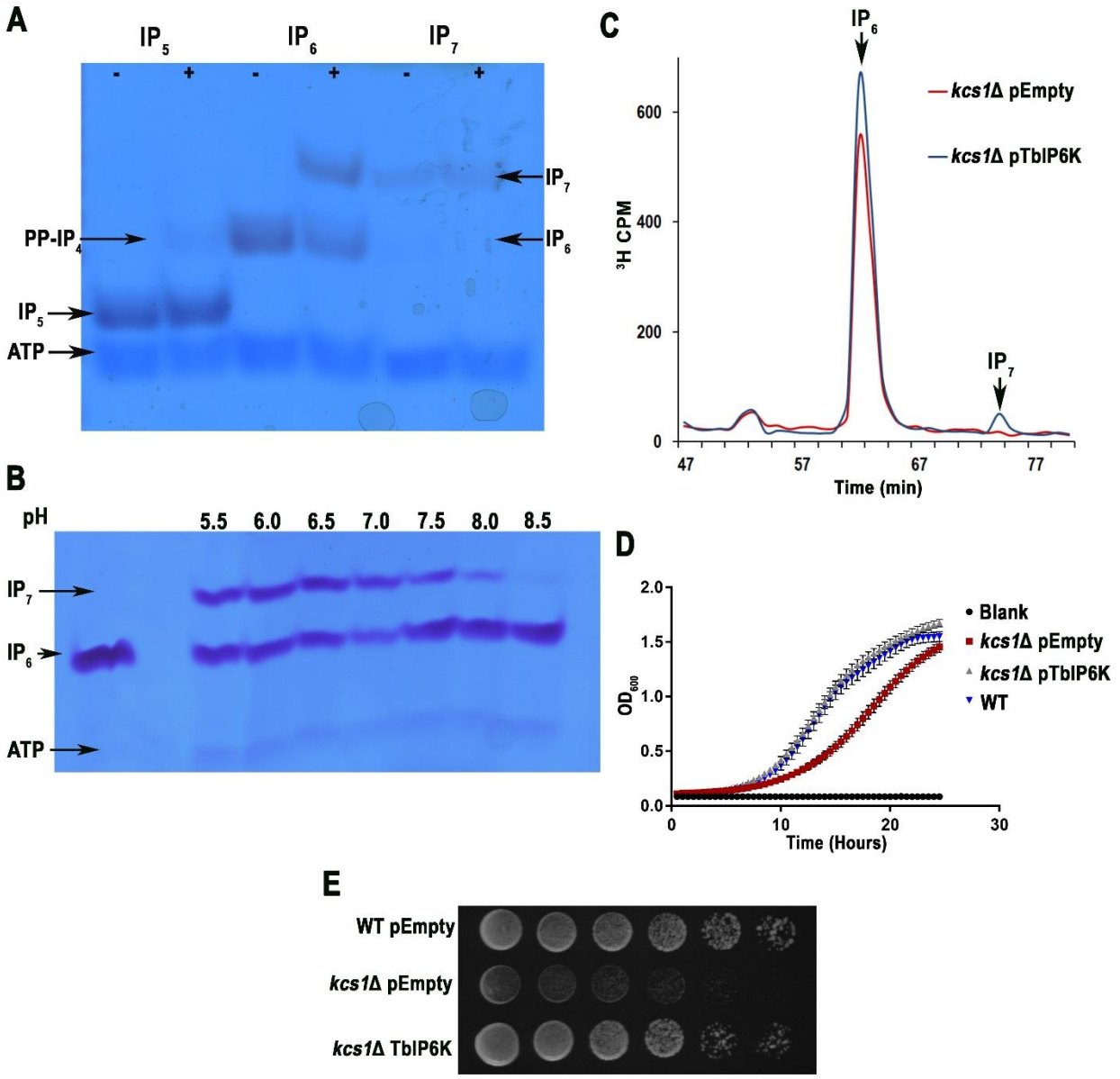

Figure 2.4. TbIP6K activity and complementation of yeast mutants. A. Kinase reactions performed with recombinant TbIP6K (2 µg) using the indicated substrates at 150 µM for 1 hour at 37ºC. TbIP6K can phosphorylate I(1,3,4,5,6)P_5 to PP-IP_4 and IP_6 to produce IP_7 (5PP-IP_5) but cannot phosphorylate IP_7 to produce IP_8. Other *arrows* show bands corresponding to ATP, and IP_5. B. HPLC analysis of soluble inositol phosphates of *S. cerevisiae kcs1*□ mutants transformed with an empty vector (*red*) or a vector containing the entire open reading frame of *TbIP6K* (*blue*). C. Growth of the same cells in liquid medium as estimated by measuring optical density at 660 nm. *kcs1*□ mutants had reduced growth, which was restored by expression of *TbIP6K*. Mean ± s.d. for three independent experiments, each one with 6 duplicates. D. WT, and *kcs1*□ transformed with empty vector or *kcs1*□ transformed with *TbIP6K* (serially diluted 10-fold, 10^6-10 cells/spot from left to right) were spotted on YPD plates and incubated at 30ºC for 2 days. E. Optimum pH for TbIP6K activity is under acidic conditions. We detected a higher activity at pH 6.0 and 6.5. All results are representative of three or more independent experiments.

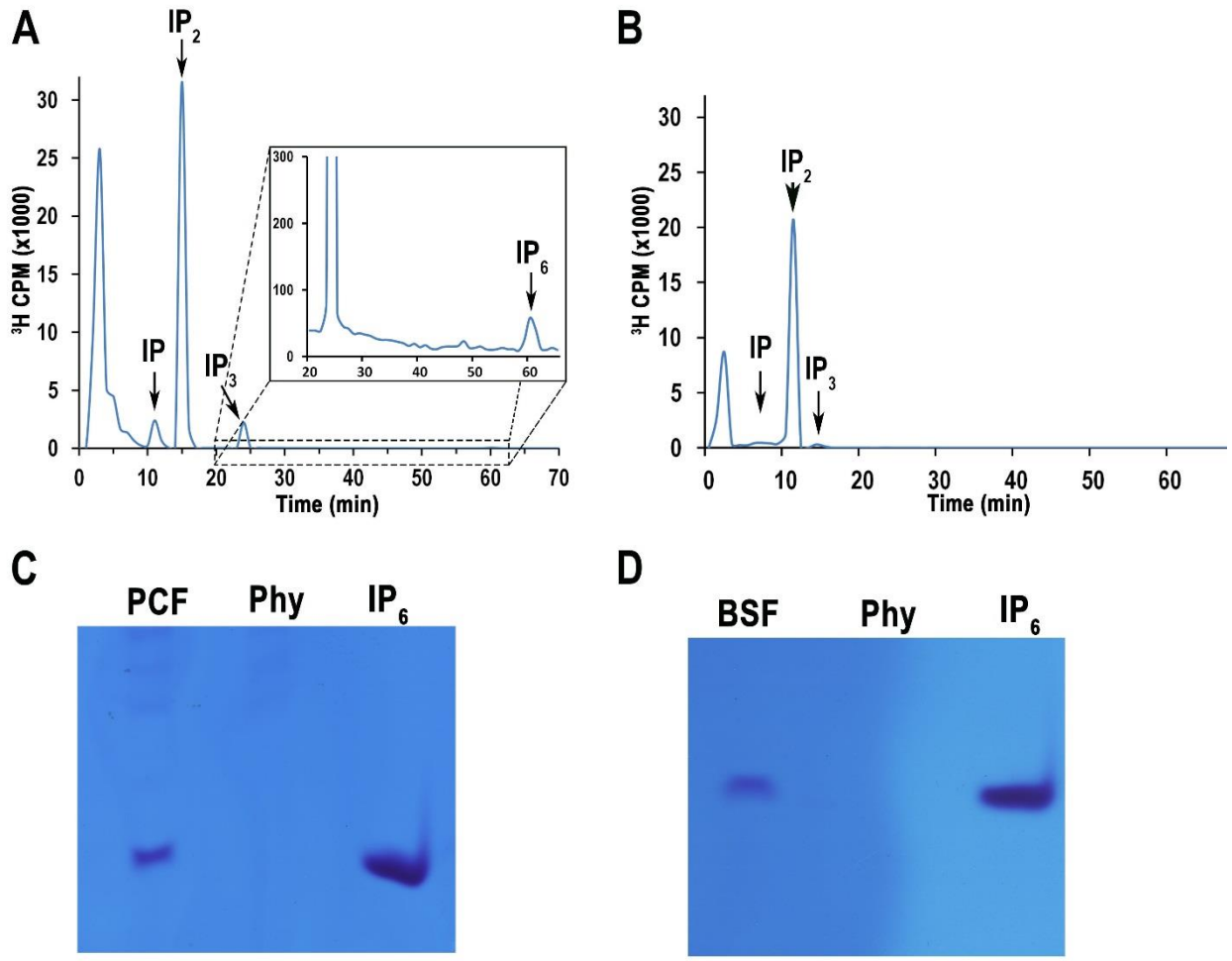

Figure 2.5. HPLC and PAGE analyses of soluble inositol phosphates from *T. brucei* PCF and BSF. A. PCF showed the presence of IP, IP_2, IP_3 and IP_6. B. BSF showed the presence of IP, and IP_2. Cells were labeled with [^{3}H]inositol as described under *Experimental Procedures*. C-E. PAGE analyses of extracts from PCF (C) or BSF (D) or standard IP_6 (E). Samples in (C) and (D) (5 x 10^9 cells) were treated with phytase (Phy) (0.1 mg/ml, pH 5.0, at 37ºC for 1 hour) to confirm that the bands correspond to IP_6. E. Phytase control activity with IP_6 standard. All results are representative of three or more independent experiments.

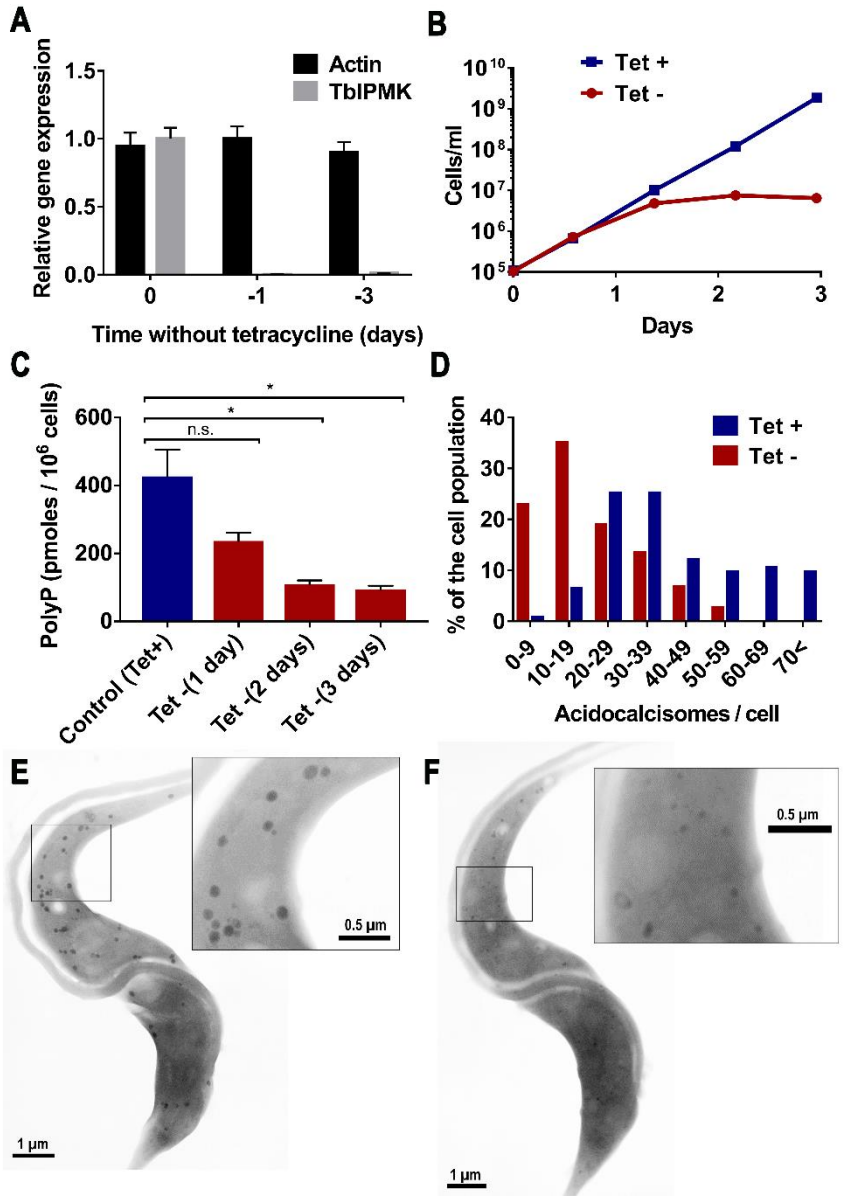

Figure 2.6. Phenotypic changes of mutant BSF deficient in TbIPMK. A. qRT-PCR analysis of gene expression of *TbIPMK* at time 0 and after 1 and 3 days in the absence of tetracycline as compared to expression of control actin. Values are means ± s.e.m., $n = 3$. $P < 0.001$ at days 1 and 3 without tetracycline. Student's *t* test.B. In vitro growth of BSF in the presence (+*Tet*) or absence (-*Tet*) of 1 µM tetracycline. Values are means ± s.e.m., $n = 3$ (bars are smaller than symbols). C. Quantification of short-chain polyphosphate in control (+*Tet*) and induced (-*Tet*) *TbIPMK* conditional knockout BSF. Values are means ± s.e.m, $n = 3$, $*P < 0.05$. Student's *t* test. D. Numeric distribution of acidocalcisomes in BSF. Whole unfixed parasites were observed by transmission electron microscopy and the number of acidocalcisomes per cell in ~100 cells of control *(+Tet*) and conditional *TbIPMK* mutants (-*Tet*) were counted (the results from 3 independent experiments were combined). E, F. Scanning transmission electron microscopy (STEM) images from control (E) or *TbIPMK* conditional mutant BSF showing acidocalcisomes. Bar = 1 µm. *Insets* show acidocalcisomes highlighted in (E) and (F) at higher magnification. Bars = 0.5 µm.

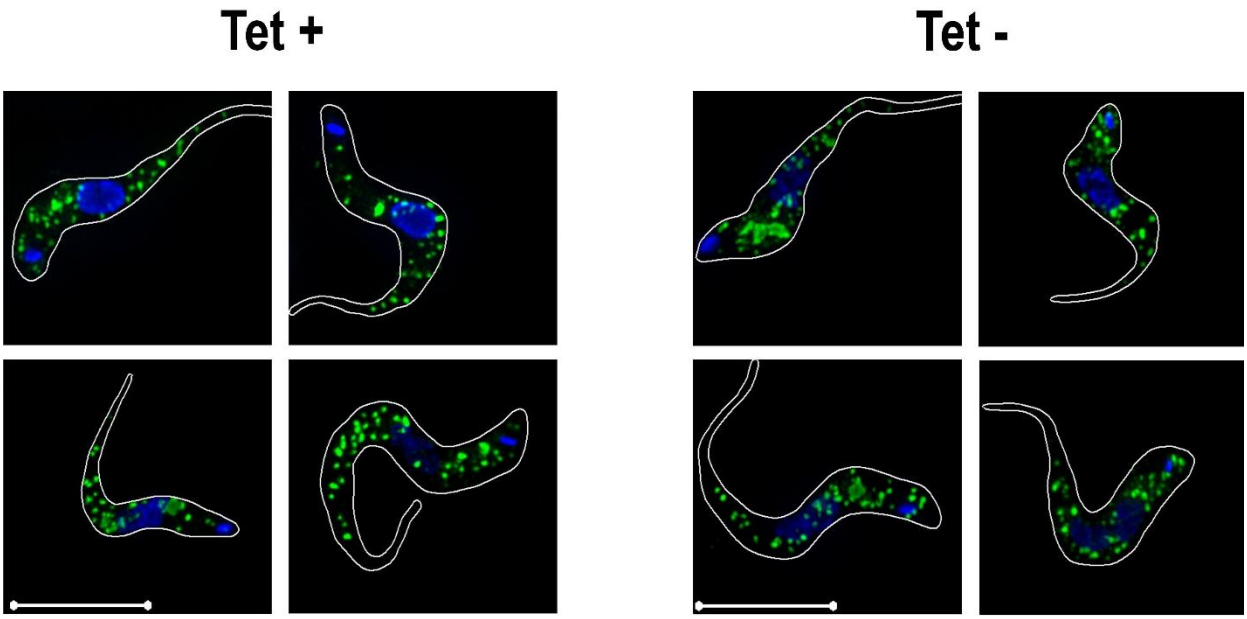

Figure 2.7. TbIPMK conditional KO does not change labeling or distribution of acidocalcisomes. Immunofluorescence of TbIPMK conditional KO with (A) or without (B) tetracycline shows acidocalcisome marker TbVP1 (*green*) and DAPI-stained DNA (*blue*) in four different cells or each condition. Bar = 5 µm.

Examination of the protein sequences of TbIPMK, TbIP5K, and TbIP6K indicated low identity with the mammalian enzymes but conservation of the putative binding site that catalyzes the transfer of phosphate from ATP to IPs, as well as of other domains required for enzymatic activity. The expression of these three kinases is very low in BSF since no clear bands were detected by western blot analyses of endogenous tagged lines, although gene expression is detectable at the mRNA level. Conversely, all three kinases can be easily identified by western blot analysis of PCF. Our results suggest, in agreement with the presence of these enzymes in other unicellular organisms such as *D. discoideum* (Europe-Finner, Gammon et al. 1991, Mayr GW 1992, Stephens, Radenberg et al. 1993), and *E. histolytica* (Martin, Bakker-Grunwald et al. 1993), an early emergence of this pathway preceding the origin of multicellularity.

The application of polyacrylamide gel electrophoresis (PAGE) and toluidine blue staining (Losito, Szijgyarto et al. 2009, Pisani, Livermore et al. 2014) allowed the characterization of the IPs synthesizing kinases of *T. brucei* and the identification of the products of each reaction bypassing the need for extraction under the strong acidic conditions required for HPLC analysis that has been shown to degrade some of the most highly phosphorylated species (Losito, Szijgyarto et al. 2009).

Previous work has indicated that TbIPMK is essential for growth (Cestari and Stuart 2015) and infectivity (Cestari, Haas et al. 2016) of *T. brucei* BSF, and partially characterized the recombinant enzyme (Cestari, Haas et al. 2016). We confirmed that TbIPMK prefers I(1,4,5)P_3 and I(1,3,4,5)P_4 as substrates (Cestari, Haas et al. 2016) and found that it does not phosphorylate I(1,3,4)P_3. We also confirmed that TbIPMK cannot phosphorylate the lipid PIP_2 to PIP_3 (Cestari, Haas et al. 2016), as the human enzyme does (Resnick, Snowman et al. 2005). In addition, we found that the enzyme can use I(1,3,4,5)P_4 and I(1,4,5,6)P_4 for the generation of I(1,3,4,5,6)P_5 indicating that TbIPMK has a dual 3-kinase/6-kinase activity. This is in contrast to the human enzyme, where the major activity of IP_4 kinase is phosphorylation at the D-5 position (Chang, Miller et al. 2002). Moreover, we demonstrated that TbIPMK is able to generate PP-IP_4 *in vitro*, using either I(1,4,5)P_3, I(1,3,4,5)P_4 or I(1,3,4,5,6)P_5, as well as IP_6 from I(1,2,4,5,6)P_5, or (I(1,2,3,4,5)P_5 as substrate, again indicating a 3/6-kinase activity. TbIPMK has a neutral pH optimum for phosphorylation of both IP_3 and IP_4. Previous work (Cestari, Haas et al. 2016) described inhibitors of this enzyme that inhibited *T. brucei* BSF growth. However, their IC_{50}s against the enzymes were higher (3.4-5.33 µM) than the EC_{50}s for their growth inhibition (0.51-0.83 µM), suggesting that either the drugs are accumulated or other targets might be involved in the sensitivity of *T. brucei* BSF to those inhibitors. The search for more specific inhibitors is

warranted to demonstrate the relevance of this pathway to human disease and drug therapy. Interestingly, a recombinant multi-domain protein from *Plasmodium knowlesi* termed PkIPK1 was shown to have IPMK-like activity and was able to generate I(1,3,4,5)P_4 from I(1,4,5)P_3 and I(1,2,4,5,6)P_5 from either I(1,2,5,6)P_4 or I(1,3,4,6)P_4, showing 3/5-kinase activity (Stritzke, Nalaskowski et al. 2012).

We were not able to detect activity of the recombinant IP5K in the presence of different isomers of IP_5 suggesting that, as proposed for the mammalian enzyme, post-translational modifications are needed for its activity (Verbsky, Wilson et al. 2002). However, *TbIP5K* was able to complement *null* mutant yeast deficient in its ortholog *IPK1* (*Ipk1Δ*), providing genetic evidence of its function.

Recombinant TbIP6K was able to generate PP-IP_4 from IP_5 and IP_7 from IP_6, but was not able to generate IP_8 using a 5-PP-IP_5 as substrate suggesting that, as IP6K from mammalian cells (Draskovic, Saiardi et al. 2008), TbIP6K phosphorylates phosphate at position D-5. Therefore, TbIP6K is able to generate two PP-IPs in vitro: PP-IP_4, and IP_7. Complementation of yeast deficient in its ortholog confirmed the function of this enzyme.

T. brucei incorporates poorly the radioactive tracer [^{3}H]inositol a feature previously observed in *Dictyostelium discoideum* (Losito, Szijgyarto et al. 2009). Nevertheless, improved metabolic labeling with [^{3}H]inositol resulted in detection of IP, IP_2, IP_3 and IP_6 by HPLC analysis of PCF extracts. In contrast to the results obtained using similar methods in yeasts (Azevedo and Saiardi 2006), plants (Phillippy, Perera et al. 2015) or animal cells (Guse, Greiner et al. 1993), only very low levels of IP_6 were detected and no labeled IP_6 was detected by HPLC using BSF extracts. However, IP_6 was clearly detected by PAGE and toluidine blue staining when large numbers of parasites were used. No inositol pyrophosphates were detected since to

purify and visualize IPs we removed the abundant inorganic polyphosphate (polyP) by acidic treatment, procedure that would degrade IP_7 to IP_6. However, the absence of IP_7 could be also attributed to the high turnover of these important signaling molecules (Glennon and Shears 1993, Burton, Hu et al. 2009). Some cells accumulate IP_6 and produce IP_7 upon signaling events. For instance, *Cryptococcus neoformans* requires synthesis of IP_7 for successful establishment of infection (Li, Lev et al. 2016). A recent study demonstrated that IP_7 binds the SPX domain of proteins involved in phosphate homeostasis in plants, yeast and humans with high affinity and specificity and postulated the role of this domain as a polyphosphate sensor domain (Wild, Gerasimaite et al. 2016, Azevedo and Saiardi 2017). Two proteins in *T. brucei* possess SPX domains, TbVtc4 (Lander, Ulrich et al. 2013), which is involved in polyphosphate synthesis and translocation, and TbPho91 (Huang, Ulrich et al. 2014), a phosphate transporter. Both proteins localize to acidocalcisomes (Huang, Ulrich et al. 2014), the main polyphosphate storage of these cells. Our results, showing lower levels of polyphosphate and altered acidocalcisomes in *TbIPMK* BSF mutants, support the link between PP-IPs and polyphosphate metabolism.

In summary, both recombinant enzymes, TbIPMK and TbIP6K, are able to generate inositol pyrophosphates. The essentiality of the first enzyme of this pathway, TbIPMK, for growth and infectivity of *T. brucei* BSF (Cestari and Stuart 2015, Cestari, Haas et al. 2016) suggests that the study of the PP-IPs pathway in trypanosomes could lead to the elucidation of potentially multiple important roles of these compounds, possibly linked to the synthesis of polyphosphate. Differences between mammalian and trypanosome metabolism of these compounds could provide potential targets for drug development.

CHAPTER 3

5-DIPHOSPHO-INOSITOL PENTAKISPHOSPHATE SIMULATE PHOSPHATE RELEASE FROM ACIDOCALCISOMES OF *TRYPANOSOMA BRUCEI* AND YEAST VACUOLES

Introduction

Inorganic phosphate (Pi) is essential for all organisms. In yeast *S. cerevisiae*, Pi is incorporated by low affinity, ScPho87 and ScPho90, and high affinity transporters, ScPho84 and ScPho89, located at the plasma membrane (Figure 5.2). The core transcriptional regulation of genes involved in phosphate acquisition, uptake and storage is performed by the PHO transduction pathway. When there is low phosphate, the Pho80-Pho85 cyclin dependent kinase complex mediate activation of transcription factor Pho4 that increase expression of phosphate homeostasis-related genes. ScPho81 is a negative regulator of Pho80-Pho85 kinase complex. ScPho81 has an SPX domain that binds 1-IP_7 and generates a conformational change thus preventing phosphorylation of Pho4, which then accumulates in nucleus and activates transcription genes, including ScPho84 and ScPho89 (Figure 5.2) (Lee, Huang et al. 2008). The low-affinity and high-affinity systems are mutually exclusive: in high phosphate conditions only low-affinity transporters are expressed and in low phosphate conditions the high-affinity are expressed, while low-affinity are downregulated preventing phosphate leakage. This regulation mechanism results in extended survival upon nutrient limitation and facilitates recovery afterwards (Secco, Wang et al. 2012). Transcription of the low-affinity Pi transporters ScPho87, ScPho90 and ScPho91 is not regulated by external Pi availability (Wykoff, Rizvi et al. 2007).

The low affinity transporter system may be regulated by post-translational modification and/or other forms of signaling as all of them have the regulatory SPX domain at the N-terminus. For example, PHO pathway activates Spl2 transcription which binds to SPX domain of ScPho87 and ScPho90. Removal of SPX domain resulted in unrestricted phosphate accumulation and lower tolerance to high phosphate conditions (Hurlimann, Pinson et al. 2009). Interestingly, most proteins from fungi and plants that contain SPX domains are involved in phosphate homeostasis (Secco, Wang et al. 2012). The crystal structure of SPX from ScVtc2 obtained with IP_6 demonstrated the ability of this domain to interact with IPs (Wild, Gerasimaite et al. 2016).

Phosphate homeostasis regulation Trypanosomes is not well understood. Studies of *T. brucei* enzymatic assays that require inorganic phosphate, like glycolytic synthesis of ATP, assumed a cytosolic phosphate concentration similar to the bloodstream around 0.5 mM (Bakker, Michels et al. 1999). However, phosphate concentration can change according to host nutrition, age and health conditions. Human normal serum Pi varies from 0.4 to 1.5 mM (Bansal 1990). Conditions may also change in different hosts: mice blood Pi was reported at 5 mM (Russo-Abrahao, Koeller et al. 2017). Trypanosomes must have evolved mechanisms to regulate intracellular cytosolic phosphate to acclimate for extracellular changes. *T. cruzi* has two independent high and low affinity Pi uptake systems, which are activated differently according to phosphate availability. *T. cruzi* Pi incorporation depends on either H^+ or Na^+ (Dick, Dos-Santos et al. 2013). On the other hand, *Leishmania spp*. only has H^+-dependent Pi uptake (Dick, Dos-Santos et al. 2014). Like yeast and *T. cruzi*, *T. brucei* has two modes of Pi acquisition that operate differently under high and low external phosphate, resulting in higher uptake with the former and low uptake in latter conditions. There is little information on *T. brucei* phosphate transporters and virtually no literature on how they adjust Pi levels. Recently, the first

characterization of *T. brucei* phosphate acquisition was published. The kinetics of the high affinity Pi uptake was described, but it remains unclear which transporters are involved. Additionally, high affinity Pi transport is more efficient in PCF than BSF and dependent on H^+ gradient (Russo-Abrahao, Koeller et al. 2017). *T. brucei* genome has orthologs of the yeast plasma membrane transporters ScPho89, annotated as phosphate-repressible phosphate permease (Tb927.1.580, Tb927.1.600) (TriTryp.org), and one protein with similarity to ScPho84 named TbHMIT (Tb927.11.5350), which is also an inositol transporter. TbHMIT can transport phosphate and it is negatively modulated by inositol concentration. RNAi knockdown of TbHMIT reduced Pi intake, what led authors to believe this transporter is directly responsible for phosphate acquisition (Russo-Abrahao, Koeller et al. 2017). However, TbHMIT was found to be in the Golgi of PCF and BSF parasites, which conflicts with the plasma membrane transporter function proposed by Russo-Abrahao et al. TbHMIT was only observed at the plasma membrane after overexpression, which could lead to mislocalization. It remains to be determined if TbHMIT really is normally a plasma membrane transporter. Moreover, TbHMIT is an essential gene that is important for the phosphatidylinositol synthesis and may affect inositol phosphate pathway (Gonzalez-Salgado, Steinmann et al. 2012, Gonzalez-Salgado, Steinmann et al. 2015). It is plausible that the TbHMIT does not directly affect Pi uptake, but rather alters signaling pathways that regulate Pi uptake resulting in the observed uptake phenotype.

Another tactic to regulate intracellular phosphate is to store Pi and utilize when needed. For example, plant cells store phosphate in vacuoles. Studies of the rice Pho91-related SPX-MFS vacuolar transporter, which contains SPX domain, concluded this family of transporters regulate phosphate efflux from stores and ultimately help maintain Pi homeostasis (Wang, Yue et al. 2015). Additionally, in *Arabidopsis thaliana*, decrease in extracellular phosphate sources leads to

subsequent reduction in cytosolic Pi and, once it reaches a threshold level, phosphate release from stores is activated (Pratt, Boisson et al. 2009). Similar regulatory mechanisms of maintaining Pi concentration by acquisition from stores exist in other organisms. Experiments with yeast inorganic phosphate (Pi) starvation by ^{31}P-NMR revealed that levels of polyP are reduced progressively to almost zero after 4 hours without extracellular Pi. However, the cytoplasmic Pi is maintained relatively stable for almost 4 hours, indicating that vacuolar polyphosphate reserves are supplying the cell with the phosphate it needs. Indeed, culture growth was maintained for about 4 hours, indicating that the exhaustion of stores stalled cell division. Mutants with vacuolar defects and lower polyP ceased growth immediately after Pi starvation (Shirahama, Yazaki et al. 1996).

Unicellular eukaryotes store phosphate mainly as polyP in acidocalcisomes or vacuoles. How is the phosphate store utilized by the cell when it needs? Arbuscular mycorrhiza Pi homeostasis is tightly regulated and the vacuolar transporter Pho91 participates in adjusting phosphate balance, but mechanisms of Pi release are not characterized (Ezawa and Saito 2018). In *S. cerevisiae*, there is evidence that polyP can leave the vacuole and reach nucleus (Lichko, Kulakovskaya et al. 2006). This phenomenon has been recently associated with polyphosphorylation of nucleolar proteins, which is not yet fully characterized (Bentley-DeSousa, Holinier et al. 2018). The current model for polyP recycling comprise polyP degradation by vacuolar endopolyphosphatases and phosphate release to cytosol by ScPho91 transporter. Still, properties of the ScPho91 transporter has not been fully reported. The first electro-physiological characterization of a Pho91 was done with *T. cruzi* TcPho91, demonstrating it is a sodium phosphate symporter (Jimenez and Docampo 2015). *T. brucei* TbPho91 and TcPho91 are 82% similar and share 70% identical amino acids. TbPho91 and all its

orthologs share same basic structural domains: one N-terminal SPX domain and one annotated sodium/sulphate symporter domain that contain several transmembrane domains (Figure 3.1 A). Alignment of Pho91 from *T. brucei* (Protozoa, Euglenozoa), *S. cerevisiae* (Fungi, Ascomycota), *Trichomonas vaginalis* (Protozoa, Metamonada), *Phytophthora infestans* (Chromista, Oomycota), *Cryptococcus neoformans* (Fungi, Basidiomycota) *Candida Albicans* (Fungi, Ascomycota) and *Chlamydomonas reinhardtii* (Viridiplantae, Chlorophyta) show the conservation of key residues for interaction with inositol phosphates in SPX domain (Figure 3.1 B). Moreover, we observed the Sodium/Sulfate symporter domain is conserved among these organisms (72% similarity and 37 % identical residues on average). Our previous data (Chapter 2) suggests acidocalcisomes polyphosphate storage is regulated by inositol phosphates. In this chapter, we investigate Pho91 participation in phosphate homeostasis and how inositol phosphates regulate Pho91 transport.

Experimental procedures

Cell cultures and Microscopy

T. brucei Lister strain PCF was cultivated as described in chapter 2. To generate a knockout cell line of TbPho91 in PCF, we replaced the genes with resistance markers using homologous recombination. We amplified the resistance marker for puromycin with primers containing 90 nucleotides of homology with the 5' and 3' UTRs of TbPho91 by PCR and transfected the product in parasite cultures as described previously (Lander, Ulrich et al. 2013). After selection of resistant parasites, we replaced the second copy of TbPho91 with the blasticidin resistance gene using same strategy. We then verified gene displacement by PCR of genomic DNA and Southern blot.

Acidocalcisomes detection by immunofluorescence microscopy was performed as described in chapter 2 using anti-VP1 antibody.

Southern Blot

Southern blot was performed as described (Lander, Ulrich et al. 2013). Briefly, we extracted genomic DNA from *T. brucei* cell cultures and digested 3 µg of DNA with EcoRI and NdeI (Probe for 5'UTR) or HindIII and NotI (Probe for CDS). Digestion products were resolved by electrophoresis in 0.8% agarose gels and the DNA was transferred to Zeta-probe blotting membranes (Bio-Rad) by capillarity using 400 mM NaOH. We amplified genomic sequences by PCR (Table 3.1) to generate probes for the 5'UTR and CDS of the genes (Figure 3.2), which were then labeled with [α-^{32}P]dCTP using the Prime-a-Gene labeling system (Promega). Membranes were hybridized with probes overnight, then washed for one hour and imaged with a Phosphorimager.

Sequence analysis

We used the Basic Local Alignment Search Tool (http://www.ncbi.nlm.nih.gov) to search and identify sequences of Pho91 orthologs from different species. We used the protein sequences from NCBI database and aligned using ClustalW Alignment.

Yeast Cultures

We used *Saccharomyces cerevisiae* strain BY4741 (MATa his3Δ1 leu2Δ0 met15Δ0 ura3Δ0). To generate Pho91Δ knockout, we amplified the sequence of Kan4 resistance marker fused with 100 nucleotides upstream and downstream of PHO91 coding sequence. PCR product was used for transformation. For hyperosmotic stress test, yeast liquid cultures were diluted to OD_{600} = 0.1, then diluted serially ½ and each dilution was plated in YPD agar supplemented with NaCl (O.8 M) or Sorbitol (1M).

Table 3.1. Primers used in this study.

Primer	Use
CATGCATATTGACTTTAGGTCCTCTTGGTACCTTTCC CTCTGCTCTTCCTGTTCCCTTCTTATTTTTAGTCCCG ACAGTGCAGGCACGCCACTGCCGCATAAACTACGGT	Knockout TbPho91 – Used to amplify resistance markers from pPOTv6 plasmids
ATAATAACAATAATGACAGCACGACGAAACCGCAGT CCAGCTCCTGTACCCTTCTGTCGATGCGAACGGAAC AAGACAACGCCAACTAAATGGGCACTCG	Knockout TbPho91 – Used to amplify resistance markers from pPOTv6 plasmids
GCGAAGTGGCGTTTTGTCTT	Southern blot probe for coding sequence of TbPho91
AGACGCTGCTACACAGCATT	Southern blot probe for coding sequence of TbPho91
TAGCGGTGCAGCTCTAGTTC	Southern blot probe for 5’ UTR sequence of TbPho91
GGGAAAGGTACCAAGAGGACC	Southern blot probe for 5’ UTR sequence of TbPho91
AGGAAAAATGCCGCTCAAAATCT	Knockout of ScPho91
CAATACAAATGGGCATTGACCAGA	Knockout of ScPho91
TTGGGTACCGGGCCCCCCCTCGAGGTGGGCCTATC CGCCTTAAT	Amplification of ScPho91 for cloning in pRS413
GGATCCCCCGGGCTGCAGGAATTCAATCATAAGTGG TGCGGCCA	Amplification of ScPho91 for cloning in pRS413
GACACGGTAACTTGCAGACTGACATGAAGTTCGGAA AGCG	Amplification of TbPho91 for fusing with ScPho91 UTRs and clone in pRS413
TTTCATTCTCTCTATGGATAATCCTACGGTTTGCCTT CAAA	Amplification of TbPho91 for fusing with ScPho91 UTRs and clone in pRS413
TTGGGTACCGGGCCCCCCCTCGAGGTGGGCCTATC CGCCTTAAT	Amplification of ScPho91 5’UTR for fusing with TbPho91
GTCAGTCTGCAAGTTACCGTGTCACCTTCACAGTTTT CTTTTTATTTG	Amplification of ScPho91 5’UTR for fusing with TbPho91
GATTATCCATAGAGAGAATGAAAGGTTACTAATATAG TATGTATACGTGC	Amplification of ScPho91 3’UTR for fusing with TbPho91
GGATCCCCCGGGCTGCAGGAATTCAATCATAAGTGG TGCGGCCA	Amplification of ScPho91 3’UTR for fusing with TbPho91
GCTGCGAAAAGGCCAGATACTTGG	Amplification of ScPho91 fragment with Y22F mutation
CCAAGTATCTGGCCTTTTCGCAGC	Amplification of ScPho91 fragment with Y22F mutation
TATGTAAATTTCAAACGGCTGAAAAAGTTCATACACA GTTCC	Amplification of TbPho91 fragment with Y22F mutation
GCCGTTTGAAATTTACATAGAAATCTTTCCACTGCTC CA	Amplification of TbPho91 fragment with Y22F mutation

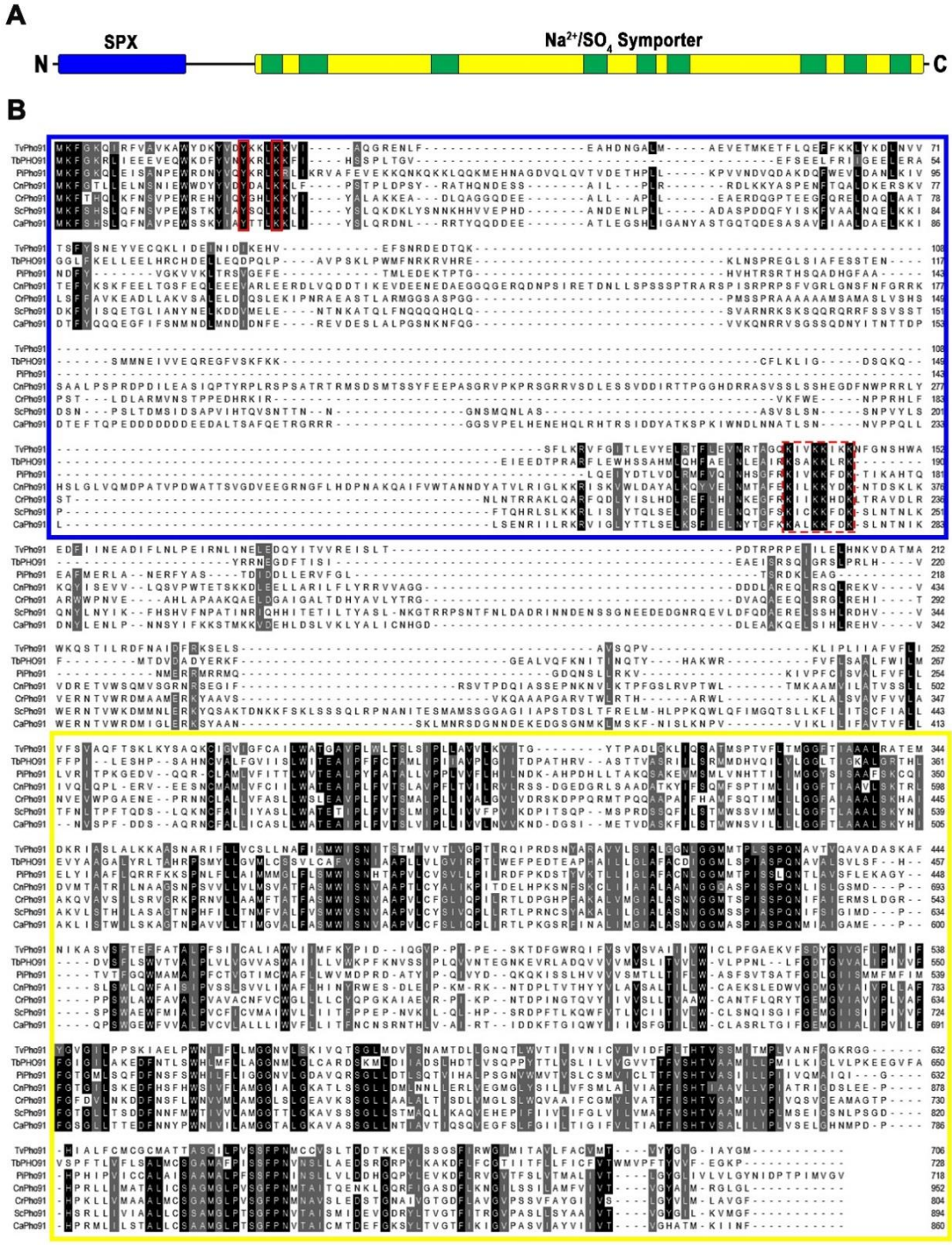

Figure 3.1. A. Conserved domains of TbPho91. The SPX domain (blue) has 190, while the conserved Sodium/Sulphate symporter domain (yellow) has 472 amino acid residues. There are 9 annotated transmembrane domains (green areas). B. Alignment of amino acid sequence of Pho91 from *T. brucei*, *S. cerevisiae*, *Trichomonas vaginalis*, *Phytophthora infestans Cryptococcus neoformans*, *Candida Albicans* and *Chlamydomonas reinhardtii*. Identical (black) and similar (gray) amino acid residues are highlighted. Notice conservation of canonical residues from the IP_6 phosphate binding cluster (solid red boxes) and the lysine surface cluster (dashed red box) (Wild, Gerasimaite et al. 2016).

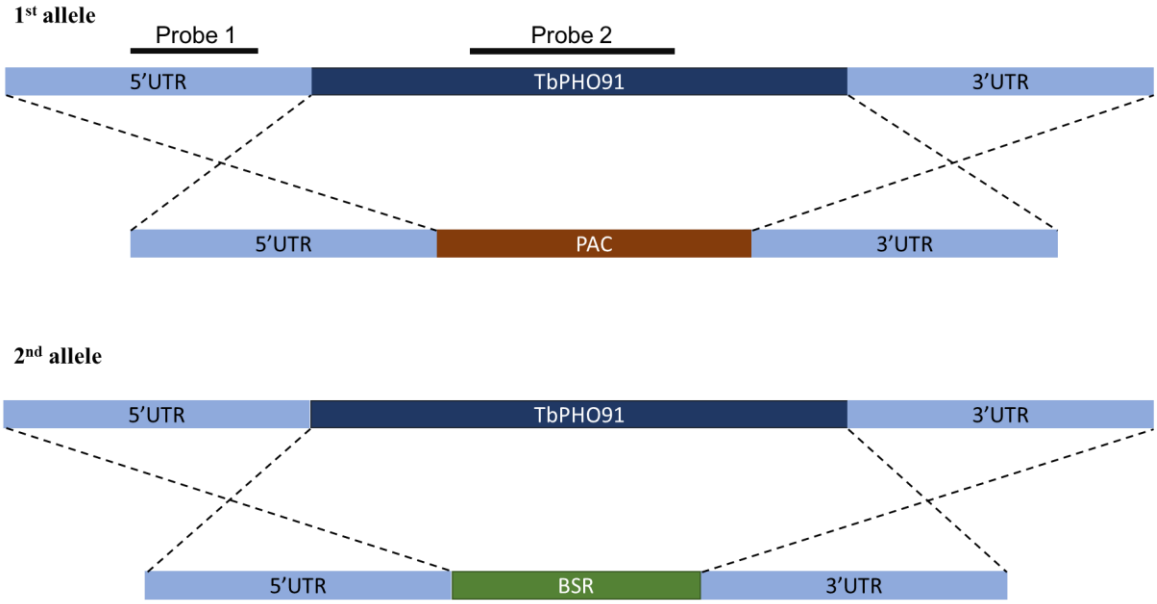

Figure 3.2. Representation of strategy used for homologous recombination replacement of TbPho91 alleles by resistance markers. One allele was replaced by Puromycin N-acetyltransferase (PAC) gene and the other was replaced by Blasticidin S-resistance (BSR) gene. Black bars represent binding targets of 5'UTR and CDS probes used for southern blot in figure 3.4 A.

Yeast transformation was done with 5ml of yeast culture at OD_{600}=1.5-2. We washed cells with water and sterile lithium acetate 0.1 M. Cells were suspended in 240 µl of 50% sterile PEG3350, 36 µl of 1.0 M lithium acetate, 50 µl 2 mg/ml SS DNA and PCR template or plasmid in 36 µl. Mixture was put in vortex for one minute until complete solubilization and then incubated at 30 ºC for 30 minutes. Next, sample was incubated at 42 ºC for 30 minutes and spun down. At last, the cells were suspended in YPD and plated in plates for selection.

Yeast vacuole staining

Vacuolar staining was performed following previous described protocol (Michaillat and Mayer 2013). Briefly, cells were suspended in YPD with 3µM FM4-64 and incubated for 30 minutes at 30 ºC. Then we spun cells and washed in regular YPD twice. We suspended cell

pellet using YPD diluted 5X with water and incubated again at 30ºC for 30 min. Then we visualized using Delta Vision Elite deconvolution microscope (Applied Precision).

Yeast complementation

Constructs for yeast complementation were built on plasmid pRS413. To generate inserts, we amplified by PCR the genomic region of ScPho91 gene, including 400 base pairs upstream and downstream of coding sequence. TbPho91 insert was built by two-step PCR in which we first amplified genomic sequence of TbPho91 and UTR genomic sequences of ScPho91 using primers with homologous 5' sequences. Then we used the previous PCR products as template to generate a new single PCR product with Phusion High-Fidelity DNA Polymerase (NEB) that was cloned in pRS413 (Figure 3.3) using Gibson Assembly® Cloning Kit (NEB) following manufacturer's recommendations. We verified constructs by Sanger sequencing.

Yeast patch clamp

Method for generating enlarged vacuoles and performed patch clamp was previously developed (Yabe, Horiuchi et al. 1999). Briefly, we washed mid-log phase yeast in TRIS-HCl 100 mM (pH 7.2), 5mM DTT, and shake slowly for 10 min. Then cells were washed in 1mM DTT and suspended in 100 mM TRIS-HCl (pH 7.2), 1 mM DTT, 1M sorbitol with 1 mg/ml Zymolyase. We incubated cells for 30 min at room temperature and verified that cells become spherical. Then we spun cells and suspended in 6 ml of YPD supplemented with 1M sorbitol and 0.05 % 2-Deoxy-D-glucose. Cells were placed in shaker at 50 RPM at 25 ºC overnight. To release vacuoles in patch clamp chamber, we used hypo-osmotic shock with 100 mM KCl, 100 mM Sorbitol, 1 mM $MgCl_2$, 10 mM HEPES, pH 7.1. Then we raised osmolarity to prevent disruption of vacuoles by keeping them in 100 mM NaCl, 200 mM Sorbitol, 1 mM $MgCl_2$, 10 mM HEPES, pH 7.1. Patch clamp recording were performed on vacuoles attached to poly-L-

lysine coated chamber. Solution inside micropipette was 100 mM NaCl, 200 mM Sorbitol, 1 mM $MgCl_2$, 5 mM NaH_2PO_4, 5mM Na_2HPO_4, 10 mM HEPES, pH 7.1.

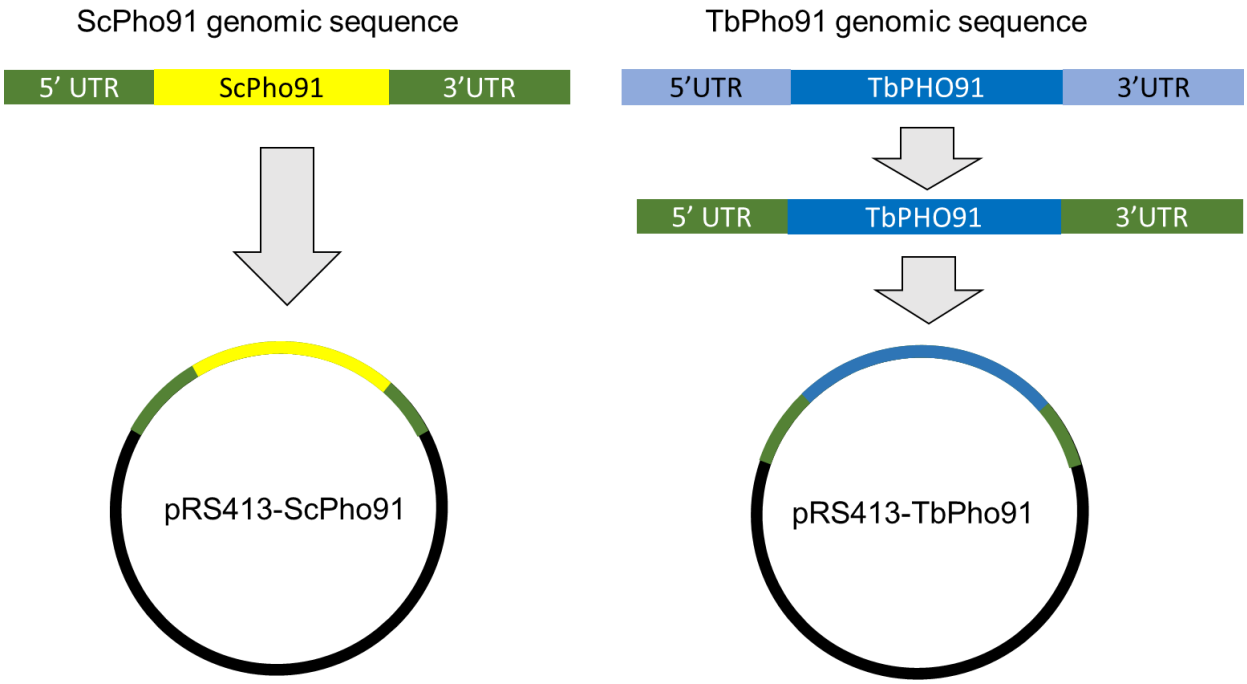

Figure 3.3. Schematic representation of strategy used for cloning of ScPho91 and TbPho91 in pRS413 plasmid for expression in yeast. Left panel. Genomic sequence of ScPho91 (including UTRs) was amplified by PCR and cloned in pRS413. Right panel. Genomic sequence of TbPho91 was fused with UTRs from ScPho91 and then cloned in pRS413.

Inorganic Phosphate and PolyP quantification

We counted cells and used parasites at approximately the same concentration of 10^6 cells per ml. Cells were washed in buffer A with glucose (BAG) twice and immediately suspended in 100 µl of ice cold perchloric acid by pipetting to break cells. Then lysate was incubated on ice for 5 min and spun 15000 g for 5 minutes at 4°C to remove cell debris. Supernatant was transferred to new tube and pH neutralized with KOH (0.8M) $KHCO_3$ (0.8M). Then sample was

spun 15000 g for 5 minutes to remove precipitated salt and supernatant transferred to new tube. Final volume of solution was adjusted to 200 µl and split in two: one half was directly used for phosphate quantification and the other half was used for polyP quantification. Samples can be stored -80 ^{o}C until further use.

Chemical quantification is based on Pi detection by malachite green assay. To quantify polyP we use recombinant ScPPX1 to specifically hydrolyse polyP and release Pi that can be precisely quantified. 100 µl of sample was digested with ScPPX1 in 50 mM TRIS, 2.5 mM $MgSO_4$, pH 7.4 for 1 hour at 37 ^{o}C. We made serial dilution of samples and Pi standards KH_2PO_4 (250 µM) in a 96-well plate immediately before adding the same volume of malachite green mix. Malachite green reagent mix was prepared at least 10 min before reading, by mixing 0.045% Malachite Green in water with 4.2% ammonium molybdate in 4 M HCl at a 1:3 ratio respectively and finally solution is filtered with syringe filter units (Millipore). After mixing samples with reagent we immediately read absorbance OD_{660}. Absorbance values that are within standard curve were adjusted for dilution factor and used to determine final phosphate or polyP concentration.

Irradiation of *T. brucei*

For evaluation of DNA damage recovery, we generated DNA damage with ionizing radiation and determined cell numbers afterwards. We diluted mid-log phase *T. brucei* PCF to 10^6 cells / ml and irradiated with 2000 rads in γ-ray source irradiator. Then cells were returned to incubator and cell number was determined 24 hours after by counting in Neubauer chamber.

Results

TbPho91-KO phenotypic changes

Fungi vacuoles and kinetoplastid acidocalcisomes share important phosphate regulatory membrane proteins: VTC complex that synthesize polyP and simultaneously translocating it to the lumen; and the Pho91 transporter, in charge of phosphate release. The basic phosphate regulation mechanism found in the yeast vacuoles seems to be conserved in trypanosomes. Our initial approach was to look at TbPho91 function in the parasite by generating mutants that do not express TbPho91. *T. brucei* cells are diploid, so we used homologous recombination to replace both copies of the TbPho91 gene with resistance markers to generate knockout cell lines in procyclic form of the parasite (Figure 3.4A). Knockout (KO) of TbPho91 in PCF cells showed no significant grown difference in SDM79 medium compared to wild type (WT) (Figure 3.4B). We then performed immunofluorescence microscopy to assess acidocalcisomes morphology and we observed an enlargement of acidocalcisomes in TbPho91 KO mutants (Figure 3.4C). We counted the larger acidocalcisomes (more than 0.2 μm) and we observed average of 6.5 acidocalcisomes per WT cell and 9.5 acidocalcisomes per TbPho91 KO cell. Distribution of larger acidocalcisomes by size indicate a tendency for enlargement on TbPho91 KO (Figure 3.4D). Given the known function of Pho91 in other organisms, we questioned what is the effect of Pho91 KO in polyP stores. Yeast ScPho91Δ strain keeps same polyP quantity as wild type (Hurlimann, Stadler-Waibel et al. 2007), but TcPho91 knockdown results in reduction in short-chain polyP (Jimenez and Docampo 2015). We used acidic extraction to obtain total inorganic phosphate and short chain polyP content from *T. brucei* cells. Quantification revealed that WT and Pho91 KO have similar amounts of polyP, but Pho91 KO accumulates significantly more inorganic phosphate, due to its inability to release Na^+/Pi (Figure 3.4E).

Survival of TbPho91-KO cells after DNA damage

We postulated that TbPho91 Pi release is important for maintaining phosphate levels, but what chemical reactions require phosphate from stores? Previous data from yeast experiments demonstrated that polyP stores are reduced when cells produce dNTPs for DNA synthesis. This happens during the S phase of the cell cycle or when there is widespread DNA damage (Bru, Samper-Martin et al. 2017). To test if phosphate stores are also important for DNA repair in *T. brucei*, our approach was to generate DNA damage by radiation. After irradiation generated double-strand breaks (DSB), *T. brucei* starts the DNA repair process through homologous recombination, which takes roughly 6 hours (Marin, da Silva et al. 2018). We irradiated *T. brucei* PCF wild type and TbPho91 KO at same cell density using γ-radiation and let cells recover for 24 hours. We then counted cell density and noticed that TbPho91 KO had reduced numbers compared to WT (Figure 3.5). This result indicates that DNA repair and growth recovery in TbPho91 KO takes longer than WT parasites.

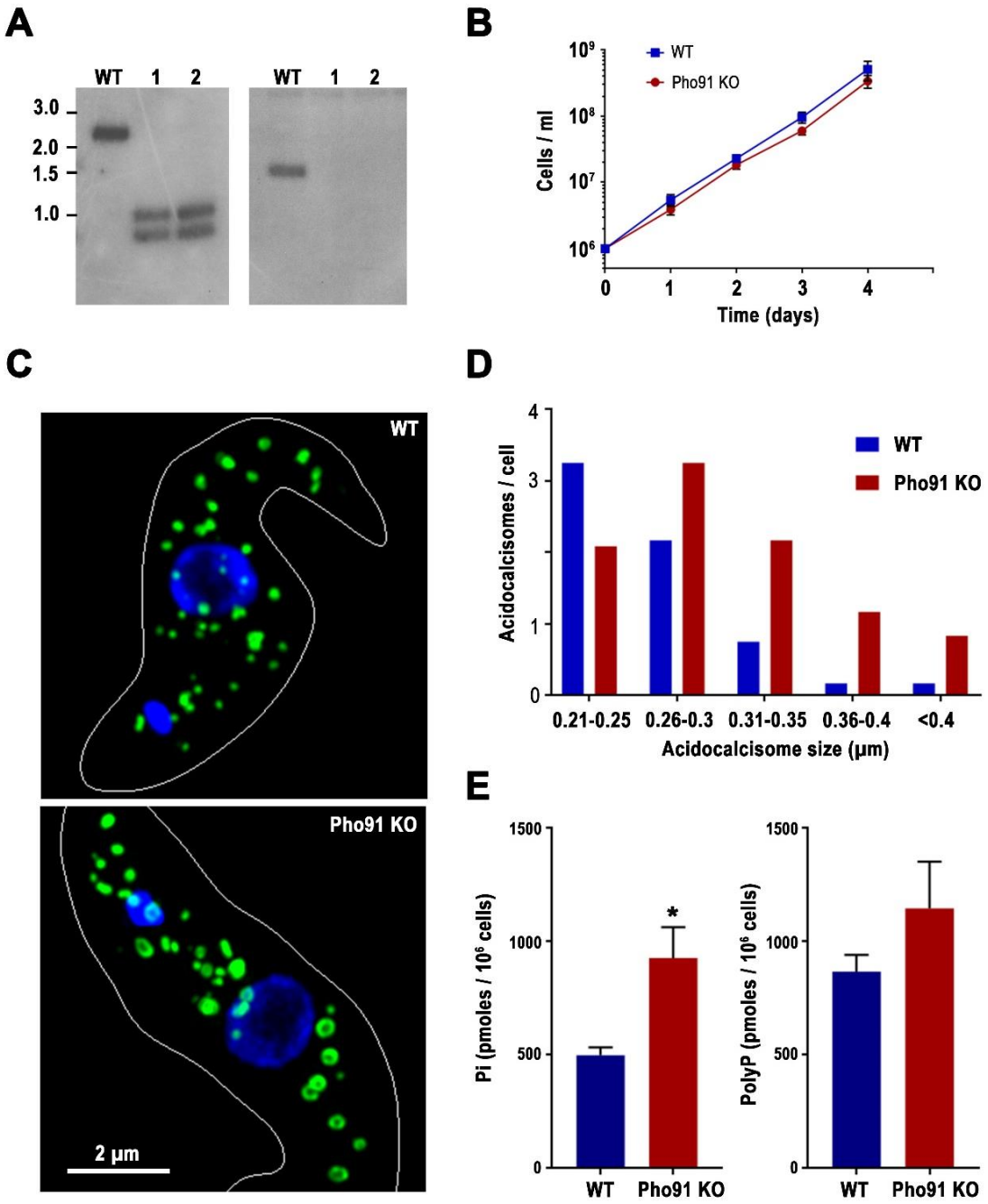

Figure 3.4. TbPho91 is important for phosphate release from acidocalcisomes. A. Southern blot of wild type (WT) cells and two populations of Pho91 knockout mutants (1, 2) generated. We used two probes to show gene displacement: 5'UTR TbPho91 probe (left panel) show CDS was replaced by puromycin and blasticidin resistance markers; and TbPho91 CDS probe (right panel) show sequence was removed from the genome. B. Growth curve of WT and Pho91 KO in *T. brucei* procyclic forms. C. Immunofluorescence microscopy using VP1 antibody to stain acidocalcisomes. D. Numeric distribution of acidocalcisomes bigger than 0.2 µm by size. Acidocalcisomes from ten cells of WT and Pho91 KO were counted, in two independent experiments. E. Quantification of total inorganic phosphate (Pi) and polyP content. Values are mean ± SD, n = 4, *P < 0.01.

Regulation of phosphate release from yeast vacuoles

How is the Na^+/Pi release from acidocalcisomes regulated? We wanted to measure Na^+/Pi release from acidocalcisomes, but it is not possible to perform patch clamp in *T. brucei* acidocalcisomes, for its small size. Due to its similarities to acidocalcisomes, we used yeast vacuole as a model to study Pho91 activation. We first generated a knockout of ScPho91 in yeast using homologous recombination to replace the genomic sequence of ScPho91 for a resistance marker. Yeast Pho91Δ was reported with slower growth under phosphate-limiting conditions, due to lack of capacity to utilize stores. Expression of repressible acid phosphatase (rAPase) Pho5 is inversely correlated with cytosolic Pi, making it an indicator of phosphate availability (Auesukaree, Homma et al. 2004). Tests of rAPase activity after phosphate starvation in ScPho91Δ found hyper-activation compared to wild type, indicating inability of ScPho91Δ cells to release phosphate from stores (Yokota, Gomi et al. 2017). To assess if Pho91p absence generates vacuolar alterations, we stained vacuoles of WT and ScPho91Δ with FM4-64 and visualized by fluorescence microscopy. We did not observe any morphological difference in ScPho91Δ (Figure 3.6A).

ScPho91 is a sodium phosphate transporter, therefore it may be important for sodium equilibrium. We investigated the possibility that sodium release from vacuoles affect survival after salt stress. Sodium chloride hyperosmotic stress leads to a vacuolar fragmentation that lasts for about 10 to 20 min. Then they recover normal size as cells acclimate to different medium composition by using long-term responses. Interestingly, Kcs1Δ (IP6K) is sensitive to NaCl and sorbitol stress, indicating that synthesis of 5-IP_7, and maybe polyP as well, is important for hyperosmotic stress response (Dubois, Scherens et al. 2002). A high throughput search for vacuole fragmentation defects reported Pho91Δ as having a small defect in vacuolar

fragmentation (Michaillat and Mayer 2013). If ScPho91 is important for vacuolar Na^+/Pi release during or after hyperosmotic shock, gene deletion may affect growth in high salt media. Thus, we tested survival of ScPho91Δ in hyperosmotic plates consisting of YPD supplemented with NaCl (0.8 M) or Sorbitol (1 M). There was no significant growth change in hyperosmotic plates (Figure 3.6 B).

To directly measure Na^+/Pi release, we used a method previously developed to generate larger vacuoles and perform whole-organelle patch clamp (Yabe, Horiuchi et al. 1999). First, we tested wild type vacuoles with the most abundant inositol phosphate IP_6 at physiological levels (1-100 µM), which did not stimulate currents. We used concentration of 1 mM IP_6 and we observed 80 pA release currents (Figure 3.7 A). We then tested the two isomers of IP_7 found in yeast: 1 µM of 5-IP_7 generated 50 pA currents (Figure 3.7 A), whereas 1-10 µM 1-IP_7 led to little or no vacuolar currents (Figure 3.7 B). ScPho91 has strong specificity to IP6K product 5-IP_7. We then tested the ScPho91Δ vacuoles and did not detect currents using the same concentration of IP_6 or 5-IP_7 (Figure 3.7 C). Next we generated plasmid constructs for expression of ScPho91 or TbPho91 in ScPho91Δ. We cloned genomic sequence of ScPho91 or TbPho91 in plasmid vector pRS413 that maintain one single copy per cell, and, to ensure expression at endogenous levels, we also inserted the upstream promoter region of ScPho91. Complementation with ScPho91 or TbPho91 restored currents upon stimulation with IP_6 or IP_7 (Figure 3.7 D,E). We then tested if SPX domain is directly involved in activation of transporters. To test this, we generated a point mutation in complementation constructs in which we replaced the tyrosine (Y) 22 of the SPX, essential for binding inositol phosphates (Wild, Gerasimaite et al. 2016), for a phenylalanine (F). Complementation using constructs that express $ScPho91^{Y22F}$ or $TbPho91^{Y22F}$ resulted in

significantly reduced or completely abolished currents induced by IP_6 or 5-IP_7 (Figure 3.7 F,G). Taken together our results show that inositol pyrophosphates trigger release of Na^+/Pi by Pho91.

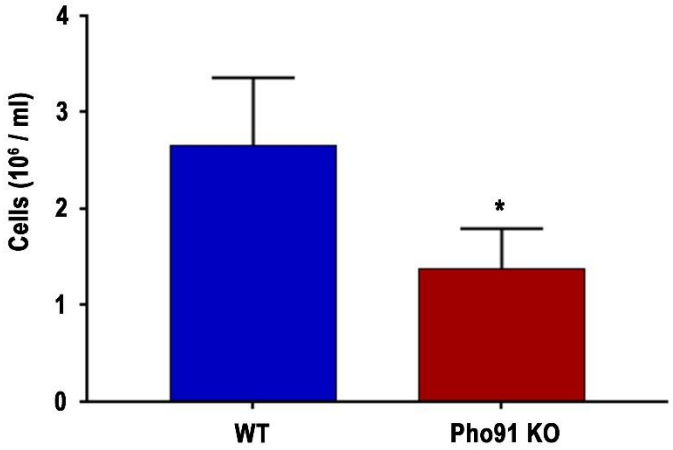

Figure 3.5. TbPho91 is important for survival after DNA damage. Cell density of irradiated parasites was estimated after 24 hours. Values are means ± SD, n=4, *P < 0.05.

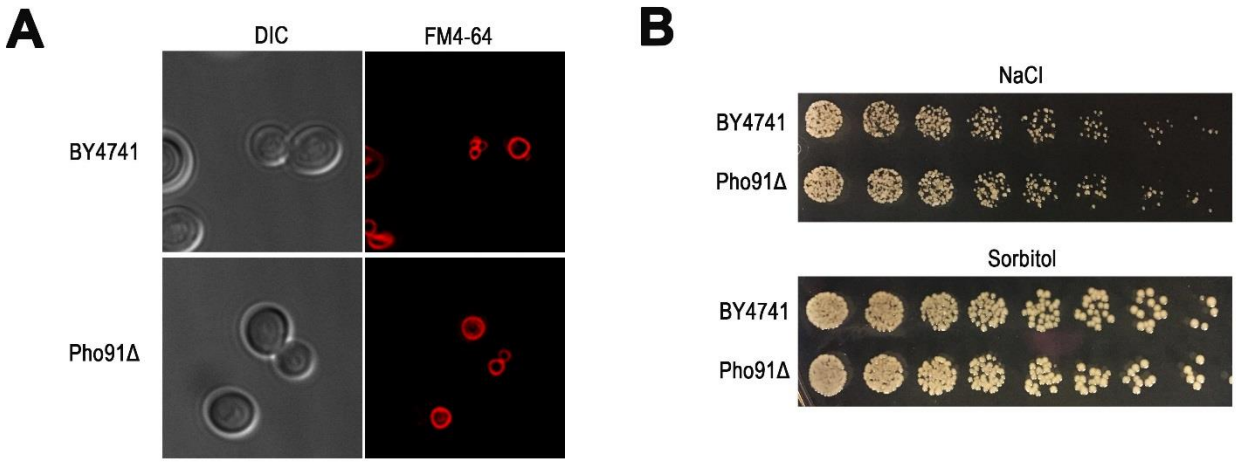

Figure 3.6. ScPho91Δ preserve vacuole integrity and normal growth in hyperosmotic medium. A. Wild type (BY4741) and Pho91Δ yeast were stained with FM4-64 to visualize vacuole morphology. B. Growth in YPD supplemented with NaCl (O.8 M) or Sorbitol (1M).

Discussion

We report here the characterization of Na^+/Pi TbPho91 and ScPho91 transport and their regulation by inositol pyrophosphates. We observed that knockout of *T. brucei* TbPho91 resulted in no change in polyP, but higher accumulation of inorganic phosphate what led to enlargement of acidocalcisomes. In yeast, polyP is also unchanged in ScPho91Δ (Hurlimann, Stadler-Waibel et al. 2007), but total inorganic phosphate was not measured. Contrary to TbPho91 KO, ScPho91Δ does not lead morphological alteration in vacuoles. We also noted that TbPho91 KO has delayed recovery after radiation-induced DNA damage, an indication that consumption of Pi stores is relevant for DNA repair. We then successfully demonstrated that the Na^+/Pi transport of TbPho91 and ScPho91 is stimulated by 5-IP_7.

Maintaining adequate levels of Pi is vital: lack of Pi stall cell replication (Shirahama, Yazaki et al. 1996)) whereas excess of Pi in yeast that have uncontrolled Pi uptake results in growth deficiency (Hurlimann, Pinson et al. 2009). What is the role of Pho91 for Pi levels maintenance? Pho91 is found Fungi, Protozoa and unicellular algae, distant organisms with diverse life strategies such as parasitism, mutualistic cooperation or free-living. Interestingly, our alignment analysis found that the key amino acids required for IP_7 binding are conserved among Pho91 orthologs. The inositol phosphate pathway is broadly distributed in eukaryotes, and so is the SPX regulatory domain. Furthermore, the majority of proteins that contain SPX domain are involved in phosphate homeostasis, so it was suggested that inositol pyrophosphates are major regulators of phosphate homeostasis (Azevedo and Saiardi 2017). We propose that management of intracellular stores may be important across various groups for maintaining adequate Pi levels, and the regulation of Pho91 symporter by inositol pyrophosphates is fundamental for this balance.

In *S. cerevisiae*, both low-affinity plasma membrane transporters, ScPho87 and ScPho90, have SPX domain. They may be also regulated by inositol phosphates or inositol pyrophosphates. Considering that these transporters are expressed only in high external Pi conditions, their transport regulation must account for maintaining stable phosphate concentration during nutrient fluctuations that do not activate PHO pathway. Upon substantial depletion of Pi, the PHO pathway is activated resulting in expression of high affinity Pi symporters, which do not have SPX domain. Yet, it is not well established how levels of 5-IP_7 vary in response to phosphate starvation. There have been conflicting results reported. Yeast cells starved of phosphate for 2 hours have increase in 1-IP_7 generated by Vip1 (PPIP5K). The HPLC IP_7 signal observed had two peaks, which could represent different isomers of IP_7 (Lee, Mulugu et al. 2007). 1-IP_7 generated by Vip1 binds to Pho80-Pho85-Pho81 complex and inactivates the kinase activity of the complex (Lee, Huang et al. 2008), leading to de-phosphorylation of the transcription factor Pho4 and its translocation to the nucleus, resulting in transcription of PHO genes (Springer, Wykoff et al. 2003). A reduction in IP_7 was reported when cells were starved of Pi for 2 hours, and when Pi was added back there was a rapid increase in IP_7 (Lonetti, Szijgyarto et al. 2011). Nevertheless, the authors did not determine which isomer was detected, but it may correspond to 5-IP_7. Pi starvation drastically reduces ATP levels, which should lead to less 5-IP_7 synthesis (IP6K has high Km for ATP). In conclusion, the current data on Pi starvation support a scenario of elevated 1-IP_7 activating PHO pathway and reduced 5-IP_7, leading to less polyP synthesis. Pi consumption from vacuoles during starvation is explained by ScPho91 leak of Na^+/Pi, as we observed before addition of IP_6 or 5-IP_7 (Figure 3.7 A). The 5-IP_7 mediated ScPho91 activation may be relevant in conditions in which PHO pathway is not active.

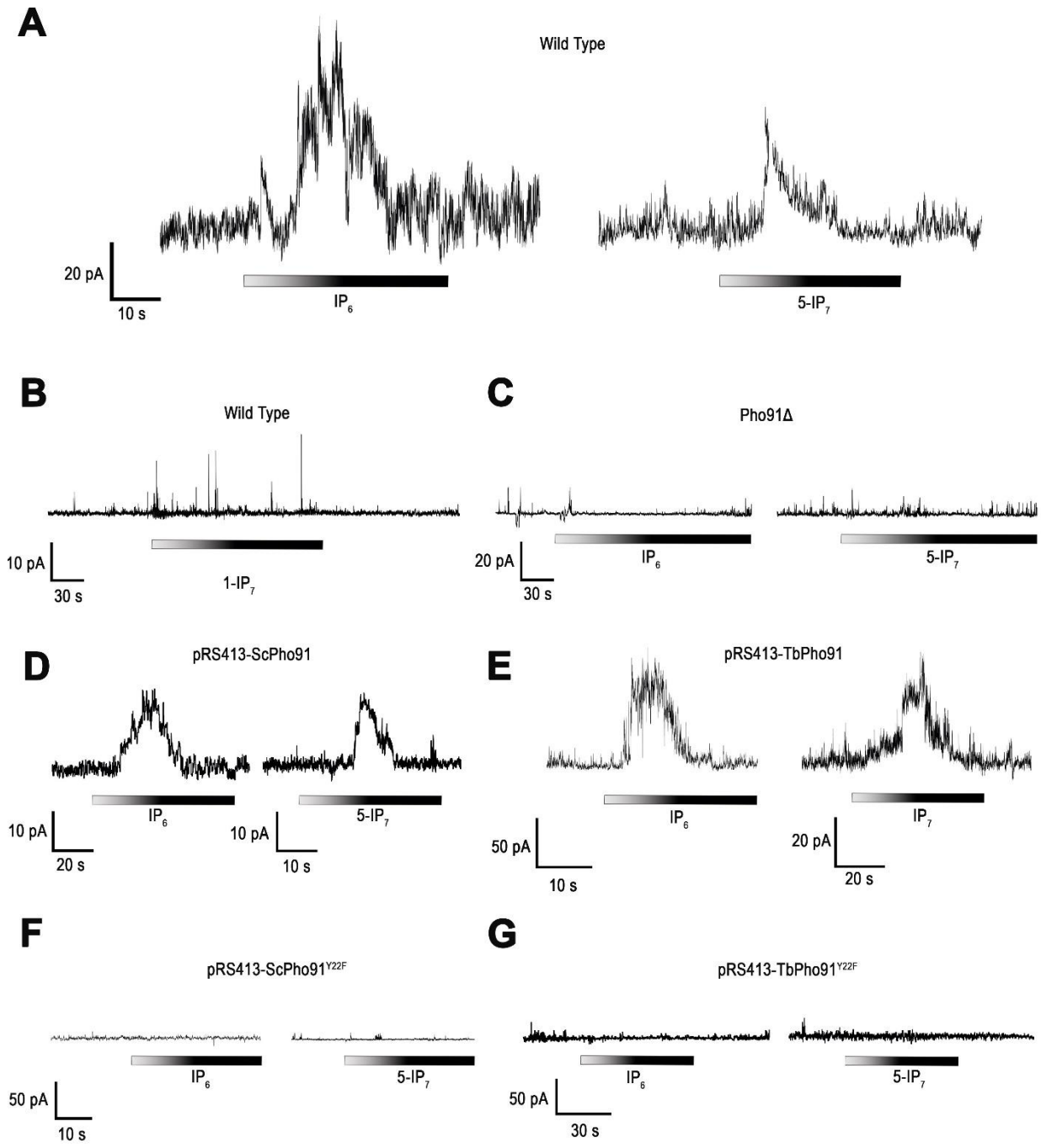

Figure 3.7. IP_6 and 5-IP_7 induce SPX domain mediated activation of Na^+/Pi currents in ScPho91 and TbPho91 expressing vacuoles. Bar under each tracing represents when solution containing the indicated compound was injected in chamber. A. Activation of Na^+/Pi currents on vacuoles from wild type yeast after injection of IP_6 (1mM) or 5-IP_7 (1µM). B. Effect of 1 µM 1-IP_7 on wild type vacuoles. C. Pho91Δ vacuoles cannot release currents after injection of IP_6 or 5-IP_7. D, E. Complementation of Pho91Δ with ScPho91 or TbPho91 restore vacuoles response to IP_6 and 5-IP_7. F, G. Complementation of Pho91Δ with mutated ScPho91^{Y22F} or TbPho91^{Y22F} does not restore vacuoles ability to release Na^+/Pi currents. Data is representative of four independent experiments.

Our data supports previous reports of SPX-containing proteins binding specifically to inositol pyrophosphates. It has been reported that 1-IP_7 binds the N-terminal segment of Pho81, which contains an SPX domain. 5-IP_7 generated by Kcs1 (IP6K) did not bind Pho81, showing its specificity for 1-IP_7 isomer (Lee, Huang et al. 2008). Likewise, the yeast VTC complex has specificity for different IP_7 or IP_8 isomers. 1-IP_7 and 5-IP_7 generated by Vip1 and Kcs1 respectively have similar capacity to induce polyP synthesis by this complex, whereas IP_6 has negligible effect under physiological conditions (Gerasimaite, Pavlovic et al. 2017). Remarkably, the higher VTC *in vitro* activity observed using isolated yeast vacuoles was registered with IP_8 (Gerasimaite, Pavlovic et al. 2017). Kcs1Δ leads to reduction in polyP synthesis, while Vip1Δ has no significant changes in polyP content (Lonetti, Szijgyarto et al. 2011, Gerasimaite, Pavlovic et al. 2017), which suggests Kcs1 activity is more relevant for polyP storage. Ipk1Δ (homolog of IP5K) generates no IP_6 synthesis and increase in polyphosphate, confirming IP_6 does not stimulate polyP synthesis in vacuole. Ipk1Δ shows elevated synthesis of PP-IP_4 (also capable of stimulating VTC activity) that would explain the higher polyP content of those cells (Lonetti, Szijgyarto et al. 2011). It was hypothesized that InsPP, mainly 5-IP7, would inhibit ScPho91 since InsPPs in general stimulate polyP synthesis (Azevedo and Saiardi 2017). Surprisingly, our data shows 5-IP_7 can trigger release of phosphate from vacuoles. We believe there may be additional forms of regulation that participates in vacuolar phosphate control. We looked at annotated post-translational modification of residues in the SPX domain of all *S. cerevisiae* and *T. brucei* SPX-containing proteins and we found plentiful targets (Table 3.1). Interestingly, lysine K26 (essential for binding with IP_7) of ScPho91 and ScVTC2 can be succinylated (Table 3.2). Succinylation of residues alter charge of lysine from positive to negative and this may affect transporter state and sensitivity to 5-IP_7 (Weinert, Scholz et al.

2013). It is tempting to speculate that this could be a mechanism to control SPX binding and alter activity. Additionally, numerous phosphorylation sites were detected, including in SPX of TbVTC4 (Table 3.2).

Another function of ScPho91 is to assist nutrient recycling in the cell, done by yeast vacuole through autophagy. For instance, in growing yeast, the majority of RNA is ribosomal and half of total protein content as well. Upon nitrogen starvation, cells cannot keep growing or producing proteins, so ribosome assembly is stalled, protein synthesis reduced, and old ribosomes are recycled. Ribosomal proteins and RNA are imported to autophagosomes and end up in the vacuole, where they are degraded along with other cellular components (Huang, Kawamata et al. 2015). RNA is degraded by RNases and phosphatases to release Pi and nucleosides. ScPho91 is important for release of phosphate that is recycled to the cytosol. Phospholipids internalized in vacuole can be degraded and release phosphate as well (Yang, Huang et al. 2017). Metabolomics of phosphate starving cells reported choline is accumulated, what indicates recycling of phospholipid phosphatidylcholine (Boer, Crutchfield et al. 2010, Klosinska, Crutchfield et al. 2011). Additionally, lack of phosphate can specifically induce ATG11-dependent autophagy by inactivation of TORC1 signaling pathway (Yokota, Gomi et al. 2017). Under phosphate limiting conditions, an efficient recycling of nutrients may result in better chances of survival.

In the cyanobacteria Synechococcus elongatus, coordination between polyphosphate bodies and DNA distribution throughout cell cycle seems to correlate with DNA replication. Researchers observed that during the light period, when cells are replicating, the polyphosphate bodies reduce in size. They attribute this size reduction to consumption of polyP for synthesis of DNA and RNA, which contain almost half of total phosphate in these cells. During the dark

period, when cells are not dividing or consuming phosphate for DNA and RNA synthesis, the polyphosphate bodies enlarge. It was proposed that polyphosphate is important for DNA replication by supplying phosphate required for nucleotide synthesis (Seki, Nitta et al. 2014). Two independent metabolomics studies examined yeast cells under depleted phosphate medium and showed nucleotide precursor metabolites are elevated while dNTPS levels are reduced (Boer, Crutchfield et al. 2010, Klosinska, Crutchfield et al. 2011). These results confirms phosphate is required for synthesis of nucleotides in yeast. Furthermore, yeast mutants that do not have polyP (Vtc4Δ) or have difficulty using polyP stores (lack polyphosphatases PPN1/PPX1) have a prolonged time for DNA duplication. These mutants also have reduced dNTPs levels in phosphate-limiting conditions compared to wild type cells in same conditions. Vtc4Δ has a decrease in genome stability when cultivated in low phosphate, probably due to lower dNTPs concentration (Bru, Martinez-Lainez et al. 2016). The DNA replication and repair require four canonical dNTPs at the right proportion. Changes in concentration of one or more dNTPs may lead to incorporation problems and increase in mutation rate (Meuth 1989). Additionally, yeast cells under stress, in which there is cell cycle arrest, accumulate longer polyP chains in the vacuole and dividing cells have smaller chains of polyP. This suggests that during growth and cell division there is a turnover of polyP (Klompmaker, Kohl et al. 2017). Indeed, polyP levels are reduced during the S phase in *S. cerevisiae*, while dNTPS levels concomitantly increase (Bru, Samper-Martin et al. 2017). Taken together, yeast cells degrade polyP and use some of the phosphate for dNTP synthesis and DNA replication. Similarly, we hypothesized that phosphate from stores in *T. brucei* helps dNTPs synthesis and therefore it is important for DNA repair. Absence of TbPho91p results in lower growth recovery after DNA damage. In conclusion, we present a new function of the transporter TbPho91 on DNA replication of

Trypanosomes. We also unveiled an evolutionary conserved regulatory mechanism for release of phosphate from stores by the transporter Pho91.

Table 3.2. Post-translational modifications in SPX domains of proteins from *S. cerevisiae* and *T. brucei*.

Protein	Residue	Modification	Reference
ScGDE1	S61	phosphorylation	(Albuquerque, Smolka et al. 2008)
ScPHO81	S42	phosphorylation	(Albuquerque, Smolka et al. 2008)
	S42	phosphorylation	(Albuquerque, Smolka et al. 2008)
ScPHO87	K89	ubiquitination	(Swaney, Beltrao et al. 2013)
	K102	ubiquitination	(Swaney, Beltrao et al. 2013)
	K102	ubiquitination	(Peng, Schwartz et al. 2003)
	K124	ubiquitination	(Swaney, Beltrao et al. 2013)
	S127	phosphorylation	(Swaney, Beltrao et al. 2013)
	K130	ubiquitination	(Swaney, Beltrao et al. 2013)
	S146	phosphorylation	(Swaney, Beltrao et al. 2013)
	S147	phosphorylation	(Swaney, Beltrao et al. 2013)
	S227	phosphorylation	(Holt, Tuch et al. 2009)
ScPHO90	K164	ubiquitination	(Swaney, Beltrao et al. 2013)
ScPHO91	K26	succinylation	(Weinert, Scholz et al. 2013)
	S191	phosphorylation	(Albuquerque, Smolka et al. 2008)
	S201	phosphorylation	(Albuquerque, Smolka et al. 2008)
ScSYG1	K35	ubiquitination	(Swaney, Beltrao et al. 2013)
	S44	phosphorylation	(Albuquerque, Smolka et al. 2008)
	K82	ubiquitination	(Swaney, Beltrao et al. 2013)
	S149	phosphorylation	(Swaney, Beltrao et al. 2013)
	S149	phosphorylation	(Albuquerque, Smolka et al. 2008)
	S149	phosphorylation	(Holt, Tuch et al. 2009)
	S172	phosphorylation	(Swaney, Beltrao et al. 2013)
	S172	phosphorylation	(Albuquerque, Smolka et al. 2008)
	S175	phosphorylation	(Swaney, Beltrao et al. 2013)
	S179	phosphorylation	(Swaney, Beltrao et al. 2013)
	S179	phosphorylation	(Holt, Tuch et al. 2009)
	S179	phosphorylation	(Albuquerque, Smolka et al. 2008)
ScVTC2	K26	succinylation	(Weinert, Scholz et al. 2013)
ScVTC3	S43	phosphorylation	(Albuquerque, Smolka et al. 2008)
	S43	phosphorylation	(Holt, Tuch et al. 2009)
	S43	phosphorylation	(Soulard, Cremonesi et al. 2010)
	S45	phosphorylation	(Holt, Tuch et al. 2009)
	S50	phosphorylation	(Holt, Tuch et al. 2009)
ScVTC4	S16	phosphorylation	(Albuquerque, Smolka et al. 2008)
	K75	ubiquitination	(Swaney, Beltrao et al. 2013)
ScVTC5	S43	phosphorylation	(Holt, Tuch et al. 2009)
TbVTC4	S93	phosphorylation	(Urbaniak, Martin et al. 2013)
	Y106	phosphorylation	(Urbaniak, Martin et al. 2013)
	S110	phosphorylation	(Urbaniak, Martin et al. 2013)

CHAPTER 4

CHARACTERIZATION OF POLYPHOSPHATASE ACTIVITY OF NUDIX HYDROLASES FROM *TRYPANOSOMA BRUCEI*

Introduction

The nudix superfamily is an ancient group of proteins that over millions of years of evolution have acquired various functions: pyrophosphohydrolases, A/G-specific adenine glycosylases, isopentenyl diphosphate isomerases and proteins with non-enzymatic activity (Srouji, Xu et al. 2017). Within the nudix superfamily, the nudix hydrolases (PF00293) are the pyrophosphohydrolases initially found to cleave nucleoside diphosphates, hence the name nudix (Nucleoside Diphosphate linked to moiety X). Nudix hydrolases have a conserved sequence called nudix box ($GX_5EX_7REUXEEXGU$) where U is a bulky alphatic residue and X is any amino acid (Srouji, Xu et al. 2017). The nudix motif is the catalytic site. Glutamic acid residues within the nudix motif bind to divalent cations cofactors like Mg^{2+} and Mn^{2+}, mutations on these residues can reduce the activity considerably (Yoshimura and Shigeoka 2015).

Human Nudix 5 can hydrolize poly(ADP-ribose) to ADP-ribose which is used to generate ATP required for nuclear cell replication (Wright, Lioutas et al. 2016). In plants, dozens of proteins containing the nudix motif have been described and there is high redundancy of nudix activity. For example, three nudix proteins from *Arabidopsis thaliana* can hydrolize ADP-ribose and NADH pyrophosphate bonds. Other substrates are 8-oxo-(d)GTP, GDP-mannose, CoA, mRNA cap, thiamin diphosphate, FAD. *A. thaliana* nudix functions are house-cleaning of harmful metabolites, metabolic control and stress response. It has been proposed that nudix can

help eliminate oxidized nucleotides that can be damaging to the cell. Hydrolisis of poly(ADP-ribose) can help regulate DNA damage repair and programmed cell death. AtNUDX7 activity regulates NADH levels important for growth and development. AtDCP2 is a decapping mRNA enzyme, knockout of this protein accumulated mRNAs and had a lethal phenotype suggesting that it is important for mRNA turnover and plant development (Yoshimura and Shigeoka 2015).

Human nudix DIPP1 is capable of hydrolyzing 5-diphosphoinositol pentakisphosphate (IP_7), 5-diphosphoinositol tetrakisphosphate ($PP\text{-}IP_4$) and 1,5-diphosphoinositol tetrakisphosphate ($1,5\text{-}IP_8$) (Safrany, Caffrey et al. 1998). DIPP activity is not restricted to inositol phosphates, it was reported that human DIPP1, DIPP2 and DIPP3 and its yeast homolog DDP1 are endopolyphosphatases that can degrade polyphosphates (PolyP). PolyP is a linear polymer of phosphate that can range from three to hundreds of phosphate units. PolyP is considered an ancient molecule, it has been found in all evolutionary groups, from bacteria to protozoa and mammals. In *Trypanosoma brucei*, polyP is synthesized by the VTC complex into the acidocalcisome, an important organelle that stores phosphate, calcium and other metal ions. There are several enzymes called polyphosphatases that can hydrolyse polyP to shorter sizes and release inorganic phosphate (Lander, Cordeiro et al. 2016). Exopolyphosphatases are enzymes that remove the terminal phosphate from polyP releasing inorganic phosphate, and endopolyphosphatases cleave internal phosphates generating shorter polyphosphate molecules (Shi and Kornberg 2005).

In *Trypanosoma brucei*, two polyphosphatases have been characterized: TbPPX1 (Luginbuehl, Kunz et al. 2011) and TbVSP (Lemercier, Espiau et al. 2004). There is no endopolyphosphatase identified, although one ortholog of yeast PPN1 is in the genome of *T. brucei* (Table 4.1). In comparison, *S. cerevisiae* has four known polyphosphatases: ScPPX

(YHR201C), ScPPN1 (YDR452W), ScPPN2 (YNL217W) and Ddp1 (YOR163W). Ddp1 and its human homologs DIPP1, DIPP2 and DIPP3 have endopolyphosphatase activity (Lonetti, Szijgyarto et al. 2011). Interestingly, these yeast and human enzymes also have an inositol pyrophosphate hydrolase that help regulate inositol pyrophosphates signaling (Lonetti, Szijgyarto et al. 2011).

Table 4.1. Phosphatases identified in *T. brucei* genome.

Name	TriTryp.org I.D.	Localization	References
TbPPX1	Tb927.9.3280	Cytosolic	(Luginbuehl, Kunz et al. 2011)
TbVSP1	Tb927.11.7060 Tb927.11.7080	Cytosolic / acidocalcisome	(Lemercier, Espiau et al. 2004, Galizzi, Bustamante et al. 2013)
TbPPN1	Tb927.4.1110	Unknown	
TbNH2	Tb927.5.4350	Glycosome	This study
TbNH4	Tb927.6.2670	Cytosol	This study

Trypanosoma brucei has five nudix proteins identified, of which two have been characterized. Nudix Hydrolase 1 (TbNH1 or MERS1) binds to the RNA-editing complex and help on stabilizing edited mRNAs (Weng, Aphasizheva et al. 2008); nudix hydrolase 4 (TbNH4 or TbDcp2) is an mRNA decapping enzyme that removes 5' cap from processed mRNAs (Ignatochkina, Takagi et al. 2015). TbNH2 and TbNH3 were identified in the latest glycosome proteome, but the localization was not validated by microscopy (Guther, Urbaniak et al. 2014). Functions of TbNH2, TbNH3 and TbNH5 have not yet been studied. We studied here the regulation of polyP metabolism by the nudix hydrolases from *T. brucei*. We identified two polyphosphatases: TbNH2 and TbNH4 that have exopolyphosphatase and endopolyphosphatase activity, respectively.

Experimental procedures

Chemicals and reagents

Chemically synthesized 5-diphosphoinositol pentakisphosphate (Gerasimaite, Pavlovic et al. 2017) was provided by Dr. Henning Jessen, Albert-Ludwigs-University of Freiburg, Germany. PolyP60 was a gift from Dr. Toshikazu Shiba, RegeneTiss Inc., Tokyo, Japan.

Cell Cultures

Trypanosoma brucei brucei procyclic (PCF) Lister 427, 29-13 TetR/T7RNAP and bloodstream (BSF) SM TetR/T7RNAP cell lines were used. Procyclic cells were cultivated at 28ºC in SDM-79 (Cunningham 1977) supplemented with 10% heat-inactivated FBS and hemin (7.5µg/ml). Drug concentrations used for selection and maintenance of procyclic cell lines were: Hygromycin (50 µg/ml), G418 (15 µg/ml), Blasticidin S (5 µg/ml). Bloodstream cells were cultivated at 37ºC with 5% CO_2 in HMI-9 medium (Hirumi and Hirumi 1989) and 10% heat-inactivated FBS. Drug concentration used for selection and maintenance of bloodstream cell lines were: G418 (5 µg/ml), Blasticidin S (2.5 µg/ml).

Cloning, primers, expression and SDS-PAGE

The sequences of TbNH1 (Tb927.11.15640), TbNH2 (Tb927.5.4350), TbNH3 (Tb927.11.9810), TbNH4 (Tb927.6.2670) and TbNH5 (Tb927.10.4680) were amplified from genomic DNA by PCR (Table 4.2) and cloned in expression vector pET32 Ek/LIC (Novagen) following manufacturer instructions. Constructs inserts were verified by Sanger sequencing and then transformed in *Escherichia coli* BL21-CodonPlus(DE3). Protein expression was induced by addition of 0.1 mM isopropyl β-D-1-thiogalactopyranoside (IPTG) to bacterial cultures in Luria Bertani broth shaking for 2h at 25ºC. Culture was chilled on ice and bacteria harvested by centrifugation. Pellet was suspended in 20 mM Tris HCl, 150 mM NaCl, pH7.4 with protease

inhibitors (Sigma P8465) and sonicated on ice. Lysate was then centrifuged 15,000 G for 30 min and then filtered on 0.8 µm syringe filter units (Millipore). Protein purification was performed using Nickel column HIS-Select® Cartridge as recommended by manufacturer. Elution fractions with purified protein were dialyzed, replacing elution buffer for 300 mM NaCl, 200 mM Tris HCl, pH 7.4 with 20% glycerol. Expression was verified by SDS-PAGE followed by coomassie blue staining and protein aliquots were stored at -80^{o}C until further use. Protein concentration was determined using Pierce BCA Protein Assay Kit (Thermo Scientific) as instructed by manufacturer.

Nudix hydrolases activity tests

Nudix activity assays were performed at 37^{o}C using 50 mM NaCl, 40 mM HEPES buffer (pH 7.4 unless stated otherwise), 0.25 µmoles of polyP60 or 5 nmoles of 5-diphosphoinositol pentakisphosphate (IP_7), 6 mM $MgCl_2$ or other specified cation and about 0.5 µg/ml of recombinant protein for 1 h or indicated time. For enzymatic reactions at different pHs, we used MES buffer for pH 5.5 to 6.5, HEPES for pH 7.0 to 8.0 and Tris-base for pH 8.5. Enzymatic reactions were stopped by addition of 3 µl of 100 mM EDTA and kept on ice or frozen until further use. Products were resolved by polyacrylamide gel electrophoresis using 30 or 35% acrylamide/bis-acrylamide 19:1 (National Diagnostics) gels in Tris/Borate/EDTA (TBE) buffer as previously described (Losito, Szijgyarto et al. 2009). Gels were then stained with toluidine blue for 1h and de-stained on 20% methanol for several hours until background staining was removed.

For kinetic measurements, the same activity test was performed at pH 8.0 using various quantities of indicated substrate for 10 min. Then inorganic phosphate released from substrates was quantified by malachite green assay. First, we prepared reagent mix (0.045% Malachite

Green with 4.2% ammonium molybdate in 4 M HCl at a 1:3 ratio respectively) and let it sit for at least 10 minutes, and then filtered the solution with 0.2 µm syringe filter units (Millipore). We then added 100 µl of reagent mix to 100 µl of reaction in a clear 96 wells plate, mixed well and immediately read absorbance at 660 nm. We quantified phosphate through comparison with standard curve made by serial dilution of KH_2PO_4. Phosphate concentration obtained was used for kinetic calculations and plotted in GraphPad Prism software.

Endogenous tagging

We generated cell lines with endogenous C-terminal tag using a one-step transfection method (Oberholzer, Morand et al. 2006). We amplified by PCR a cassette from pMOTag4H using primers that contained 80 nt homologous region of the 3' end of CDS and 3'UTR of TbNH2 and TbNH4. Construct was verified by agarose gel electrophoresis, PCR purified using Minelute PCR purification kit (Qiagen) and transfected in *T. brucei* Lister 427 PCF cells. Transfection was performed as described before and cells were selected using Hygromycin (Cordeiro, Saiardi et al. 2017). Culture lysates, SDS-PAGE and western blot using anti-HA antibody (Covance) were performed to verify expression of tagged proteins (Cordeiro, Saiardi et al. 2017). We used microscopy to localize tagged proteins, sample preparation for immunofluorescence microscopy was performed as described before (Cordeiro, Saiardi et al. 2017).

Table 4.2. Primers used in this study.

Primer	Use
GACGACGACAAGATGCGCAAGCAATTATTTTTC	(fwd); cloning of TbNH1 in pET32
GAGGAGAAGCCCGGTTCACGATGCATCTTCCC	(rev); cloning of TbNH1 in pET32
GACGACGACAAGATGTACCGAAAAAATGTATGTGTGGTA	(fwd); cloning of TbNH2 in pET32
GAGGAGAAGCCCGGTTTATATGGAAGACCTTGTTTTCAAAAATGC	(rev); cloning of TbNH2 in pET32
GACGACGACAAGATGAGGGACCGCTATATCAG	(fwd); cloning of TbNH3 in pET32
GAGGAGAAGCCCGGTTCAGAGAGTTGCTATTTTCAGAC	(rev); cloning of TbNH3 in pET32
GACGACGACAAGATGCCAAACGAAACCGCGG	(fwd); cloning of TbNH4 in pET32
GAGGAGAAGCCCGGTTCACTCGCAGGAGGTGGG	(rev); cloning of TbNH4 in pET32
GACGACGACAAGATGGCTATGGGAAGAGTTT	(fwd); cloning of TbNH5 in pET32
GAGGAGAAGCCCGGTCTAACGCTTTCCAAGTGGG	(rev); cloning of TbNH5 in pET32
GAACGTTGCCCGAAAGAAAAGCAACATATTTTTGTTGCGGTATCGAAGGTGGCGATCCCCATGGCTAAGGCATTTTTGAAAACAAGGTCTTCCATAGGTACCGGGCCCCCCCTCGAG	(fwd); C-terminal tagging of TbNH2; template pMOTag4H
TCTCCTCTCTCCTTCCCCCTTCCCTCACCTTCCTTCTCCCTTTCCGTATAAAATTCAAGTAACAGCATGGACAGTTTGAAGAGAGAGAGAAATGGCGGCCGCTCTAGAACTAGTGGAT	(rev); C-terminal tagging of TbNH2; template pMOTag4H
AATCAATTGTTACATGAGGAGGGAGGTTCCCCTCAGATGAATTTACTTGGAAACCCCACCTCCTGCGAGCGAGACGGGTGGGGGTTTTCGGGTACCGGGCCCCCCCTCGAG	(fwd); C-terminal tagging of TbNH4; template pMOTag4H
CGAGGAGCCAAATGCAAAGAGGATATTAAACATTATTTTTATGCGATGTTACAATGCCACTGTGAGAGCTATACGAGGTGTCGTTTTTCTTGGCGGCCGCTCTAGAACTAGTGGAT	(rev); C-terminal tagging of TbNH4; template pMOTag4H
TAAAATTCACAAGCTTATGTACCGAAAAAATGTATGTGTGGTAATA	(fwd); cloning of TbNH2 in pLEW100v5b1d-BSD
TAAATGGGCAGGATCCTTATATGGAAGACCTTGTTTTCAAAA	(rev); cloning of TbNH2 in pLEW100v5b1d-BSD
TAAAATTCACAAGCTTATGCCAAACGAAACCGCGGGTAA	(fwd); cloning of TbNH4 in pLEW100v5b1d-BSD
TAAATGGGCAGGATCCTTACGAAAACCCCCACCCGTC	(rev); cloning of TbNH4 in pLEW100v5b1d-BSD
GCAAAGCAGGAGTTCTCCCA	(fwd); qRT-PCR of TbNH2
CCACCTTCGATACCGCAACA	(rev); qRT-PCR of TbNH2
GGAAACGACGGCGTAAGAGA	(fwd); qRT-PCR of TbNH4
ACCCGTCTCGCTCGCA	(rev); qRT-PCR of TbNH24
GTATAGCGTGTGGATTGGCGG	(fwd); qRT-PCR of Actin
TGCTGTGTACGATGCTGGG	(rev); qRT-PCR of Actin

Construct overexpression

Sequences of TbNH2 (Tb427. 05.4350) and TbNH4 (Tb427.06.2670) were amplified by PCR using Q5® high-fidelity polymerase (NED) and cloned in the vector pLEW100v5b1d-BSD using the Gibson Assembly® Cloning kit (NEB). Sequences were verified by Sanger sequencing and plasmids transfected in *T. brucei* procyclic 29-13 TetR/T7RNAP and bloodstream SM TetR/T7RNAP cell lines. Cells were cultured for 2 days with Tetracycline (1 µg/ml) for induction of overexpression.

To verify overexpression we extracted RNA, synthesized cDNA and performed by qRT-PCR as described previously (Cordeiro, Saiardi et al. 2017). Relative gene expression data was obtained by comparison with actin expression levels. We also used western blot analysis with specific antibody to validate increase in TbNH2 protein translation.

Antibody Production

We digested the recombinant protein construct of TbNH2 with Thrombin (Sigma) to remove thioredoxin and HIS-tag from the construct. Then we applied products in HIS-Select® Cartridge column to remove tag from mixture, allowing us to collect pure TbNH2 in the flow-through. This protein was quantified using Pierce BCA Protein Assay Kit (Thermo Scientific) and used for antibody production. The antigen was injected to six female CD-1 mice (Charles River Laboratories) intraperitoneally. The primary inoculation contained 100 µg purified protein mixed in equal parts with Freund's complete adjuvant (Sigma). Subsequent boosts, spaced in 2 weeks intervals, contained 50 µg purified protein mixed in equal parts with Freund's incomplete adjuvant (Sigma). Final bleeds were collected via cardiac puncture.

Results

Characterization of Nudix hydrolases from *T. brucei*

Human Nudix Hydrolase DIPP has been previously identified as a polyphosphatase. To test nudix hydrolases phosphatase activity, we amplified the sequences from *T. brucei* genomic DNA by PCR, cloned and expressed the recombinant proteins in bacteria. We were able to obtain purified proteins that were used on activity tests with polyP. A qualitative analysis of polyphosphate size using polyacrylamide gel electrophoresis (PAGE) shows if each enzyme can degrade polyP. We first tested activity of TbNH1, TbNH2, TbNH3, TbNH4, TbNH5 with polyP60 and polyP700. Then the enzymatic products were resolved by polyacrylamide gel electrophoresis (PAGE). We observed that TbNH2 and TbNH4 can degrade polyP60, however only TbNH4 was able to degrade polyP700 (Figure 4.1). This result indicates that TbNH2 have higher affinity to polyP of smaller sizes. TbNH1, TbNH3 and TbNH5 did not show any activity under the same conditions. We also tested the enzymes activity on 5-diphosphoinositol pentakisphosphate (IP_7) at pH 6.5, 7.5 and 8.5 without success (Figure 4.2).

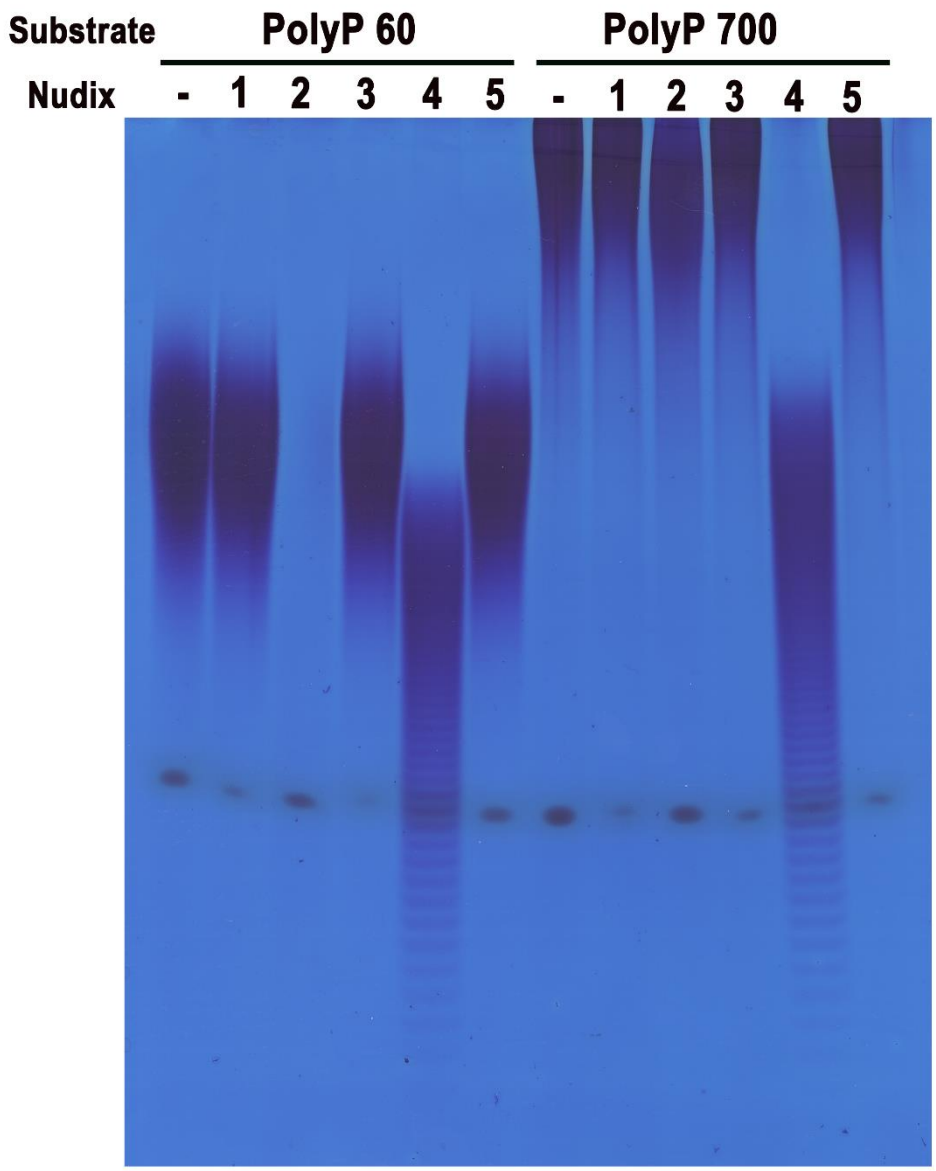

Figure 4.1. Activity test of nudix hydrolases identified two polyphosphatases in *T. brucei*. We tested the capacity of nudix hydrolases to degrade short polyP (polyP60) and long polyP (polyP700). Control (-) and enzymatic products from nudix 1, 2, 3, 4 and 5 were assayed and resolved in 30% acrylamide gel. TbNH2 has high activity with polyP60 and apparently no activity with polyP700. TbNH4 has activity with both polyP60 and polyP700, as evidenced by shorter polyP sizes. Data are representative of 3 independent experiments.

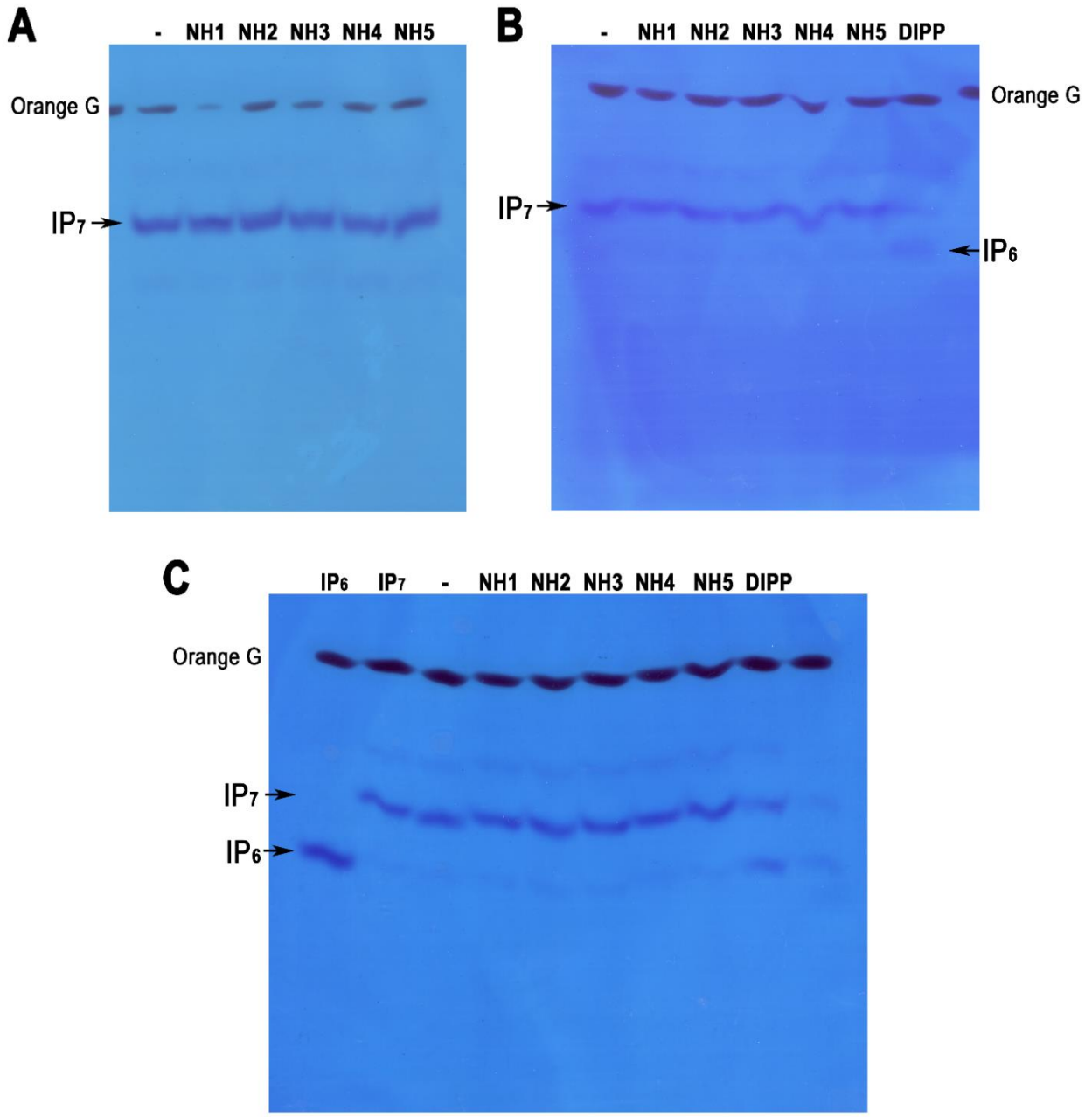

Figure 4.2. Nudix hydrolases from *T. brucei* do not hydrolyze IP_7. We tested activity of TbNH1, TbNH2, TbNH3, TbNH4 and TbNH5 on substrate 5-diphosphoinositol pentakisphosphate (IP_7) at pH 6.5 (A), 7.5 (B) or 8.5 (C). We used recombinant human DIPP as control for enzymatic reaction and we observed about half of the IP_7 hydrolyzed into IP_6. Gel images are representative images of 3 independent experiments.

Characterization of TbNH2

We tested the activity of TbNH2 on polyP60 over the course of one hour and resolved the products by PAGE (Figure 4.3 A). Yeast Ddp1 has been reported to have higher activity at slightly acidic pH, while human DIPPs have preference for higher pH (Lonetti, Szijgyarto et al. 2011). TbNH2 has highest activity at basic pH 8.0 (Figure 4.3 B). We tested activity of TbNH2 with different cofactors. TbNH2 was able to hydrolyze polyP with magnesium and cobalt, and it also has lower activity with manganese (Figure 4.3 C). We used the malachite green assay to detect free phosphate released from polyphosphate or ATP/ADP. The kinetic curve of TbNH2 with polyP60 and polyP700 confirmed the higher affinity to shorter lengths of polyP compared to longer polyP700 (Figure 4.3 D, top). The Km for polyP60 is 200.5 μM with Vmax of 20.6 $pmol*\mu g^{-1}*min^{-1}$, and the Km for polyP700 is 125.6 μM with Vmax of 1.1 $pmol*\mu g^{-1}*min^{-1}$. This difference in affinity based on polyP size indicates the enzyme work by removing terminal phosphate from polyP chains, exopolyphosphatase activity. Interestingly, using same method we detected TbNH2 also has activity to release the γ and β phosphates from ATP and ADP (Figure 4.3 D, bottom).

Characterization of TbNH4

We also tested the activity of TbNH4 over the course of one hour (Figure 4.4 A). TbNH4 has a slightly lower activity on polyP60 than TbNH2. Activity tests at various pHs showed TbNH4 has optimum activity at pH 8.0 (Figure 4.4 B). We then tested TbNH4 activity using several common cofactors, and we determined that it is active in presence of magnesium or manganese only (Figure 4.4 C). Unlike TbNH2, TbNH4 does not use cobalt as cofactor. The malachite green assay for detection of phosphate released shows 50% higher affinity for polyP60 than polyp700 (Figure 4.4 D). Km for polyP60 is 90.1 μM with Vmax of 9.1 $pmol*\mu g^{-1}*min^{-1}$

and Km for polyP700 is 71.0 µM with Vmax of 4.9 pmol*µg^{-1}*min^{-1}. TbNH4 does not have phosphatase activity on ATP or ADP.

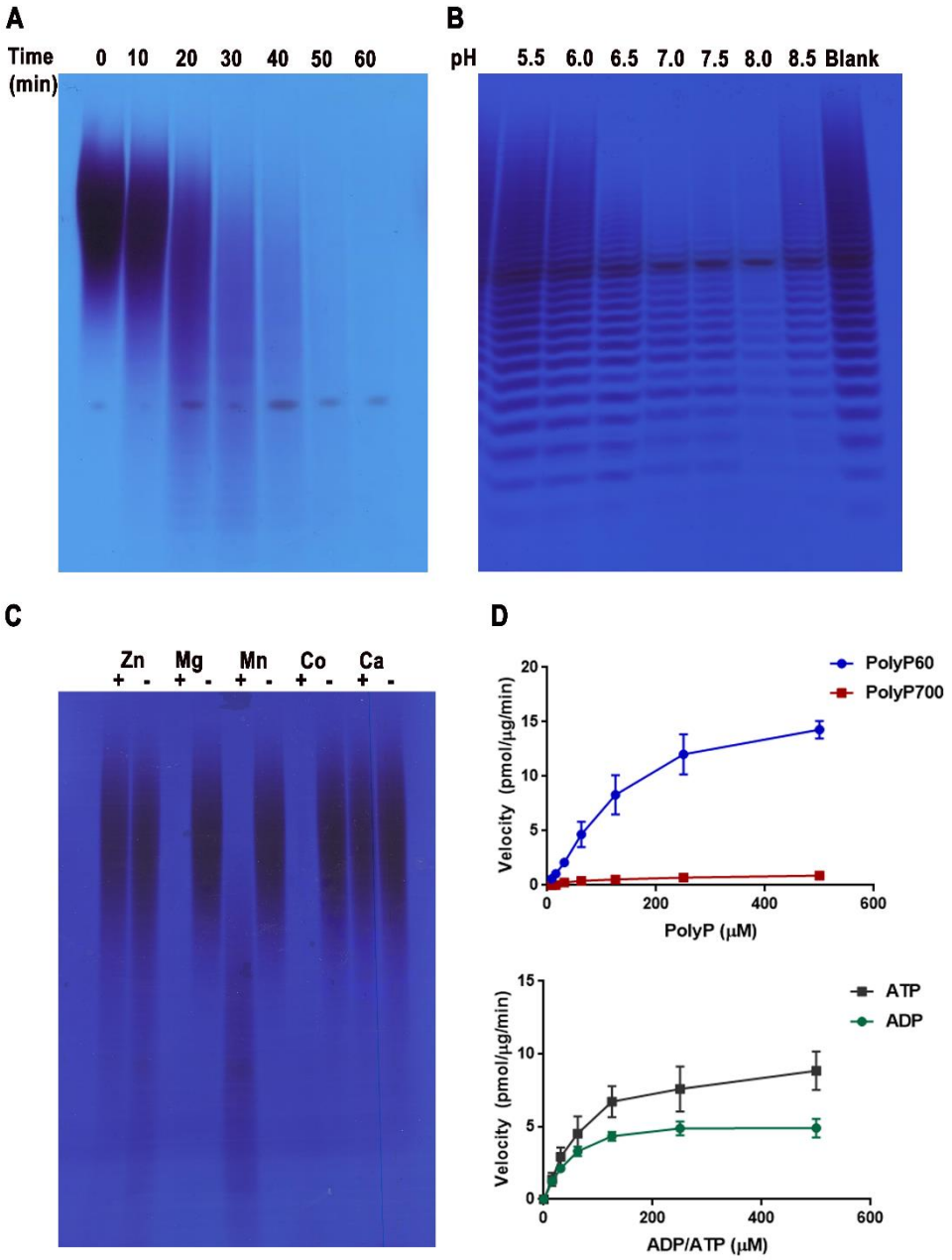

Figure 4.3. TbNH2 activity characterization. A, Degradation of polyP by TbNH2 over time. B, TbNH2 activity at various pH conditions. C, TbNH2 activity with ions zinc (Zn), magnesium (Mg), manganese (Mn), cobalt (Co) and calcium (Ca). D, kinetic curves of TbNH2 measured by quantification of phosphate released from polyP60, poly700, ATP and ADP. Notice that there is some activity on polyP700, which is about 10 times lower than activity with polyP60.

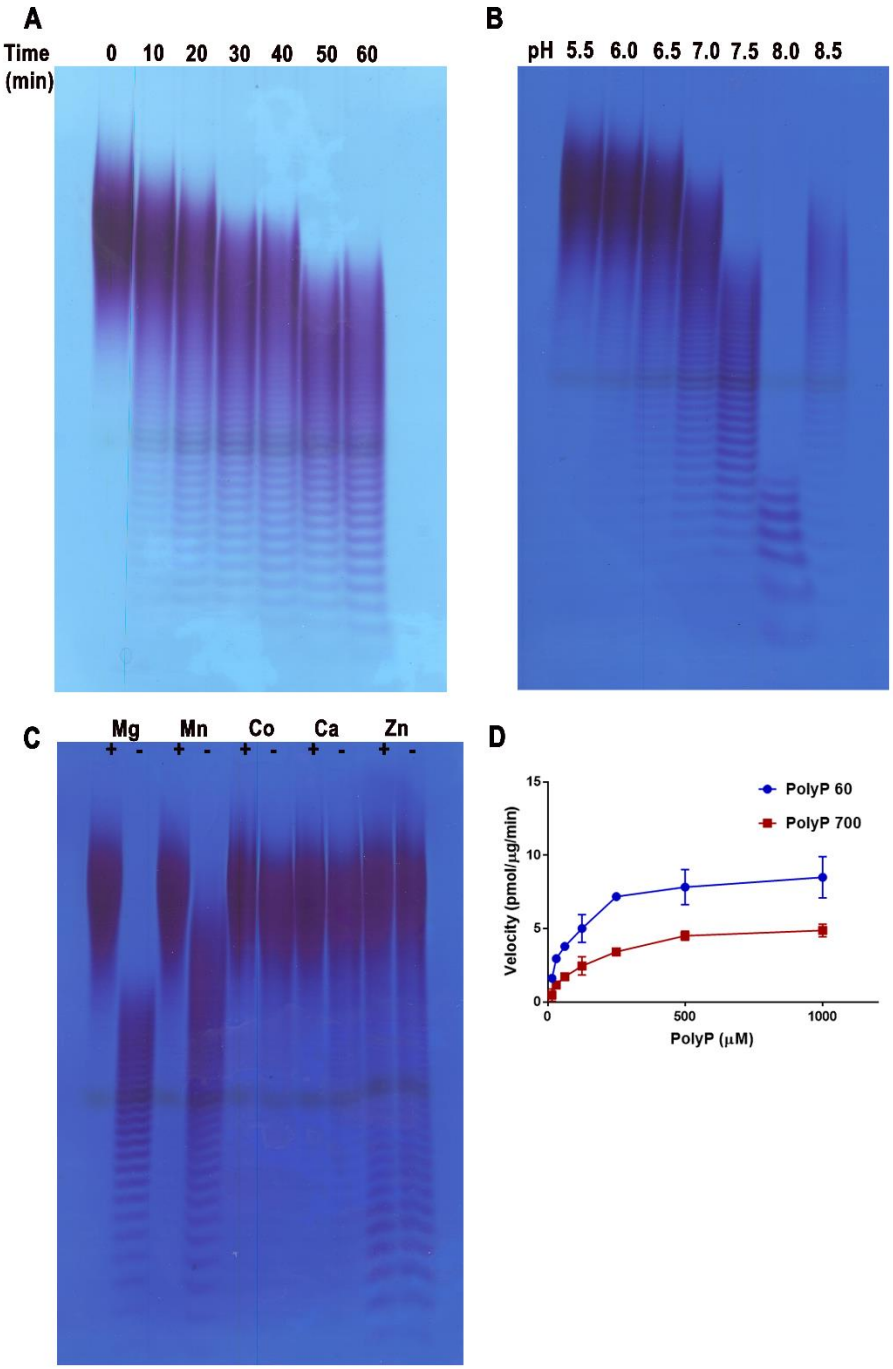

Figure 4.4. TbNH4 activity characterization. A, Degradation of polyP by NH4 over time. B, NH4 activity at various pH conditions. C, TbNH4 activity with ions magnesium (Mg), manganese (Mn), cobalt (Co), calcium (Ca) and zinc (Zn). D, kinetic curves of TbNH4 measured by quantification of phosphate released from polyP60 and polyP700.

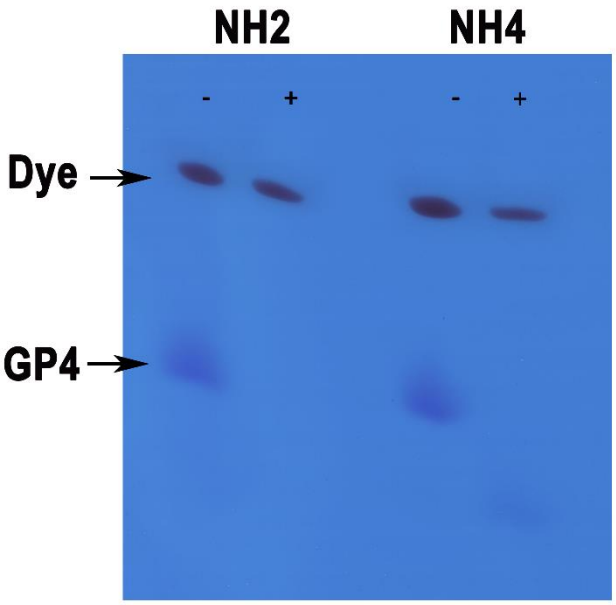

Figure 4.5. TbNH2 and TbNH4 can degrade guanosine tetraphosphate (GP4). Enzymatic reaction incubated with (+) and without (-) purified enzymes were resolved PAGE 35%, showing a band that corresponds to the orange dye used for loading and GP4.

Finally, we wondered if TbNH2 and TbNH4 can dephosphorylate other molecules that have several phosphates attached. To test this hypothesis, we assayed the activity of TbNH2 and TbNH4 with guanosine 5'-tetraphosphate (GP4) and we observed degradation of GP4 (Figure 4.5).

Localization studies

Trypanosomes accumulate substantial amounts of polyphosphate. Acidocalcisomes are a significant storage of polyphosphate, pyrophosphate and phosphate (Moreno, Urbina et al. 2000). Polyphosphate has also been found in glycosomes and nucleus of *T. brucei* by using a polyphosphate binding domain (PPBD) (unpublished data). To determine the localization of TbNH2 and TbNH4, we used *in situ* tagging to generate endogenous C-terminal tag in procyclic forms of *T. brucei*. Western blot analysis using anti-HA antibodies confirmed that TbNH2 and

TbNH4 are expressed in PCF and have expected size of 23 kDa and 37 kDa with tag respectively (Figure 4.6 A). Immunofluorescence microscopy shows NH4 localize in cytosol of the cells (Figure 4.6 D). NH2 has been found in independent proteomes of the glycosome (Colasante, Ellis et al. 2006, Guther, Urbaniak et al. 2014) and has a glycosomal localization signal at the C-terminus (SSI) that could be blocked by the HA tag, leading to mislocalization of the protein. Our attempts to use N-terminal tag to confirm glycosomal localization of TbNH2 were unsuccessful, therefore we decided to use specific antibody to localize NH2. We cloned TbNH2 and TbNH4 in vector pLEW100 for overexpression of protein in *T. brucei* 2913 cell lines. We performed real time PCR of parasites induced with tetracycline for 2 days (Figure 4.6 B) to confirm increase in transcripts. For native protein detection, we produced antibody against TbNH2 in mice. Our polyclonal antibody recognized a weak band at the expected size of 19 kDa and we observed a significant increase in the corresponding band area after overexpression (Figure 4.6 C). Then we performed immunofluorescence microscopy to co-localize TbNH2 signal with the glycosomal marker Pyruvate Phosphate Dikinase (PPDK) (Figure 4.6 D). Overexpression did not lead to mislocalization as the TbNH2 signal was restricted to glycosomes.

Knockout of any of the known yeast polyphosphatases alone have no significant effect on total polyphosphate content observed by gel electrophoresis (Lonetti, Szijgyarto et al. 2011, Gerasimaite and Mayer 2017). Still, a multiple knockout of PPN1 and PPN2, the two vacuolar polyphosphatases, lead to reduction in polyP turnover and accumulation of long chain polyP due to its inability to degrade vacuolar polyP (Gerasimaite and Mayer 2017). We performed knockdown of TbNH2 or TbNH4, but we did not observe a significant decrease in growth or change in polyphosphate content in the cells (data not shown).

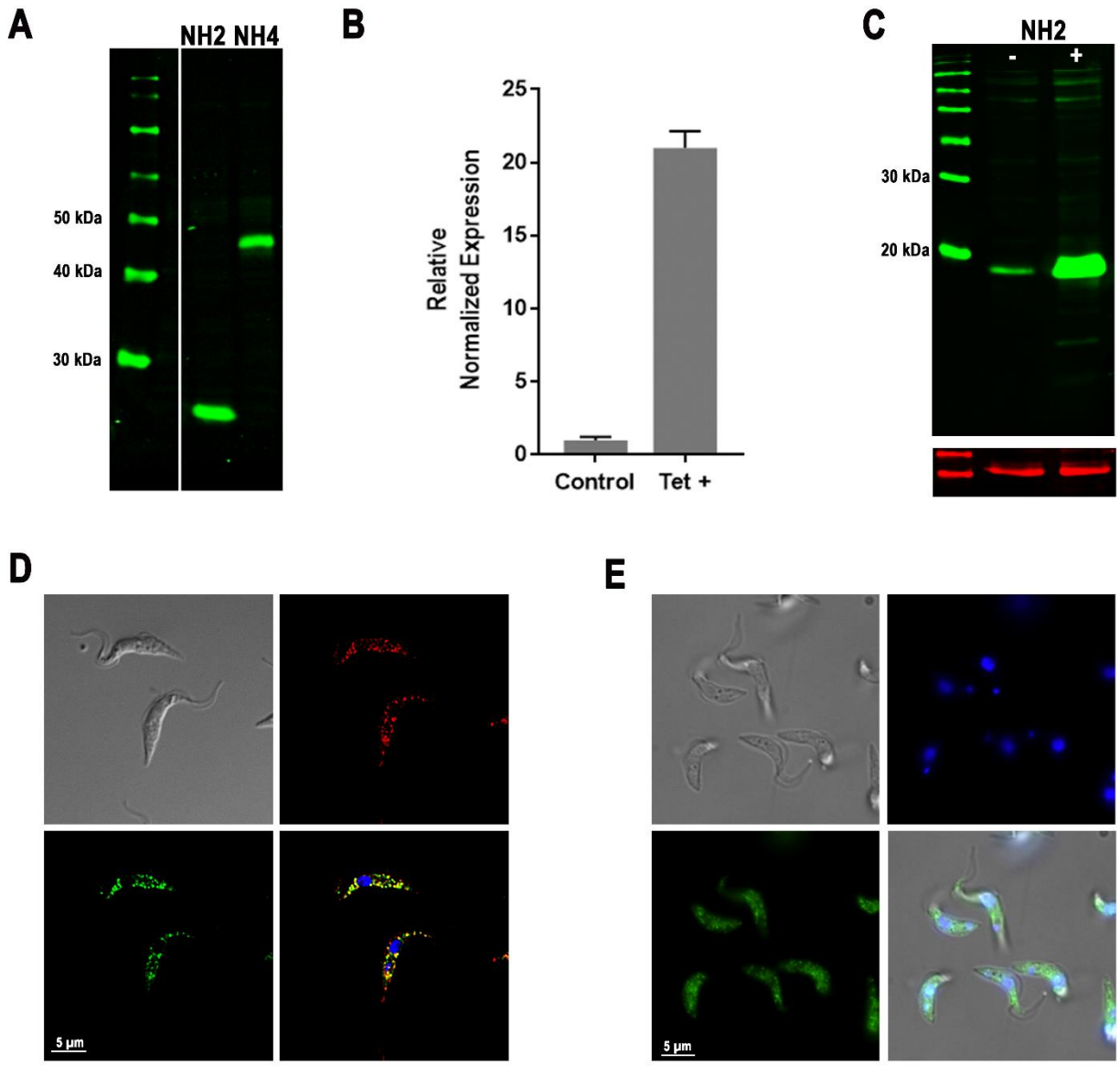

Figure 4.6. TbNH2 is a glycosomal and TbNH4 is a cytosolic protein. A, Western blot showing expression of C-terminal tagged TbNH2 (19 kDa) and TbNH4 (34 kDa). B, Real time PCR showing relative expression levels of TbNH2 and TbNH4 overexpression cells lines of *T. brucei* PCF. Values are means ± SD, n=3. C, Western blot of cells lines overexpressing TbNH2. D-E, Immunofluorescence microscopy was used to determine co-localization of TbNH2 (green) with glycosomal marker PPDK(red) (D) and TbNH4 cytosolic distribution (E).

Discussion

Our investigation discovered two new polyphosphatases from *T. brucei*: TbNH2 and TbNH4. TbNH2 is glycosomal and TbNH4 is cytosolic. We also tested activity of all *T. brucei* nudix on 5-IP_7 without success, demonstrating a difference from mammalian DIPP and yeast nudix Ddp1.

There is little information on polyP processing enzymes of *T. brucei*, so we characterized TbNH2 and TbNH4 activity on polyphosphate degradation. TbNH2 has higher activity than TbNH4 on polyP60, but TbNH2 has low activity on polyP700. PolyP is a linear polymer made only of phosphate, so there is no chemical difference among different chain lengths. However, there is a difference on the number of terminal phosphates available for an exopolyphosphatase. This is a measurement artifact created by the way polyP is quantified. The convention is to quantify amounts of polyP by molarity of phosphate units in the sample. Therefore, polyP60 and polyP700 at same molarity have the same amount of phosphate units, but not the same number of molecules. The activity of an exopolyphosphatase should be the same only if there is the same number of molecules in solution. Our kinetic curves show about 10 times reduction in Vmax between polyP60 and polyP700. This result confirms TbNH2 has exopolyphosphatase activity.

Alkaline pH and divalent ions (Mg^{2+}) have been found before to be important for Nudix activity (Yoshimura and Shigeoka 2015). TbNH2 and TbNH4 have similar optimum pH around 8.0. We observed that TbNH2 and TbNH4 require mainly Mg^{2+}, but they both work with less efficiency with Mn^{2+}. Nudix hydrolases typically require Mg^{2+} or Mn^{2+} (McLennan 2006), but some nudix from *Myxococcus xanthus* have preference for Co^{2+} (Kimura, Yamamoto et al. 2018). Yeast Ddp1 polyphosphatase activity requires Mg^{2+} or Co^{2+} (Lonetti, Szijgyarto et al. 2011). We also detected similar activity of TbNH2 with Mg^{2+} or Co^{2+}. Considering Mg^{2+} is the

more abundant than Mn^{2+} or Co^{2+}, it must be the main cofactor (Fuad, Fothergill-Gilmore et al. 2011). Interestingly, activity tests of another *T. brucei* glycosomal protein Phosphoglycerate Mutase revealed maximum activity in presence of Co^{2+} instead of Mg^{2+} or Mn^{2+} *(Fuad, Fothergill-Gilmore et al. 2011)*. There is little information on cobalt in Trypanosomes, but our finding suggests it could be also relevant for TbNH2 activity.

We discovered here a new function of TbNH4. TbNH4 is an important mRNA decaping enzyme, therefore it was expected to be found in cytosol. Nudix mRNA decapping function have been widely conserved, among mammalian, yeast and plant cells. Interestingly, the polyphosphatase activity is also conserved (Lonetti, Szijgyarto et al. 2011). Polyphosphatase activity can have significant physiological effects, and our kinetic data suggest a strong affinity for polyP, suggesting TbNH4 may be important to regulate cytosolic polyphosphate accumulation. TbNH4 has a similar activity on polyP60 and polyP700, suggesting it is an endopolyphosphatase. Yet, we detected inorganic phosphate release typical of exopolyphosphatase activity. Together, our results show that TbNH4 is exo and endo-polyphosphatase. Similarly, yeast endopolyphosphatase 1 (PPN1) has been characterized as capable of switching between exo and endopolyphosphatase activities (Andreeva, Trilisenko et al. 2015). Kinetic analysis shows a higher affinity to polyP60 than polyp700, which could be due to the detection method. Although the enzyme can hydrolyse polyP at any position, only the inorganic orthophosphate is detected by malachite green assay used. Therefore, shorter chains of polyP will have more available ends to release inorganic phosphate at higher pace than longer chains.

The vacuolar soluble pyrophosphatase is capable of degrading polyphosphate and pyrophosphate inside the acidocalcisome to produce inorganic phosphate that can be released to

the cytosol (Lemercier, Espiau et al. 2004). A knockout of the VTC4, the kinase that makes polyP, results in partial reduction of total cellular short chain polyP, found inside acidocalcisomes, and alteration of acidocalcisome morphology (Lander, Ulrich et al. 2013, Ulrich, Lander et al. 2014). This result suggests there is high concentration of extra-acidocalcisomal polyP in the cell. In fact, polyphosphate was recently found in nucleus and glycosomes of *T. brucei* (unpublished data). Moreover, a cytosolic exopolyphosphate (TbPPX1) from *T. brucei* was characterized, but a gene knockdown indicated this gene is not essential (Luginbuehl, Kunz et al. 2011). Our findings demonstrate a redundancy in polyphosphatase activity, which suggests that polyphosphate regulation is important for the parasites. For instance, *S. cerevisiae* overexpression experiments indicate that elevated cytosolic polyP is toxic for the cells (Gerasimaite, Sharma et al. 2014) and we propose that nudix TbNH4 help maintain optimum levels of cytosolic polyP. Additionally, overexpression of the *T. cruzi* TcPPX leads to reduction in polyphosphates and delayed hypo-osmotic response (Fang, Ruiz et al. 2007). Polyphosphate levels control seem to be crucial for various organisms.

Alternative possible function for nudix hydrolases is removing polyP from proteins that are polyphosphorylated. Polyphosphorylation happens when the polyacidic serine lysine rich (PASK) domain binds to polyP independently of enzymes. The polyP concentration is a crucial factor to determine this event so the reduction of polyP pools in yeast cells lead to concomitant reduction in protein polyphosphorylation. Conversely, an increase in cytosolic polyP concentration leads to polyphosphorylation of multiple targets. For example, expression of EcPPK1 in human cells generated polyphosphorylation of conserved proteins that contain PASK domains, although this post-translational modification was not detected in native conditions (Bentley-DeSousa, Holinier et al. 2018). Another experiment that lead to similar conclusion was

the inactivation of both yeast PPN1 and PPN2, leading to accumulation of long chain polyP (Gerasimaite and Mayer 2017) and alteration of polyphosphorylation sizes which are observed as a large shifts in protein migration pattern in polyacrylamide gels. Polyphosphatases may be important for regulating polyphosphate concentration and preventing excess or unwanted polyphosphorylation, which could be harmful for cells (Bentley-DeSousa, Holinier et al. 2018). TbNH2 and TbNH4 may be regulation of polyphosphorylation in cytosol and glycosomes. Furthermore, nucleoside polyphosphates or other compounds with phosphoanhydride bonds may also be targets of Nudix hydrolases as shown by the activity test of TbNH2 and TbNH4 on guanosine 5'-tetraphosphate. In summary, we characterized the enzymatic activity of *T. brucei* nudix hydrolases on polyP, which may be important for regulating polyP in different compartments.

CHAPTER 5

CONCLUSIONS AND FUTURE DIRECTIONS

When we started this work, there was no information on inositol phosphate kinases in trypanosomes. We successfully characterized the activity of the inositol pyrophosphate synthetic pathway that includes TbIPMK, TbIP5K and TbIP6K. We also demonstrated the ability of *T. brucei* TbIPMK, TbIP5K and TbIP6K to complement yeast knockouts *in vivo*. This work was important to build the foundation to following work on the function and relevance of inositol phosphates and identify the molecules that are synthesized in trypanosomes. Additionally, we demonstrated for the first time that *T. brucei* procyclic and bloodstream forms produce IP_6. We did not detect IP_7 previously, so we used mass spectrometry to confirm synthesis of IP_7 in procyclic forms of the parasite (Figure 5.1). This more sensitive method of detection also identified IP_4, IP_5 and IP_6. We propose this could be an interesting approach to determine inositol phosphates levels in parasites.

There is scarce information on inositol phosphates in protozoan parasites. One of the few studies described the IPMK from *Plasmodium knowlesi* with specific activity on Ins(1,4,5,)P_3. Like the human IPMK and TbIPMK, it phosphorylates positions 3 and 6, generating Ins(1,3,4,5)P_4 and then Ins(1,3,4,5,6)P_5. Interestingly, inhibitors of the mammalian IPMKs are not effective on *P. knowlesi* IPMK (Stritzke, Nalaskowski et al. 2012). A difference between TbIPMK and mammalian IPMK is the activity on PIPs. The activity of human IPMK as a PI3-Kinase of PI(4,5)P_2 that generates PI(3,4,5,)P_3 was observed and suggested as important for

regulating nuclear processes (Nalaskowski, Deschermeier et al. 2002, Resnick, Snowman et al. 2005). We attempted to detect PI3K activity unsuccessfully (data not shown), and Cestari and collaborators (Cestari, Haas et al. 2016) likewise failed to detect this kind of activity *in vitro*. This difference suggests that inhibitors of IPMK from distant organisms could have a minimal effect on human orthologs, therefore making it an interesting drug target.

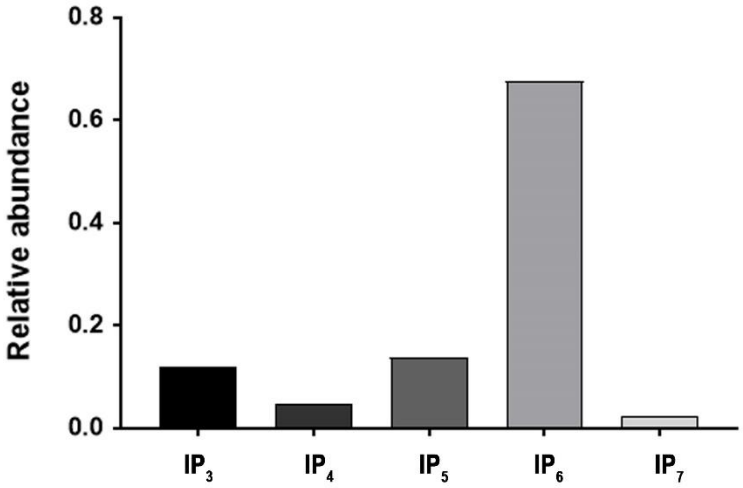

Figure 5.1. Mass spectrometry revealed presence of IP_7 in *Trypanosoma brucei*. We performed mass spectrometry as described previously (Couso, Evans et al. 2016) and relative abundance to total inositol phosphates mass was calculated. Data represents average of two experiments.

Synthesis of higher inositol phosphates by TbIPMK is essential for *T. brucei*, as demonstrated by the decline in growth and eventual death after TbIPMK depletion. Still, it is not established yet all the functions it has in parasites. Previous experiments have encountered multiple pleiotropic effects on yeast knockout mutants. In *T. brucei*, there are still many phenotypes to study to unveil new functions of this pathway, like DNA repair regulation, protein pyrophosphorylation, autophagy and cell cycle regulation. A recent study of TbIPMK knockout

revealed IPs regulate *T. brucei* differentiation. Overexpression of TbIPMK inhibits differentiation from BSF to PCF. In contrast, reduction of TbIPMK reduced VSG levels, increased procyclin expression and allowed cells to transform into PCF. Moreover, genes related to the respiratory chain were up-regulated in TbIPMK knockout, which is expected to happen when cells differentiate from BSF to PCF. Another interesting observation was that TbIPMK knockouts had elevated ATP (Cestari, Anupama et al. 2018), a phenotype also observed in yeast knockouts of IP6K (Szijgyarto, Garedew et al. 2011), an indication that IPs may be regulators of energy metabolism as in yeast and mammalian cells.

Our approach to investigate the functions of the IP pathway was to study the TbIPMK knockout mutant. Quantification of polyP after depletion of TbIPMK expression indicated a reduction in total short chain polyphosphate in the cells and resulted in less electrodense acidocalcisomes. We attributed this difference to a reduction in TbVTC4 activity, analogous to what has been described in yeast (Wild, Gerasimaite et al. 2016). Together, these results indicate that acidocalcisome storage of polyphosphate is linked to inositol phosphate synthesis (Figure 5.2). TbVTC4 has an N-terminal SPX domain which may bind to an inositol phosphate to regulate its own activity. Yeast ScVTC4 is stimulated by 5-IP_7, therefore 5-IP_7 synthesized by TbIP6K is a candidate TbVTC4 regulator.

We then inquired whether inositol phosphates also regulate phosphate release from intracellular stores. Previous studies in yeast have explored ScPho91 function for phosphate metabolism (Hurlimann, Stadler-Waibel et al. 2007) and during phosphate starvation (Yokota, Gomi et al. 2017), but the mechanism that controls the release has been elusive. We established that 5-IP_7 is a potent activator of ScPho91 Na^+/Pi transport (Figure 5.2) and we eliminated 1-IP_7 as a potential ScPho91 effector. We detected vacuole release currents with 1 μM 5-IP_7. The

concentration of IP_7 in yeast ranges from 500 nM to 5 µM and consists mainly of 5-IP_7 (Thota and Bhandari 2015). Additionally, IP_6 can also stimulate ScPho91 phosphate release at the relatively high concentration of 1 mM, which is above the physiological range of 10-100 µM (Thota and Bhandari 2015). However, we cannot discard the possibility that IP_6 concentration may rise above threshold levels and activate ScPho91 under certain circumstances. Our findings open the possibility that other phosphate transporters are also regulated by IPs via the SPX domain (Figure 5.2). The SPX domain from the yeast low affinity phosphate transporter ScPho90 has been associated with regulation of phosphate uptake. When the SPX domain was removed to generate a truncated form of the ScPho90, there was increased accumulation of phosphate which was presented as an evidence that SPX is a regulatory domain that inhibits phosphate transport (Hurlimann, Pinson et al. 2009). However, the SPX removal experiments provided no mechanistic evidence on how SPX regulates the transporters. The truncated version of Pho90 without the SPX domain may have altered its conformation rendering it in an open state. To answer this question, electro-physiological characterization of ScPho90 and ScPho87 could reveal how inositol phosphates and the SPX domain regulates phosphate uptake by low-affinity transporters.

Our experiments successfully demonstrated the inability of TbPho91 KO to release phosphate from acidocalcisomes, which suggests the absence of an alternative phosphate release transporter in this organelle. The TbPho91 transporter is not essential for growth under the culture conditions we tested. Nonetheless, during natural infection the utilization of phosphate stores may be important for survival. We observed a reduction in recovery after DNA damage in TbPho91 KO, suggesting that phosphate stores help supply extra phosphate to the cells when consumption is elevated as occurs during DNA repair. We learned that 1 µM 5-IP_7 can activate

TbPho91, regulating its activity through binding SPX domain. However, concentration of 5-IP_7 and how it varies in *T. brucei* is not known, hence characterization of inositol phosphates concentration in *T. brucei* is required to better understand this regulation mechanism. Furthermore, the conservation of polyP storage and Pi release control by inositol phosphates among distant organisms is evidence of its evolutionary importance. Both VTC complex and Pho91 are not found in animals, therefore they are interesting potential drug targets against kinetoplastid and fungal parasites.

Unlike TbPho91, TcPho91 ortholog from *T. cruzi* was found in the contractile vacuole membrane. This localization was obtained by overexpression of the transporter fused with a green fluorescent protein tag (Jimenez and Docampo 2015). Overexpression of acidocalcisomal IP_3R in *T. cruzi* previously led to an altered localization to the ER, which was only discovered to be an artefact later by using endogenous tagging (Lander, Chiurillo et al. 2016). Moreover, fusion of the acidocalcisomes and contractile vacuole has been reported (Rohloff, Montalvetti et al. 2004), raising the possibility that TcPho91 localization resulted from fusion events. Endogenous tagging may answer the question as to whether TcPho91 is also acidocalcisomal, which could shed light on phosphate homeostasis regulation of *T. cruzi* as well.

Polyphosphate in *T. brucei* is not restricted to acidocalcisomes. Previous experiments entailing depletion of TbVTC4 revealed reduced short chain polyP and smaller acidocalcisomes, but the cells retained themajority of its total polyP (Lander, Ulrich et al. 2013, Ulrich, Lander et al. 2014). This data is evidence that polyP is found outside of acidocalcisomes, and it may be synthesized by another polyP kinase in *T. brucei* as well. The localization, function or properties of extra-acidocalcisomal polyP is unkown. We identified two new phosphatases that may

regulate polyP in different compartments: TbNH2 is an exopolyphosphatase located in glycosomes and TbNH4 is an endopolyphosphatase found in cytosol.

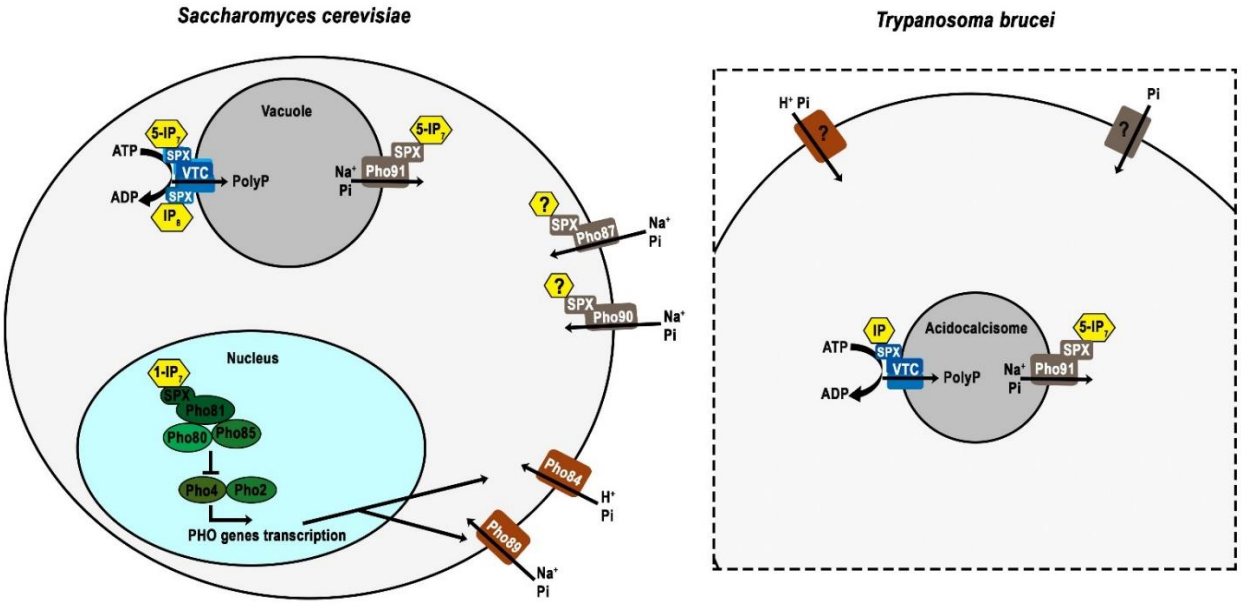

Figure 5.2. Inositol phosphates regulate phosphate stores in yeast and *T. brucei*. We represent here the known phosphate transporters in *S. cerevisiae* and *T. brucei* that are involved in phosphate uptake and management of stores. Top panel. *S. cerevisiae* PHO pathway is the classical response to low extracellular phosphate. Activation of PHO pathway is mediated by 1-IP_7 binding to SPX domain of Pho81 that triggers the inhibition of the cyclin-dependent kinase complex Pho80-Pho85, resulting in inhibition of phosphorylation of transcription factor Pho4. Pho4 then accumulates in nucleus where it interacts with its activator and promotes transcription of genes important for phosphate homeostasis, like the high-affinity transporters Pho84 and Pho89. Low-affinity transporters Pho87 and Pho90 have SPX domain, whose binding effectors are not yet identified. PolyP is stored in vacuoles and synthesized by VTC complex, which convert ATP to ADP and generates polyP in lumen. VTC is formed by different combinations of five VTC proteins that have SPX domain, with exception of VTC1. Currently, several inositol phosphates have been found to stimulate vacuole polyP synthesis (Gerasimaite, Pavlovic et al. 2017), and the activity of IP6K generating 5-IP_7 and IP_8 is essential for polyP synthesis (Lonetti, Szijgyarto et al. 2011). Yeast Pho91 Na^+/Pi release is also triggered by 5-IP_7. Bottom panel. *Trypanosoma brucei* transporters that uptake phosphate are not identified. Similar to vacuoles, acidocalcisomes polyP synthesis is performed by VTC complex that is composed of TbVTC1 and TbVTC4, which has an SPX that binds an unspecified inositol phosphate. TbPho91 is the transporter that release Na^+/Pi from acidocalcisomes when activated by 5-IP_7.

Elevated polyphosphate in the cytosol has been found to be toxic for yeast cells resulting in lower growth (Gerasimaite, Sharma et al. 2014). Although, it is not clear why elevated cytosolic polyP has this effect, one study observed that expression of cytosolic PPK leads to increase in protein polyphosphorylation in yeast cells (Bentley-DeSousa, Holinier et al. 2018). TbNH4 may be important for maintenance of cytosolic polyphosphate levels. Additionally, a proteome of polyP-binding proteins found several glycosomal proteins with a high score (Lander N.M. 2013), suggesting that polyP may interact with glycosomal proteins and therefore be found inside glycosomes. Our data support this intriguing possibility as we present the first report of an enzyme that can degrade polyP in glycosomes. Moving forward, there are many interesting questions to pursue. To confirm the existence of glycosomal polyP, one approach is to use polyphosphate binding domain of bacterial PPX as it was used for localization of nucleolar polyP in human cells (Jimenez-Nunez, Moreno-Sanchez et al. 2012). Additionally, activity tests of glycosomal enzymes in the presence of polyP may help understand if it affects glycosomal enzymatic activity. A novel experiment would be to test glycosomal proteins for polyphosphorylation, which has not been tested in any protozoan parasite yet.

Numerous experiments are required to advance the understanding of phosphate regulation in *T. brucei*. It is necessary to identify other phosphate transporters and players that participate in maintaining phosphate levels. There is no characterized plasma membrane Pi uptake symporter in *T. brucei*. As an initial approach one could be the investigate transporters based on their homology with other known proteins. Another interesting experiment is to investigate gene expression changes during phosphate depletion using RNA sequencing. This could help identify key regulators of phosphate homeostasis. We discovered the importance of inositol phosphates for Pi homeostasis, and it may be worth searching for additional binding partners of IPs that may

play complementary roles for this pathway. A pull-down of proteins that interact with IP_6 or IP_7 as performed yeast (Wu, Chong et al. 2016) will provide insights into new targets of inositol phosphate pathway in *T. brucei*. One candidate is a protein that contains SPX domain, which is annotated as ribose-phosphate pyrophosphokinase. This protein is normally involved in the synthesis of nucleotides, but it has not been studied in trypanosomes. The characterization of its enzymatic activity and interaction with inositol phosphates will provide additional insights into functions of inositol phosphates.

REFERENCES

Albert, C., S. T. Safrany, M. E. Bembenek, K. M. Reddy, K. Reddy, J. Falck, M. Brocker, S. B. Shears and G. W. Mayr (1997). "Biological variability in the structures of diphosphoinositol polyphosphates in Dictyostelium discoideum and mammalian cells." Biochem J **327 (Pt 2)**: 553-560.

Albuquerque, C. P., M. B. Smolka, S. H. Payne, V. Bafna, J. Eng and H. Zhou (2008). "A multidimensional chromatography technology for in-depth phosphoproteome analysis." Mol Cell Proteomics **7**(7): 1389-1396.

Andreeva, N., L. Trilisenko, M. Eldarov and T. Kulakovskaya (2015). "Polyphosphatase PPN1 of Saccharomyces cerevisiae: switching of exopolyphosphatase and endopolyphosphatase activities." PLoS One **10**(3): e0119594.

Auesukaree, C., T. Homma, H. Tochio, M. Shirakawa, Y. Kaneko and S. Harashima (2004). "Intracellular phosphate serves as a signal for the regulation of the PHO pathway in Saccharomyces cerevisiae." J Biol Chem **279**(17): 17289-17294.

Azevedo, C., A. Burton, E. Ruiz-Mateos, M. Marsh and A. Saiardi (2009). "Inositol pyrophosphate mediated pyrophosphorylation of AP3B1 regulates HIV-1 Gag release." Proc Natl Acad Sci U S A **106**(50): 21161-21166.

Azevedo, C., T. Livermore and A. Saiardi (2015). "Protein polyphosphorylation of lysine residues by inorganic polyphosphate." Mol Cell **58**(1): 71-82.

Azevedo, C. and A. Saiardi (2006). "Extraction and analysis of soluble inositol polyphosphates from yeast." Nature protocols **1**(5): 2416-2422.

Azevedo, C. and A. Saiardi (2017). "Eukaryotic Phosphate Homeostasis: The Inositol Pyrophosphate Perspective." Trends Biochem Sci **42**(3): 219-231.

Bakker, B. M., P. A. Michels, F. R. Opperdoes and H. V. Westerhoff (1999). "What controls glycolysis in bloodstream form Trypanosoma brucei?" J Biol Chem **274**(21): 14551-14559.

Bansal, V. K. (1990). Serum Inorganic Phosphorus. Clinical Methods: The History, Physical, and Laboratory Examinations. rd, H. K. Walker, W. D. Hall and J. W. Hurst. Boston.

Bentley-DeSousa, A., C. Holinier, H. Moteshareie, Y. C. Tseng, S. Kajjo, C. Nwosu, G. F. Amodeo, E. Bondy-Chorney, Y. Sai, A. Rudner, A. Golshani, N. E. Davey and M. Downey (2018). "A Screen for Candidate Targets of Lysine Polyphosphorylation Uncovers a Conserved Network Implicated in Ribosome Biogenesis." Cell Rep **22**(13): 3427-3439.

Berridge, M. J. (2009). "Inositol trisphosphate and calcium signalling mechanisms." Biochim Biophys Acta **1793**(6): 933-940.

Bertsch, U., C. Deschermeier, W. Fanick, I. Girkontaite, K. Hillemeier, H. Johnen, W. Weglohner, F. Emmrich and G. W. Mayr (2000). "The second messenger binding site of inositol 1,4,5-trisphosphate 3-kinase is centered in the catalytic domain and related to the inositol trisphosphate receptor site." J Biol Chem **275**(3): 1557-1564.

Bhandari, R., A. Saiardi, Y. Ahmadibeni, A. M. Snowman, A. C. Resnick, T. Z. Kristiansen, H. Molina, A. Pandey, J. K. Werner, Jr., K. R. Juluri, Y. Xu, G. D. Prestwich, K. Parang and S. H. Snyder (2007). "Protein pyrophosphorylation by inositol pyrophosphates is a posttranslational event." Proc Natl Acad Sci U S A **104**(39): 15305-15310.

Boer, V. M., C. A. Crutchfield, P. H. Bradley, D. Botstein and J. D. Rabinowitz (2010). "Growth-limiting intracellular metabolites in yeast growing under diverse nutrient limitations." Mol Biol Cell **21**(1): 198-211.

Bru, S., J. M. Martinez-Lainez, S. Hernandez-Ortega, E. Quandt, J. Torres-Torronteras, R. Marti, D. Canadell, J. Arino, S. Sharma, J. Jimenez and J. Clotet (2016). "Polyphosphate is involved in cell cycle progression and genomic stability in Saccharomyces cerevisiae." Mol Microbiol **101**(3): 367-380.

Bru, S., B. Samper-Martin, E. Quandt, S. Hernandez-Ortega, J. M. Martinez-Lainez, E. Gari, M. Rafel, J. Torres-Torronteras, R. Marti, M. P. C. Ribeiro, J. Jimenez and J. Clotet (2017). "Polyphosphate is a key factor for cell survival after DNA damage in eukaryotic cells." DNA Repair (Amst) **57**: 171-178.

Burton, A., C. Azevedo, C. Andreassi, A. Riccio and A. Saiardi (2013). "Inositol pyrophosphates regulate JMJD2C-dependent histone demethylation." Proc Natl Acad Sci U S A **110**(47): 18970-18975.

Burton, A., X. Hu and A. Saiardi (2009). "Are inositol pyrophosphates signalling molecules?" J Cell Physiol **220**(1): 8-15.

Cestari, I., A. Anupama and K. Stuart (2018). "Inositol polyphosphate multikinase regulation of Trypanosoma brucei life stage development." Mol Biol Cell **29**(9): 1137-1152.

Cestari, I., P. Haas, N. S. Moretti, S. Schenkman and K. Stuart (2016). "Chemogenetic Characterization of Inositol Phosphate Metabolic Pathway Reveals Druggable Enzymes for Targeting Kinetoplastid Parasites." Cell Chem Biol **23**(5): 608-617.

Cestari, I. and K. Stuart (2015). "Inositol phosphate pathway controls transcription of telomeric expression sites in trypanosomes." Proc Natl Acad Sci U S A **112**(21): E2803-2812.

Chakraborty, A., M. A. Koldobskiy, N. T. Bello, M. Maxwell, J. J. Potter, K. R. Juluri, D. Maag, S. Kim, A. S. Huang, M. J. Dailey, M. Saleh, A. M. Snowman, T. H. Moran, E. Mezey and S. H. Snyder (2010). "Inositol pyrophosphates inhibit Akt signaling, thereby regulating insulin sensitivity and weight gain." Cell **143**(6): 897-910.

Chang, S. C., A. L. Miller, Y. Feng, S. R. Wente and P. W. Majerus (2002). "The human homolog of the rat inositol phosphate multikinase is an inositol 1,3,4,6-tetrakisphosphate 5-kinase." J Biol Chem **277**(46): 43836-43843.

Choi, J. H., J. Williams, J. Cho, J. R. Falck and S. B. Shears (2007). "Purification, sequencing, and molecular identification of a mammalian PP-InsP5 kinase that is activated when cells are exposed to hyperosmotic stress." J Biol Chem **282**(42): 30763-30775.

Cocco, L., M. Y. Follo, L. Manzoli and P. G. Suh (2015). "Phosphoinositide-specific phospholipase C in health and disease." J Lipid Res **56**(10): 1853-1860.

Colasante, C., M. Ellis, T. Ruppert and F. Voncken (2006). "Comparative proteomics of glycosomes from bloodstream form and procyclic culture form Trypanosoma brucei brucei." Proteomics **6**(11): 3275-3293.

Cordeiro, C. D., A. Saiardi and R. Docampo (2017). "The inositol pyrophosphate synthesis pathway in Trypanosoma brucei is linked to polyphosphate synthesis in acidocalcisomes." Mol Microbiol **106**(2): 319-333.

Couso, I., B. Evans, J. Li, Y. Liu, F. Ma, S. Diamond, D. K. Allen and J. G. Umen (2016). "Synergism between inositol polyphosphates and TOR kinase signaling in nutrient sensing, growth control and lipid metabolism in Chlamydomonas." Plant Cell.

Cremers, C. M., D. Knoefler, S. Gates, N. Martin, J. U. Dahl, J. Lempart, L. Xie, M. R. Chapman, V. Galvan, D. R. Southworth and U. Jakob (2016). "Polyphosphate: A Conserved Modifier of Amyloidogenic Processes." Mol Cell **63**(5): 768-780.

Cross, G. A. (1975). "Identification, purification and properties of clone-specific glycoprotein antigens constituting the surface coat of Trypanosoma brucei." Parasitology **71**(3): 393-417.

Cunningham, I. (1977). "New culture medium for maintenance of tsetse tissues and growth of trypanosomatids." J Protozool **24**(2): 325-329.

Dick, C. F., A. L. Dos-Santos, D. Majerowicz, L. S. Paes, N. L. Giarola, K. C. Gondim, A. Vieyra and J. R. Meyer-Fernandes (2013). "Inorganic phosphate uptake in Trypanosoma cruzi is coupled to K(+) cycling and to active Na(+) extrusion." Biochim Biophys Acta **1830**(8): 4265-4273.

Dick, C. F., A. L. Dos-Santos and J. R. Meyer-Fernandes (2014). "Inorganic phosphate uptake in unicellular eukaryotes." Biochim Biophys Acta **1840**(7): 2123-2127.

Docampo, R. and G. Huang (2016). "Acidocalcisomes of eukaryotes." Curr Opin Cell Biol **41**: 66-72.

Docampo, R. and S. N. Moreno (2011). "Acidocalcisomes." Cell Calcium **50**(2): 113-119.

Docampo, R. and O. P. Pignataro (1991). "The inositol phosphate/diacylglycerol signalling pathway in Trypanosoma cruzi." Biochem J **275 (Pt 2)**: 407-411.

Docampo, R., D. A. Scott, A. E. Vercesi and S. N. Moreno (1995). "Intracellular Ca2+ storage in acidocalcisomes of Trypanosoma cruzi." Biochem J **310 (Pt 3)**: 1005-1012.

Draskovic, P., A. Saiardi, R. Bhandari, A. Burton, G. Ilc, M. Kovacevic, S. H. Snyder and M. Podobnik (2008). "Inositol hexakisphosphate kinase products contain diphosphate and triphosphate groups." Chem Biol **15**(3): 274-286.

Dubois, E., B. Scherens, F. Vierendeels, M. M. Ho, F. Messenguy and S. B. Shears (2002). "In Saccharomyces cerevisiae, the inositol polyphosphate kinase activity of Kcs1p is required for resistance to salt stress, cell wall integrity, and vacuolar morphogenesis." J Biol Chem **277**(26): 23755-23763.

Europe-Finner, G. N., B. Gammon and P. C. Newell (1991). "Accumulation of [3H]-inositol into inositol polyphosphates during development of Dictyostelium." Biochem Biophys Res Commun **181**(1): 191-196.

Ezawa, T. and K. Saito (2018). "How do arbuscular mycorrhizal fungi handle phosphate? New insight into fine-tuning of phosphate metabolism." New Phytol.

Fang, J., P. Rohloff, K. Miranda and R. Docampo (2007). "Ablation of a small transmembrane protein of Trypanosoma brucei (TbVTC1) involved in the synthesis of polyphosphate alters acidocalcisome biogenesis and function, and leads to a cytokinesis defect." Biochem J **407**(2): 161-170.

Fang, J., F. A. Ruiz, M. Docampo, S. Luo, J. C. Rodrigues, L. S. Motta, P. Rohloff and R. Docampo (2007). "Overexpression of a Zn2+-sensitive soluble exopolyphosphatase from Trypanosoma cruzi depletes polyphosphate and affects osmoregulation." J Biol Chem **282**(44): 32501-32510.

Franco, J. R., P. P. Simarro, A. Diarra and J. G. Jannin (2014). "Epidemiology of human African trypanosomiasis." Clin Epidemiol **6**: 257-275.

Freimoser, F. M., H. C. Hurlimann, C. A. Jakob, T. P. Werner and N. Amrhein (2006). "Systematic screening of polyphosphate (poly P) levels in yeast mutant cells reveals strong interdependence with primary metabolism." Genome Biol **7**(11): R109.

Fuad, F. A., L. A. Fothergill-Gilmore, M. W. Nowicki, L. J. Eades, H. P. Morgan, I. W. McNae, P. A. Michels and M. D. Walkinshaw (2011). "Phosphoglycerate mutase from Trypanosoma brucei is hyperactivated by cobalt in vitro, but not in vivo." Metallomics **3**(12): 1310-1317.

Galizzi, M., J. M. Bustamante, J. Fang, K. Miranda, L. C. Soares Medeiros, R. L. Tarleton and R. Docampo (2013). "Evidence for the role of vacuolar soluble pyrophosphatase and inorganic polyphosphate in Trypanosoma cruzi persistence." Mol Microbiol **90**(4): 699-715.

Gerasimaite, R. and A. Mayer (2017). "Ppn2, a novel Zn(2+)-dependent polyphosphatase in the acidocalcisome-like yeast vacuole." J Cell Sci **130**(9): 1625-1636.

Gerasimaite, R., I. Pavlovic, S. Capolicchio, A. Hofer, A. Schmidt, H. J. Jessen and A. Mayer (2017). "Inositol Pyrophosphate Specificity of the SPX-Dependent Polyphosphate Polymerase VTC." ACS Chem Biol **12**(3): 648-653.

Gerasimaite, R., S. Sharma, Y. Desfougeres, A. Schmidt and A. Mayer (2014). "Coupled synthesis and translocation restrains polyphosphate to acidocalcisome-like vacuoles and prevents its toxicity." J Cell Sci **127**(Pt 23): 5093-5104.

Ghosh, S., D. Shukla, K. Suman, B. J. Lakshmi, R. Manorama, S. Kumar and R. Bhandari (2013). "Inositol hexakisphosphate kinase 1 maintains hemostasis in mice by regulating platelet polyphosphate levels." Blood **122**(8): 1478-1486.

Glennon, M. C. and S. B. Shears (1993). "Turnover of inositol pentakisphosphates, inositol hexakisphosphate and diphosphoinositol polyphosphates in primary cultured hepatocytes." Biochem J **293 (Pt 2)**: 583-590.

Gokhale, N. A., A. Zaremba, A. K. Janoshazi, J. D. Weaver and S. B. Shears (2013). "PPIP5K1 modulates ligand competition between diphosphoinositol polyphosphates and PtdIns(3,4,5)P3 for polyphosphoinositide-binding domains." Biochem J **453**(3): 413-426.

Gonzalez-Salgado, A., M. Steinmann, L. L. Major, E. Sigel, J. L. Reymond, T. K. Smith and P. Butikofer (2015). "Trypanosoma brucei Bloodstream Forms Depend upon Uptake of myo-Inositol for Golgi Complex Phosphatidylinositol Synthesis and Normal Cell Growth." Eukaryot Cell **14**(6): 616-624.

Gonzalez-Salgado, A., M. E. Steinmann, E. Greganova, M. Rauch, P. Maser, E. Sigel and P. Butikofer (2012). "myo-Inositol uptake is essential for bulk inositol phospholipid but not glycosylphosphatidylinositol synthesis in Trypanosoma brucei." J Biol Chem **287**(16): 13313-13323.

Gray, M. J., W. Y. Wholey, N. O. Wagner, C. M. Cremers, A. Mueller-Schickert, N. T. Hock, A. G. Krieger, E. M. Smith, R. A. Bender, J. C. Bardwell and U. Jakob (2014). "Polyphosphate is a primordial chaperone." Mol Cell **53**(5): 689-699.

Gueldener, U., J. Heinisch, G. J. Koehler, D. Voss and J. H. Hegemann (2002). "A second set of loxP marker cassettes for Cre-mediated multiple gene knockouts in budding yeast." Nucleic Acids Res **30**(6): e23.

Guse, A. H., E. Greiner, F. Emmrich and K. Brand (1993). "Mass changes of inositol 1,3,4,5,6-pentakisphosphate and inositol hexakisphosphate during cell cycle progression in rat thymocytes." J Biol Chem **268**(10): 7129-7133.

Guther, M. L., M. D. Urbaniak, A. Tavendale, A. Prescott and M. A. Ferguson (2014). "High-confidence glycosome proteome for procyclic form Trypanosoma brucei by epitope-tag organelle enrichment and SILAC proteomics." J Proteome Res **13**(6): 2796-2806.

Hirumi, H. and K. Hirumi (1989). "Continuous cultivation of Trypanosoma brucei blood stream forms in a medium containing a low concentration of serum protein without feeder cell layers." J Parasitol **75**(6): 985-989.

Holt, L. J., B. B. Tuch, J. Villen, A. D. Johnson, S. P. Gygi and D. O. Morgan (2009). "Global analysis of Cdk1 substrate phosphorylation sites provides insights into evolution." Science **325**(5948): 1682-1686.

Huang, G., P. J. Bartlett, A. P. Thomas, S. N. Moreno and R. Docampo (2013). "Acidocalcisomes of Trypanosoma brucei have an inositol 1,4,5-trisphosphate receptor that is required for growth and infectivity." Proc Natl Acad Sci U S A **110**(5): 1887-1892.

Huang, G., P. N. Ulrich, M. Storey, D. Johnson, J. Tischer, J. A. Tovar, S. N. Moreno, R. Orlando and R. Docampo (2014). "Proteomic analysis of the acidocalcisome, an organelle conserved from bacteria to human cells." PLoS Pathog **10**(12): e1004555.

Huang, H., T. Kawamata, T. Horie, H. Tsugawa, Y. Nakayama, Y. Ohsumi and E. Fukusaki (2015). "Bulk RNA degradation by nitrogen starvation-induced autophagy in yeast." EMBO J **34**(2): 154-168.

Hurlimann, H. C., B. Pinson, M. Stadler-Waibel, S. C. Zeeman and F. M. Freimoser (2009). "The SPX domain of the yeast low-affinity phosphate transporter Pho90 regulates transport activity." EMBO Rep **10**(9): 1003-1008.

Hurlimann, H. C., M. Stadler-Waibel, T. P. Werner and F. M. Freimoser (2007). "Pho91 Is a vacuolar phosphate transporter that regulates phosphate and polyphosphate metabolism in Saccharomyces cerevisiae." Mol Biol Cell **18**(11): 4438-4445.

Ignatochkina, A. V., Y. Takagi, Y. Liu, K. Nagata and C. K. Ho (2015). "The messenger RNA decapping and recapping pathway in Trypanosoma." Proc Natl Acad Sci U S A **112**(22): 6967-6972.

Illies, C., J. Gromada, R. Fiume, B. Leibiger, J. Yu, K. Juhl, S. N. Yang, D. K. Barma, J. R. Falck, A. Saiardi, C. J. Barker and P. O. Berggren (2007). "Requirement of inositol

pyrophosphates for full exocytotic capacity in pancreatic beta cells." Science **318**(5854): 1299-1302.

Irvine, R. F. and M. J. Schell (2001). "Back in the water: the return of the inositol phosphates." Nature reviews. Molecular cell biology **2**(5): 327-338.

Jadav, R. S., M. V. Chanduri, S. Sengupta and R. Bhandari (2013). "Inositol pyrophosphate synthesis by inositol hexakisphosphate kinase 1 is required for homologous recombination repair." J Biol Chem **288**(5): 3312-3321.

Jimenez-Nunez, M. D., D. Moreno-Sanchez, L. Hernandez-Ruiz, A. Benitez-Rondan, A. Ramos-Amaya, B. Rodriguez-Bayona, F. Medina, J. A. Brieva and F. A. Ruiz (2012). "Myeloma cells contain high levels of inorganic polyphosphate which is associated with nucleolar transcription." Haematologica **97**(8): 1264-1271.

Jimenez, V. and R. Docampo (2015). "TcPho91 is a contractile vacuole phosphate sodium symporter that regulates phosphate and polyphosphate metabolism in Trypanosoma cruzi." Mol Microbiol **97**(5): 911-925.

Kimura, Y., Y. Yamamoto, S. Kajimoto, A. Sakai and K. Takegawa (2018). "Substrate specificity of Nudix hydrolases from Myxococcus xanthus." J Gen Appl Microbiol.

King-Keller, S., C. A. Moore, R. Docampo and S. N. Moreno (2015). "Ca2+ Regulation of Trypanosoma brucei Phosphoinositide Phospholipase C." Eukaryot Cell **14**(5): 486-494.

Klompmaker, S. H., K. Kohl, N. Fasel and A. Mayer (2017). "Magnesium uptake by connecting fluid-phase endocytosis to an intracellular inorganic cation filter." Nat Commun **8**(1): 1879.

Klosinska, M. M., C. A. Crutchfield, P. H. Bradley, J. D. Rabinowitz and J. R. Broach (2011). "Yeast cells can access distinct quiescent states." Genes Dev **25**(4): 336-349.

Laha, D., P. Johnen, C. Azevedo, M. Dynowski, M. Weiss, S. Capolicchio, H. Mao, T. Iven, M. Steenbergen, M. Freyer, P. Gaugler, M. K. de Campos, N. Zheng, I. Feussner, H. J. Jessen, S. C. Van Wees, A. Saiardi and G. Schaaf (2015). "VIH2 Regulates the Synthesis of Inositol Pyrophosphate InsP8 and Jasmonate-Dependent Defenses in Arabidopsis." Plant Cell **27**(4): 1082-1097.

Lander, N., M. A. Chiurillo, M. Storey, A. E. Vercesi and R. Docampo (2016). "CRISPR/Cas9-mediated endogenous C-terminal Tagging of Trypanosoma cruzi Genes Reveals the Acidocalcisome Localization of the Inositol 1,4,5-Trisphosphate Receptor." J Biol Chem **291**(49): 25505-25515.

Lander, N., C. Cordeiro, G. Huang and R. Docampo (2016). "Polyphosphate and acidocalcisomes." Biochem Soc Trans **44**(1): 1-6.

Lander, N., P. N. Ulrich and R. Docampo (2013). "Trypanosoma brucei vacuolar transporter chaperone 4 (TbVtc4) is an acidocalcisome polyphosphate kinase required for in vivo infection." The Journal of biological chemistry **288**(47): 34205-34216.

Lander, N., P. N. Ulrich and R. Docampo (2013). "Trypanosoma brucei vacuolar transporter chaperone 4 (TbVtc4) is an acidocalcisome polyphosphate kinase required for in vivo infection." J Biol Chem **288**(47): 34205-34216.

Lee, Y. S., K. Huang, F. A. Quiocho and E. K. O'Shea (2008). "Molecular basis of cyclin-CDK-CKI regulation by reversible binding of an inositol pyrophosphate." Nat Chem Biol **4**(1): 25-32.

Lee, Y. S., S. Mulugu, J. D. York and E. K. O'Shea (2007). "Regulation of a cyclin-CDK-CDK inhibitor complex by inositol pyrophosphates." Science **316**(5821): 109-112.

Lemercier, G., B. Espiau, F. A. Ruiz, M. Vieira, S. Luo, T. Baltz, R. Docampo and N. Bakalara (2004). "A pyrophosphatase regulating polyphosphate metabolism in acidocalcisomes is essential for Trypanosoma brucei virulence in mice." J Biol Chem **279**(5): 3420-3425.

Lev, S., C. Li, D. Desmarini, A. Saiardi, N. L. Fewings, S. D. Schibeci, R. Sharma, T. C. Sorrell and J. T. Djordjevic (2015). "Fungal Inositol Pyrophosphate IP7 Is Crucial for Metabolic Adaptation to the Host Environment and Pathogenicity." MBio **6**(3): e00531-00515.

Li, C., S. Lev, A. Saiardi, D. Desmarini, T. C. Sorrell and J. T. Djordjevic (2016). "Identification of a major IP5 kinase in Cryptococcus neoformans confirms that PP-IP5/IP7, not IP6, is essential for virulence." Sci Rep **6**: 23927.

Li, S. C. and P. M. Kane (2009). "The yeast lysosome-like vacuole: endpoint and crossroads." Biochim Biophys Acta **1793**(4): 650-663.

Lichko, L. P., T. V. Kulakovskaya and I. S. Kulaev (2006). "Inorganic polyphosphate and exopolyphosphatase in the nuclei of Saccharomyces cerevisiae: dependence on the growth phase and inactivation of the PPX1 and PPN1 genes." Yeast **23**(10): 735-740.

Lonetti, A., Z. Szijgyarto, D. Bosch, O. Loss, C. Azevedo and A. Saiardi (2011). "Identification of an evolutionarily conserved family of inorganic polyphosphate endopolyphosphatases." J Biol Chem **286**(37): 31966-31974.

Lonetti, A., Z. Szijgyarto, D. Bosch, O. Loss, C. Azevedo and A. Saiardi (2011). "Identification of an evolutionarily conserved family of inorganic polyphosphate endopolyphosphatases." The Journal of biological chemistry **286**(37): 31966-31974.

Losito, O., Z. Szijgyarto, A. C. Resnick and A. Saiardi (2009). "Inositol pyrophosphates and their unique metabolic complexity: analysis by gel electrophoresis." PLoS One **4**(5): e5580.

Luginbuehl, E., S. Kunz, L. Wentzinger, F. Freimoser and T. Seebeck (2011). "The exopolyphosphatase TbrPPX1 of Trypanosoma brucei." BMC Microbiol **11**: 4.

Luo, H. R., Y. E. Huang, J. C. Chen, A. Saiardi, M. Iijima, K. Ye, Y. Huang, E. Nagata, P. Devreotes and S. H. Snyder (2003). "Inositol pyrophosphates mediate chemotaxis in Dictyostelium via pleckstrin homology domain-PtdIns(3,4,5)P3 interactions." Cell **114**(5): 559-572.

Luo, H. R., A. Saiardi, H. Yu, E. Nagata, K. Ye and S. H. Snyder (2002). "Inositol pyrophosphates are required for DNA hyperrecombination in protein kinase c1 mutant yeast." Biochemistry **41**(8): 2509-2515.

Marin, P. A., M. S. da Silva, R. S. Pavani, C. R. Machado and M. C. Elias (2018). "Recruitment kinetics of the homologous recombination pathway in procyclic forms of Trypanosoma brucei after ionizing radiation treatment." Sci Rep **8**(1): 5405.

Martin, J. B., T. Bakker-Grunwald and G. Klein (1993). "31P-NMR analysis of Entamoeba histolytica. Occurrence of high amounts of two inositol phosphates." Eur J Biochem **214**(3): 711-718.

Mayr GW, R. T., THiel U, Vogel G., Stephens LR (1992). "Phosphoinositol diphosphates: non-enzymic formation in vitro and occurrence in vivo in the cellular slime mold Dictysotelium." Carbohydrate Research **234**: 247-262.

McInerney, P., T. Mizutani and T. Shiba (2006). "Inorganic polyphosphate interacts with ribosomes and promotes translation fidelity in vitro and in vivo." Mol Microbiol **60**(2): 438-447.

McLennan, A. G. (2006). "The Nudix hydrolase superfamily." Cell Mol Life Sci **63**(2): 123-143.

Menniti, F. S., R. N. Miller, J. W. Putney, Jr. and S. B. Shears (1993). "Turnover of inositol polyphosphate pyrophosphates in pancreatoma cells." J Biol Chem **268**(6): 3850-3856.

Meuth, M. (1989). "The molecular basis of mutations induced by deoxyribonucleoside triphosphate pool imbalances in mammalian cells." Exp Cell Res **181**(2): 305-316.

Michaillat, L. and A. Mayer (2013). "Identification of genes affecting vacuole membrane fragmentation in Saccharomyces cerevisiae." PLoS One **8**(2): e54160.

Miranda, K., R. Docampo, O. Grillo and W. de Souza (2004). "Acidocalcisomes of trypanosomatids have species-specific elemental composition." Protist **155**(4): 395-405.

Moreno, B., J. A. Urbina, E. Oldfield, B. N. Bailey, C. O. Rodrigues and R. Docampo (2000). "31P NMR spectroscopy of Trypanosoma brucei, Trypanosoma cruzi, and Leishmania major. Evidence for high levels of condensed inorganic phosphates." J Biol Chem **275**(37): 28356-28362.

Moreno, S. N., R. Docampo and A. E. Vercesi (1992). "Calcium homeostasis in procyclic and bloodstream forms of Trypanosoma brucei. Lack of inositol 1,4,5-trisphosphate-sensitive Ca2+ release." The Journal of biological chemistry **267**(9): 6020-6026.

Morrison, B. H., J. A. Bauer, D. V. Kalvakolanu and D. J. Lindner (2001). "Inositol hexakisphosphate kinase 2 mediates growth suppressive and apoptotic effects of interferon-beta in ovarian carcinoma cells." J Biol Chem **276**(27): 24965-24970.

Nagata, E., H. R. Luo, A. Saiardi, B. I. Bae, N. Suzuki and S. H. Snyder (2005). "Inositol hexakisphosphate kinase-2, a physiologic mediator of cell death." J Biol Chem **280**(2): 1634-1640.

Nagata, E., A. Saiardi, H. Tsukamoto, T. Satoh, Y. Itoh, J. Itoh, M. Shibata, S. Takizawa and S. Takagi (2010). "Inositol hexakisphosphate kinases promote autophagy." Int J Biochem Cell Biol **42**(12): 2065-2071.

Nalaskowski, M. M., C. Deschermeier, W. Fanick and G. W. Mayr (2002). "The human homologue of yeast ArgRIII protein is an inositol phosphate multikinase with predominantly nuclear localization." Biochem J **366**(Pt 2): 549-556.

Nishizuka, Y. (1986). "Studies and perspectives of protein kinase C." Science **233**(4761): 305-312.

Niyogi, S., V. Jimenez, W. Girard-Dias, W. de Souza, K. Miranda and R. Docampo (2015). "Rab32 is essential for maintaining functional acidocalcisomes, and for growth and infectivity of Trypanosoma cruzi." J Cell Sci **128**(12): 2363-2373.

Njiokou, F., C. Laveissiere, G. Simo, S. Nkinin, P. Grebaut, G. Cuny and S. Herder (2006). "Wild fauna as a probable animal reservoir for Trypanosoma brucei gambiense in Cameroon." Infect Genet Evol **6**(2): 147-153.

Oberholzer, M., S. Morand, S. Kunz and T. Seebeck (2006). "A vector series for rapid PCR-mediated C-terminal in situ tagging of Trypanosoma brucei genes." Mol Biochem Parasitol **145**(1): 117-120.

Oberholzer, M., S. Morand, S. Kunz and T. Seebeck (2006). "A vector series for rapid PCR-mediated C-terminal in situ tagging of Trypanosoma brucei genes." Molecular and biochemical parasitology **145**(1): 117-120.

Onnebo, S. M. and A. Saiardi (2009). "Inositol pyrophosphates modulate hydrogen peroxide signalling." Biochem J **423**(1): 109-118.

Pavlovic, I., D. T. Thakor, J. R. Vargas, C. J. McKinlay, S. Hauke, P. Anstaett, R. C. Camuna, L. Bigler, G. Gasser, C. Schultz, P. A. Wender and H. J. Jessen (2016). "Cellular delivery and photochemical release of a caged inositol-pyrophosphate induces PH-domain translocation in cellulo." Nat Commun **7**: 10622.

Peng, J., D. Schwartz, J. E. Elias, C. C. Thoreen, D. Cheng, G. Marsischky, J. Roelofs, D. Finley and S. P. Gygi (2003). "A proteomics approach to understanding protein ubiquitination." Nat Biotechnol **21**(8): 921-926.

Pesesse, X., K. Choi, T. Zhang and S. B. Shears (2004). "Signaling by higher inositol polyphosphates. Synthesis of bisdiphosphoinositol tetrakisphosphate ("InsP8") is selectively activated by hyperosmotic stress." J Biol Chem **279**(42): 43378-43381.

Phillippy, B. Q., I. Y. Perera, J. L. Donahue and G. E. Gillaspy (2015). "Certain Malvaceae Plants Have a Unique Accumulation of myo-Inositol 1,2,4,5,6-Pentakisphosphate." Plants (Basel) **4**(2): 267-283.

Piast, R. W. and R. M. Wieczorek (2017). "Origin of Life and the Phosphate Transfer Catalyst." Astrobiology **17**(3): 277-285.

Pisani, F., T. Livermore, G. Rose, J. R. Chubb, M. Gaspari and A. Saiardi (2014). "Analysis of Dictyostelium discoideum inositol pyrophosphate metabolism by gel electrophoresis." PloS one **9**(1): e85533.

Prasad, A., Y. Jia, A. Chakraborty, Y. Li, S. K. Jain, J. Zhong, S. G. Roy, F. Loison, S. Mondal, J. Sakai, C. Blanchard, S. H. Snyder and H. R. Luo (2011). "Inositol hexakisphosphate kinase 1 regulates neutrophil function in innate immunity by inhibiting phosphatidylinositol-(3,4,5)-trisphosphate signaling." Nat Immunol **12**(8): 752-760.

Pratt, J., A. M. Boisson, E. Gout, R. Bligny, R. Douce and S. Aubert (2009). "Phosphate (Pi) starvation effect on the cytosolic Pi concentration and Pi exchanges across the tonoplast in plant cells: an in vivo 31P-nuclear magnetic resonance study using methylphosphonate as a Pi analog." Plant Physiol **151**(3): 1646-1657.

Rao, N. N., M. R. Gomez-Garcia and A. Kornberg (2009). "Inorganic polyphosphate: essential for growth and survival." Annu Rev Biochem **78**: 605-647.

Resnick, A. C., A. M. Snowman, B. N. Kang, K. J. Hurt, S. H. Snyder and A. Saiardi (2005). "Inositol polyphosphate multikinase is a nuclear PI3-kinase with transcriptional regulatory activity." Proc Natl Acad Sci U S A **102**(36): 12783-12788.

Rohloff, P., A. Montalvetti and R. Docampo (2004). "Acidocalcisomes and the contractile vacuole complex are involved in osmoregulation in Trypanosoma cruzi." J Biol Chem **279**(50): 52270-52281.

Ross, C. A., J. Meldolesi, T. A. Milner, T. Satoh, S. Supattapone and S. H. Snyder (1989). "Inositol 1,4,5-trisphosphate receptor localized to endoplasmic reticulum in cerebellar Purkinje neurons." Nature **339**(6224): 468-470.

Ruiz, F. A., C. O. Rodrigues and R. Docampo (2001). "Rapid changes in polyphosphate content within acidocalcisomes in response to cell growth, differentiation, and environmental stress in Trypanosoma cruzi." J Biol Chem **276**(28): 26114-26121.

Russo-Abrahao, T., C. M. Koeller, M. E. Steinmann, S. Silva-Rito, T. Marins-Lucena, M. Alves-Bezerra, N. L. Lima-Giarola, I. F. de-Paula, A. Gonzalez-Salgado, E. Sigel, P. Butikofer, K. C. Gondim, N. Heise and J. R. Meyer-Fernandes (2017). "H(+)-dependent inorganic phosphate uptake in Trypanosoma brucei is influenced by myo-inositol transporter." J Bioenerg Biomembr **49**(2): 183-194.

Safrany, S. T., J. J. Caffrey, X. Yang, M. E. Bembenek, M. B. Moyer, W. A. Burkhart and S. B. Shears (1998). "A novel context for the 'MutT' module, a guardian of cell integrity, in a diphosphoinositol polyphosphate phosphohydrolase." EMBO J **17**(22): 6599-6607.

Saiardi, A. (2012). "Cell signalling by inositol pyrophosphates." Subcell Biochem **59**: 413-443.

Saiardi, A. (2016). "Protein pyrophosphorylation: moving forward." Biochem J **473**(21): 3765-3768.

Saiardi, A. (2017). "Has Inositol Played Any Role in the Origin of Life?" Life (Basel) **7**(2).

Saiardi, A., J. J. Caffrey, S. H. Snyder and S. B. Shears (2000). "The inositol hexakisphosphate kinase family. Catalytic flexibility and function in yeast vacuole biogenesis." J Biol Chem **275**(32): 24686-24692.

Saiardi, A., E. Nagata, H. R. Luo, A. Sawa, X. Luo, A. M. Snowman and S. H. Snyder (2001). "Mammalian inositol polyphosphate multikinase synthesizes inositol 1,4,5-trisphosphate and an inositol pyrophosphate." Proc Natl Acad Sci U S A **98**(5): 2306-2311.

Saiardi, A., A. C. Resnick, A. M. Snowman, B. Wendland and S. H. Snyder (2005). "Inositol pyrophosphates regulate cell death and telomere length through phosphoinositide 3-kinase-related protein kinases." Proc Natl Acad Sci U S A **102**(6): 1911-1914.

Saiardi, A., C. Sciambi, J. M. McCaffery, B. Wendland and S. H. Snyder (2002). "Inositol pyrophosphates regulate endocytic trafficking." Proc Natl Acad Sci U S A **99**(22): 14206-14211.

Scheffzek, K. and S. Welti (2012). "Pleckstrin homology (PH) like domains - versatile modules in protein-protein interaction platforms." FEBS Lett **586**(17): 2662-2673.

Secco, D., C. Wang, H. Shou and J. Whelan (2012). "Phosphate homeostasis in the yeast Saccharomyces cerevisiae, the key role of the SPX domain-containing proteins." FEBS Lett **586**(4): 289-295.

Seki, Y., K. Nitta and Y. Kaneko (2014). "Observation of polyphosphate bodies and DNA during the cell division cycle of Synechococcus elongatus PCC 7942." Plant Biol (Stuttg) **16**(1): 258-263.

Seufferheld, M. J., K. M. Kim, J. Whitfield, A. Valerio and G. Caetano-Anolles (2011). "Evolution of vacuolar proton pyrophosphatase domains and volutin granules: clues into the early evolutionary origin of the acidocalcisome." Biol Direct **6**: 50.

Shears, S. B. (2015). "Inositol pyrophosphates: why so many phosphates?" Adv Biol Regul **57**: 203-216.

Shi, X. and A. Kornberg (2005). "Endopolyphosphatase in Saccharomyces cerevisiae undergoes post-translational activations to produce short-chain polyphosphates." FEBS Lett **579**(9): 2014-2018.

Shirahama, K., Y. Yazaki, K. Sakano, Y. Wada and Y. Ohsumi (1996). "Vacuolar function in the phosphate homeostasis of the yeast Saccharomyces cerevisiae." Plant Cell Physiol **37**(8): 1090-1093.

Smith, S. A., N. J. Mutch, D. Baskar, P. Rohloff, R. Docampo and J. H. Morrissey (2006). "Polyphosphate modulates blood coagulation and fibrinolysis." Proc Natl Acad Sci U S A **103**(4): 903-908.

Soulard, A., A. Cremonesi, S. Moes, F. Schutz, P. Jeno and M. N. Hall (2010). "The rapamycin-sensitive phosphoproteome reveals that TOR controls protein kinase A toward some but not all substrates." Mol Biol Cell **21**(19): 3475-3486.

Springer, M., D. D. Wykoff, N. Miller and E. K. O'Shea (2003). "Partially phosphorylated Pho4 activates transcription of a subset of phosphate-responsive genes." PLoS Biol **1**(2): E28.

Srouji, J. R., A. Xu, A. Park, J. F. Kirsch and S. E. Brenner (2017). "The evolution of function within the Nudix homology clan." Proteins **85**(5): 775-811.

Steidle, E. A., L. S. Chong, M. Wu, E. Crooke, D. Fiedler, A. C. Resnick and R. J. Rolfes (2016). "A Novel Inositol Pyrophosphate Phosphatase in Saccharomyces cerevisiae: Siw14

PROTEIN SELECTIVELY CLEAVES THE beta-PHOSPHATE FROM 5-DIPHOSPHOINOSITOL PENTAKISPHOSPHATE (5PP-IP5)." J Biol Chem **291**(13): 6772-6783.

Stephens, L., T. Radenberg, U. Thiel, G. Vogel, K. H. Khoo, A. Dell, T. R. Jackson, P. T. Hawkins and G. W. Mayr (1993). "The detection, purification, structural characterization, and metabolism of diphosphoinositol pentakisphosphate(s) and bisdiphosphoinositol tetrakisphosphate(s)." J Biol Chem **268**(6): 4009-4015.

Stephens, L. R. and R. F. Irvine (1990). "Stepwise phosphorylation of myo-inositol leading to myo-inositol hexakisphosphate in Dictyostelium." Nature **346**(6284): 580-583.

Steverding, D. (2008). "The history of African trypanosomiasis." Parasit Vectors **1**(1): 3.

Streb, H., R. F. Irvine, M. J. Berridge and I. Schulz (1983). "Release of Ca2+ from a nonmitochondrial intracellular store in pancreatic acinar cells by inositol-1,4,5-trisphosphate." Nature **306**(5938): 67-69.

Stritzke, C., M. M. Nalaskowski, W. Fanick, H. Lin and G. W. Mayr (2012). "A Plasmodium multi-domain protein possesses multiple inositol phosphate kinase activities." Mol Biochem Parasitol **186**(2): 134-138.

Swaney, D. L., P. Beltrao, L. Starita, A. Guo, J. Rush, S. Fields, N. J. Krogan and J. Villen (2013). "Global analysis of phosphorylation and ubiquitylation cross-talk in protein degradation." Nat Methods **10**(7): 676-682.

Szijgyarto, Z., A. Garedew, C. Azevedo and A. Saiardi (2011). "Influence of inositol pyrophosphates on cellular energy dynamics." Science **334**(6057): 802-805.

Thota, S. G. and R. Bhandari (2015). "The emerging roles of inositol pyrophosphates in eukaryotic cell physiology." J Biosci **40**(3): 593-605.

Thota, S. G., C. P. Unnikannan, S. R. Thampatty, R. Manorama and R. Bhandari (2015). "Inositol pyrophosphates regulate RNA polymerase I-mediated rRNA transcription in Saccharomyces cerevisiae." Biochem J **466**(1): 105-114.

Ulrich, P. N., N. Lander, S. P. Kurup, L. Reiss, J. Brewer, L. C. Soares Medeiros, K. Miranda and R. Docampo (2014). "The acidocalcisome vacuolar transporter chaperone 4 catalyzes the synthesis of polyphosphate in insect-stages of Trypanosoma brucei and T. cruzi." J Eukaryot Microbiol **61**(2): 155-165.

Ulrich, P. N., N. Lander, S. P. Kurup, L. Reiss, J. Brewer, L. C. Soares Medeiros, K. Miranda and R. Docampo (2014). "The Acidocalcisome Vacuolar Transporter Chaperone 4 Catalyzes the Synthesis of Polyphosphate in Insect-stages of Trypanosoma brucei and T. cruzi." The Journal of eukaryotic microbiology **61**(2): 155-165.

Urbaniak, M. D., D. M. Martin and M. A. Ferguson (2013). "Global quantitative SILAC phosphoproteomics reveals differential phosphorylation is widespread between the procyclic and bloodstream form lifecycle stages of Trypanosoma brucei." J Proteome Res **12**(5): 2233-2244.

Van Dijken, P., J. C. Bergsma and P. J. Van Haastert (1997). "Phospholipase-C-independent inositol 1,4,5-trisphosphate formation in Dictyostelium cells. Activation of a plasma-membrane-bound phosphatase by receptor-stimulated Ca2+ influx." Eur J Biochem **244**(1): 113-119.

Van Dijken, P., J. R. de Haas, A. Craxton, C. Erneux, S. B. Shears and P. J. Van Haastert (1995). "A novel, phospholipase C-independent pathway of inositol 1,4,5-trisphosphate formation in Dictyostelium and rat liver." J Biol Chem **270**(50): 29724-29731.

Verbsky, J. W., M. P. Wilson, M. V. Kisseleva, P. W. Majerus and S. R. Wente (2002). "The synthesis of inositol hexakisphosphate. Characterization of human inositol 1,3,4,5,6-pentakisphosphate 2-kinase." J Biol Chem **277**(35): 31857-31862.

Vercesi, A. E., S. N. Moreno and R. Docampo (1994). "Ca2+/H+ exchange in acidic vacuoles of Trypanosoma brucei." Biochem J **304 (Pt 1)**: 227-233.

Voglmaier, S. M., M. E. Bembenek, A. I. Kaplin, G. Dorman, J. D. Olszewski, G. D. Prestwich and S. H. Snyder (1996). "Purified inositol hexakisphosphate kinase is an ATP synthase: diphosphoinositol pentakisphosphate as a high-energy phosphate donor." Proc Natl Acad Sci U S A **93**(9): 4305-4310.

Wang, C., W. Yue, Y. Ying, S. Wang, D. Secco, Y. Liu, J. Whelan, S. D. Tyerman and H. Shou (2015). "Rice SPX-Major Facility Superfamily3, a Vacuolar Phosphate Efflux Transporter, Is Involved in Maintaining Phosphate Homeostasis in Rice." Plant Physiol **169**(4): 2822-2831.

Weinert, B. T., C. Scholz, S. A. Wagner, V. Iesmantavicius, D. Su, J. A. Daniel and C. Choudhary (2013). "Lysine succinylation is a frequently occurring modification in prokaryotes and eukaryotes and extensively overlaps with acetylation." Cell Rep **4**(4): 842-851.

Weng, J., I. Aphasizheva, R. D. Etheridge, L. Huang, X. Wang, A. M. Falick and R. Aphasizhev (2008). "Guide RNA-binding complex from mitochondria of trypanosomatids." Mol Cell **32**(2): 198-209.

Werner, T. P., N. Amrhein and F. M. Freimoser (2007). "Inorganic polyphosphate occurs in the cell wall of Chlamydomonas reinhardtii and accumulates during cytokinesis." BMC Plant Biol **7**: 51.

Werner, T. P., N. Amrhein and F. M. Freimoser (2007). "Specific localization of inorganic polyphosphate (poly P) in fungal cell walls by selective extraction and immunohistochemistry." Fungal Genet Biol **44**(9): 845-852.

Wickner, R. B., A. C. Kelly, E. E. Bezsonov and H. K. Edskes (2017). "[PSI+] prion propagation is controlled by inositol polyphosphates." Proc Natl Acad Sci U S A.

Wickramasinghe, V. O., J. M. Savill, S. Chavali, A. B. Jonsdottir, E. Rajendra, T. Gruner, R. A. Laskey, M. M. Babu and A. R. Venkitaraman (2013). "Human inositol polyphosphate multikinase regulates transcript-selective nuclear mRNA export to preserve genome integrity." Mol Cell **51**(6): 737-750.

Wild, R., R. Gerasimaite, J. Y. Jung, V. Truffault, I. Pavlovic, A. Schmidt, A. Saiardi, H. J. Jessen, Y. Poirier, M. Hothorn and A. Mayer (2016). "Control of eukaryotic phosphate homeostasis by inositol polyphosphate sensor domains." Science **352**(6288): 986-990.

Wilson, M. S., S. J. Bulley, F. Pisani, R. F. Irvine and A. Saiardi (2015). "A novel method for the purification of inositol phosphates from biological samples reveals that no phytate is present in human plasma or urine." Open Biol **5**(3): 150014.

Wilson, M. S., T. M. Livermore and A. Saiardi (2013). "Inositol pyrophosphates: between signalling and metabolism." Biochem J **452**(3): 369-379.

Wright, R. H., A. Lioutas, F. Le Dily, D. Soronellas, A. Pohl, J. Bonet, A. S. Nacht, S. Samino, J. Font-Mateu, G. P. Vicent, M. Wierer, M. A. Trabado, C. Schelhorn, C. Carolis, M. J. Macias, O. Yanes, B. Oliva and M. Beato (2016). "ADP-ribose-derived nuclear ATP synthesis by NUDIX5 is required for chromatin remodeling." Science **352**(6290): 1221-1225.

Wu, M., L. S. Chong, D. H. Perlman, A. C. Resnick and D. Fiedler (2016). "Inositol polyphosphates intersect with signaling and metabolic networks via two distinct mechanisms." Proc Natl Acad Sci U S A **113**(44): E6757-E6765.

Wundenberg, T., N. Grabinski, H. Lin and G. W. Mayr (2014). "Discovery of InsP6-kinases as InsP6-dephosphorylating enzymes provides a new mechanism of cytosolic InsP6 degradation driven by the cellular ATP/ADP ratio." Biochem J **462**(1): 173-184.

Wykoff, D. D., A. H. Rizvi, J. M. Raser, B. Margolin and E. K. O'Shea (2007). "Positive feedback regulates switching of phosphate transporters in S. cerevisiae." Mol Cell **27**(6): 1005-1013.

Yabe, I., K. Horiuchi, K. Nakahara, T. Hiyama, T. Yamanaka, P. C. Wang, K. Toda, A. Hirata, Y. Ohsumi, R. Hirata, Y. Anraku and I. Kusaka (1999). "Patch clamp studies on V-type ATPase of vacuolar membrane of haploid Saccharomyces cerevisiae. Preparation and utilization of a giant cell containing a giant vacuole." J Biol Chem **274**(49): 34903-34910.

Yang, S. Y., T. K. Huang, H. F. Kuo and T. J. Chiou (2017). "Role of vacuoles in phosphorus storage and remobilization." J Exp Bot **68**(12): 3045-3055.

Yokota, H., K. Gomi and T. Shintani (2017). "Induction of autophagy by phosphate starvation in an Atg11-dependent manner in Saccharomyces cerevisiae." Biochem Biophys Res Commun **483**(1): 522-527.

York, J. D., A. R. Odom, R. Murphy, E. B. Ives and S. R. Wente (1999). "A phospholipase C-dependent inositol polyphosphate kinase pathway required for efficient messenger RNA export." Science **285**(5424): 96-100.

York, S. J., B. N. Armbruster, P. Greenwell, T. D. Petes and J. D. York (2005). "Inositol diphosphate signaling regulates telomere length." J Biol Chem **280**(6): 4264-4269.

Yoshimura, K. and S. Shigeoka (2015). "Versatile physiological functions of the Nudix hydrolase family in Arabidopsis." Biosci Biotechnol Biochem **79**(3): 354-366.

Zhang, T., J. J. Caffrey and S. B. Shears (2001). "The transcriptional regulator, Arg82, is a hybrid kinase with both monophosphoinositol and diphosphoinositol polyphosphate synthase activity." FEBS Lett **494**(3): 208-212.